PEOPLE'S DEMOCRATIC REPUBLIC OF ALGERIA

Ministry of Higher Education and Scientific Research

Memory

Presented with a view to obtaining the Master's degree in MechanicalEngineering

University Echahid Hamma Lakhdar d'El Oued

Faculty of Technology

Department**:** Mechanical Engineering

Option: *Electromechanical Engineering*

Presented by:

BALI mohammed fouad - ARID Marouane - BOUTAYEB Achouak

Title

Smart electromechanical agitator based on magnetic induction and combined with a plasma generator

Directed by:

Dr.Labiod Chouaib	MCB	Supervisor
Dr.Miloudi Khaled	MCB	President
Dr.Ferhat Mohammed Fouad	MCB	Assistant supervisor
Dr.Mahmoudi Abdelkader	MCB	Examiner
Dr.Mansouri Khaled	MCB	Incubator Representative

College year 2022/2023

Thanks

First and foremost, we would like to thank Allah , Almighty, for granting us the strength to persevere and overcome all challenges.

A special thank you goes to **Dr. Labiod Chouaib**, for accepting the role of our thesis supervisor. We are truly grateful for the trust he placed in us and for his invaluable guidance, expertise, and insightful directions throughout the entire process.

We would also like to extend our sincere appreciation to the members of the thesis jury for their interest in our research and for their valuable feedback and evaluation.

Furthermore, we would like to express our gratitude to all the teachers of the Electromechanical Engineering department who have contributed to our education and training. Their dedication and expertise have played a significant role in shaping our knowledge and skills.

Lastly, we would like to acknowledge and thank all other individuals, such as our family, friends, and colleagues, who have provided us with support, encouragement, and understanding throughout this journey.

Dedications

In the name of Allah, the Most Merciful, the Most Compassionate.

We dedicate this humble work as an expression of respect, gratitude, and appreciation:

To our dear mothers, who embody love, care, and selflessness. Your unwavering support, nurturing guidance, and unconditional love have shaped us into who we are today. We are forever grateful for your sacrifices and endless devotion.

To our dear fathers, who exemplify strength, wisdom, and guidance. Your constant presence, encouragement, and belief in us have been a source of inspiration and motivation. We are thankful for your sacrifices, protection, and unwavering love.

May Allah bless our mothers and fathers with good health, happiness, and long lives. May He reward them abundantly for their love, care, and sacrifices.

to our dear siblings, whose continuous support and encouragement have been a constant source of motivation. We would also like to express our deep gratitude to our extended family, the Boutayeb, Bali, and Arid families.

To all those who have contributed to the development of this humble work and to all our dear ones, your presence in our lives has made a significant impact, and we are grateful for your continuous support and encouragement.

With heartfelt appreciation

Abstract

This thesis presents a comprehensive study on the design and implementation of a smart electromechanical agitator that integrates magnetic stirring and plasma technology. The aim is to streamline and enhance the mixing process in laboratory settings by combining these two traditional devices into one advanced and user-friendly device. The thesis consists of three main chapters.

The first chapter provides an overview of magnetic stirrers and their applications in laboratory science, along with an introduction to plasma technology and its diverse uses. Additionally, the chapter explores the growing significance of IoT devices in laboratory settings.

The second chapter focuses on DC motors used in electromechanical mixers, specifically emphasizing the characteristics of permanent magnet DC motors and control techniques employed to regulate their performance. The chapter also covers the identification of motor-specific parameters.

The third chapter delves into the practical implementation of the smart electromechanical mixer. It includes the selection and integration of electronic components, the design of electronic circuits, and the configuration of mechanical parts for the mixer. The chapter also discusses the development of a remote control application interface for monitoring the mixing process and logging data. The device is connected to a microcontroller (Arduino) with a built-in Wi-Fi module, enabling wireless control of the motor speed through a smartphone application that displays temperature and treatment information. This design reduces the need for a separate display screen, simplifying user experience while ensuring static electricity protection.

Keywords: smart electromechanical agitator, magnetic stirring, plasma technology, DC motor control, IoT devices, remote control, microcontroller, Wi-Fi connectivity.

الملخص

تقدم هذه الرسالة العلمية دراسة شاملة حول تصميم وتنفيذ جهاز مزج كهرومغناطيسي ذكي يدمج بين تقنية الخلط المغناطيسي وتقنية البلازما. الهدف هو تبسيط وتعزيز عملية الخلط في بيئة المختبر عن طريق دمج هاتين الأداة التقليديتين في جهاز واحد متطور وسهل الاستخدام. تتألف الرسالة من ثلاثة فصول رئيسية.

يقدم الفصل الأول نظرة عامة على أجهزة الخلط المغناطيسي وتطبيقاتها في علوم المختبر، بالإضافة إلى مقدمة عن تقنية البلازما واستخداماتها المتنوعة. بالإضافة إلى ذلك، يتناول الفصل أهمية الأجهزة المتصلة بالإنترنت (IoT) في بيئة المختبر ونمو أهميتها.

يتمحور الفصل الثاني حول محركات التيار المباشر المستخدمة في أجهزة الكهرومغناطيسي، مع التركيز بشكل خاص على خصائص المحركات الدائمة المغناطيسية التيار المباشر وتقنيات التحكم المستخدمة لتنظيم أدائها. يشمل الفصل أيضًا المحولات الإلكترونية المستخدمة للتحكم في المحرك وتحديد المعلمات الخاصة بالمحرك.

يستكشف الفصل الثالث تنفيذ جهاز المختلط الكهرومغناطيسي الذكي عمليًا. يشمل اختيار ودمج المكونات الإلكترونية، وتصميم الدوائر الالكترونية وتكوين الأجزاء الميكانيكية. يناقش الفصل أيضًا تطوير واجهة تطبيق التحكم عن بعد لمراقبة عملية الخلط وتسجيل البيانات. يتصل الجهاز بمتحكم مدمج (أردوينو) يحتوي على وحدة واي فاي مدمجة، مما يتيح التحكم اللاسلكي في سرعة المحرك من خلال تطبيق على الهاتف الذكي يعرض معلومات الحرارة والمعالجة. يسهم هذا التصميم في تقليل تكلفة شاشة العرض المستقلة، وتبسيط تجربة المستخدم مع ضمان حماية كاملة من الكهرباء الساكنة.

الكلمات المفتاحية: جهاز الخلط الكهرومغناطيسي الذكي، الخلط المغناطيسي، تقنية البلازما، التحكم في محركات التيار المباشر، أجهزة انترنت الاشياء ، التحكم عن بعد متحكم مدمج، واي فاي.

List of Figures

List of tables

Acronyms

DC: direct courent

AC: alternatif courent

Iot: Internet of things

DIY: Do-It-Yourself

USB: Universal Serial Bus

GaAsP: Gallium Arsenide Phosphide

LED: Light-Emitting Diode

IGBT: Insulated Gate Bipolar Transistor

MOSFET: Metal-Oxide-Semiconductor Field-Effect

DC/DC: Direct Current to Direct Current

PLC: Programmable Logic Controller

CMR: Mode Rejection

UVLO: Under Voltage Lockout (UVLO) with hysteresis.

VCC: Voltage Common Collector

UL: Underwriters Laboratories.

CSA: Compliance with safety approval standards such as CSA.

DIN: EN 60747-5-2: Deutsche Industrie Norm

IGBT: Insulated Gate Bipolar Transistor.

DIP: Dual In-Line Package

SMD: Surface-Mount Device

CTR: Current Transfer Ratio

IF: Input Current

VCE: Collector-Emitter Voltage

RoHS: Restriction of Hazardous Substances

VDE: Verband der Elektrotechnik

SEMKO: Svenska Elektriska Materielkontrollanstalten

NEMKO: Norsk Elektrisk Materiellkontroll

DEMKO: Dansk Elektrisk Materielkontrol

FIMKO: Finnish Electrical Inspection Authority

CSA: Canadian Standards Association

MOS: Metal-Oxide-Semiconductor

VGS: Gate-to-Source Voltage

ID: Drain Current

IGBT: Insulated Gate Bipolar Transistor

ESS: Energy Storage Systems

PFC: Power Factor Correction

TV-5: Terminal Verzeichnis 5

VDE: Verband der Elektrotechnik (Association for Electrical, Electronic & Information Technologies)

TÜV: Technischer Überwachungsverein (Technical Inspection Association)

N.O: Normally Open

Class B: Coil insulation class B

Class F: Coil insulation class F

EN60335-1 GWT: EN60335-1 Glow Wire Test

3D: Three-dimensional

2D: Two-dimensional

CNC: Computer Numerical Control

PWM: Pulse Width Modulation

IP: Internet Protocol

Summary

Chapter III : Implementation of Smart Agitator

General introduction

General Introduction

In modern industrial and laboratory applications, efficient mixing and stirring of liquids are essential processes. The development of smart electromechanical agitators that incorporate magnetic induction and plasma generation has revolutionized the field of mixing technology. This thesis focuses on the design and implementation of a smart electromechanical agitator, integrating magnetic induction and plasma technology to enhance the mixing process.

The magnetic stirrer, has been widely utilized in laboratories for liquid mixing. It operates based on the principle of a rotating stir bar driven by a magnetic field generated by an external magnet [Hal 07],[Ros 13]. The use of magnetic induction in the agitator allows for precise control over the stirring speed, direction, and other critical parameters, leading to improved productivity and quality control.

Furthermore, the incorporation of plasma technology in the agitator introduces additional benefits. Plasma, a state of matter formed by ionizing a gas [Ale 08],[Wel 18],[Šim 19].offers unique properties and applications. It has been extensively employed in various fields, including industrial processing, medical treatments, and environmental analysis. The combination of magnetic induction and plasma technology provides a comprehensive solution for achieving efficient mixing and enhanced chemical reactions.

Laboratories face numerous challenges in dealing with conventional mixers, and to overcome these challenges, innovative solutions are being developed to meet the needs of researchers and laboratories. This memorandum presents a comprehensive study on the development and implementation of a smart electromechanical mixer that relies on magnetic stimulation and combines it with plasma generation. The aim of this research is to provide an efficient and safe mixing solution that integrates advanced control mechanisms and harnesses.

By utilizing advanced control mechanisms and intelligent features, this agitator promises to revolutionize the mixing process in terms of productivity, quality control, and cost-effectiveness.

The main chapters of this thesis will cover the following aspects:

The first chapter provides an in-depth understanding of magnetic stirrers and their various applications in laboratory settings. Additionally, it explores the fundamentals of plasma technology and its wide range of uses. The chapter sets the foundation for the subsequent chapters by discussing the principles and characteristics of magnetic stirrers and plasma technology.

The second chapter, the focus will be on the different types of motors used in electromechanical agitators, with a specific emphasis on DC motors. The characteristics of permanent magnet DC motors will be examined, and various control techniques for DC motors will be explored. Additionally, electronic converters used for DC motor control and the identification of parameters specific to DC motors will be discussed.

In the last chapter of our project, will delve into the practical implementation of the smart electromechanical agitator. It will cover the selection and integration of electronic components, the design of electronic circuits, and the hardware configuration of the agitator. The chapter will also discuss the development of an application interface for remote control, monitoring of the mixing process, and data logging. The testing and evaluation process, including the analysis of performance results, will be presented to assess the efficiency and reliability of the smart agitator.

Chapter I: The description of the Magnetic stirrer and the concept of Plasma

I.1 Introduction :

This chapter discusses the magnetic stirrer and the concept of plasma technology. Magnetic stirrers are widely used in laboratories to mix liquids, and they are available in different types, including mini magnetic stirrers, magnetic stirrers with timers, heavy-duty magnetic stirrers, battery-powered magnetic stirrers, and air-operated turbine magnetic stirrers [Hal 07], [Ros 13],[Kor 80]125.These devices operate based on the principle of the magnetic field generated by an external magnet that causes a stir bar to rotate within a container of liquid. Heating magnetic stirrers can also be used in the laboratory, and they can operate through heating induction or heating resistance. Magnetic stirrers are commonly used in various laboratory applications, such as chemical synthesis, biological research, and environmental analysis .

Plasma technology is another topic discussed in this chapter. Plasma is a state of matter that occurs when a gas is ionized [Ale 08], [Wel 18], [Šim 19] . and it is widely used in various applications, including space research, industrial processing, and medical treatments. Plasma can exist in nature, such as in lightning and stars, or it can be generated in the laboratory through various methods. Atmospheric non-thermal plasmas, such as corona discharge, are widely used in industrial processing and air purification, water purification, electrophotography, copying machines, printers, liquid spray guns, and powder coating [Cha91], [Gol 85] . The temperature of plasma can vary depending on the application, and it can range from a few thousand to millions of degrees Celsius.

Finally, the chapter briefly touches on the topic of The Internet of Things (IoT) technology is rapidly evolving, and it has become a crucial component in various industries[Gub 13], [Mio 12] ,[Sil 18] . including laboratory science. IoT devices in laboratory settings provide an efficient and cost-effective way to monitor, control, and analyze data in real-time, This not only enhances the accuracy and reliability of experimental results but also reduces the time and effort required for data collection and analysis. In this chapter, we will explore the various applications of IoT devices in laboratory science, their benefits.

I.2 Magnetic Laboratory Stirrers :

One piece of equipment that is widely used in science in chemistry and biology laboratories is the magnetic stirrer.

A magnetic stirrer or magnetic mixer is a laboratory device that employs a rotating magnetic field to cause a stir bar (or flea) that rotates at adjustable speeds immersed in a reaction vessel. This rotation allows efficient mixing and stirring of any liquid contained within through the strong fluid motion generated by the bar [Hal 07].

The rotating field may be created either by a rotating magnet or a set of stationary electromagnets, placed beneath the vessel with the liquid So, the bar inside the bottle would be driven at the time the motor is working [Ros 13].

This concept was introduced the first time by inventor named Arthur Rosinger at 1944 [Ros 13] ,[Han 17] invented a new tool to help a laborist to mix their chemistry liquid by using ,a coated bar magnet inside a reaction bottle as a stirrer. In 1917 , R.H. String ham had invented an early concept to rotate the stirrer by utilizing a stationary electromagnet in the base of a mixer rather than using a rotating permanent magnet to rotate the stirrer. However, The first multipoint magnetic stirrer was developed and patented by Salvador Bonet Company in 1977 a complete version of a magnetic stirrer was, Bonet also invented a standardized level of a stirring power in “liters of water” , This standard is used globally in the market [Han 17].

I.3 Types of Magnetic Stirrers :

There are several types of magnetic stirrers available and it all depends Based on the size choice of size, application and configuration. The different types are listed below:

I.3.1 Mini magnetic stirrer :

A mini magnetic stirrer is a small laboratory instrument used for mixing small volumes of liquids or solutions.. Mini magnetic stirrers are usually compact and portable, making them ideal for use in small workspaces or for field work. They are also generally less expensive than larger magnetic stirrers, making them a popular choice for students or for small-scale experiments. Some mini magnetic stirrers also come with additional features such as variable speed control, temperature monitoring, and built-in timers. Overall, mini magnetic stirrers provide a convenient and efficient way to mix small volumes of liquids or solutions in a laboratory or field setting.

Figure I. 1: Mini magnetic stirrer.

I.3.2 Magnetic stirrer with timer :

Magnetic stirrers with timers are useful for a variety of laboratory applications that require precise mixing times. The timer function can be programmed to turn off the motor after a set amount of time, which can be beneficial for experiments that require a specific amount of mixing or for applications where the operator needs to step away from the instrument for a period of time. Some magnetic stirrers with timers also have the ability to adjust the stirring speed during the mixing process, which can be useful for applications that require changes in mixing intensity. Additionally, some models may include other features such as temperature control, digital displays, and memory functions to store frequently used settings. The timer function is typically controlled through a digital interface on the instrument, which allows for easy programming and adjustment of the mixing time. Overall, magnetic stirrers with timers provide a convenient and efficient way to ensure accurate and consistent mixing in a laboratory setting.

Figure I.2: Magnetic stirrer with timer.

I.3.3 Heavy-duty magnetic stirrer :

Heavy-duty magnetic stirrers can come in various sizes and configurations to meet different laboratory needs. Some models can accommodate up to 50 - 600 liters of liquid, while others may have multiple stirring positions to mix several solutions simultaneously. The motors used in heavy-duty magnetic stirrers are typically high-performance AC or DC motors that can produce higher torque and rotate at higher speeds than standard magnetic stirrers. Additionally, heavy-duty magnetic stirrers may feature a variety of stirring bar shapes and sizes to optimize mixing efficiency for different types of solutions. Some common materials used for the construction of heavy-duty magnetic stirrers include stainless steel, aluminum, and polycarbonate, which provide high chemical resistance and durability

Figure I. 3: Heavy-duty magnetic stirrer**.**

I.3.4 Battery-powered magnetic stirrer :

The battery-powered magnetic stirrer is a convenient solution for mixing applications where a power outlet is not available, making it particularly useful in incubators or other remote locations. These devices are typically compact and portable, allowing them to be easily moved between different work areas or facilities. Alkaline batteries are commonly used with these devices although rechargeable batteries can also be used as an alternative. Battery-powered magnetic stirrers are commonly used in scientific research and analytical laboratories, as well as in educational settings where mobility and convenience are important factors

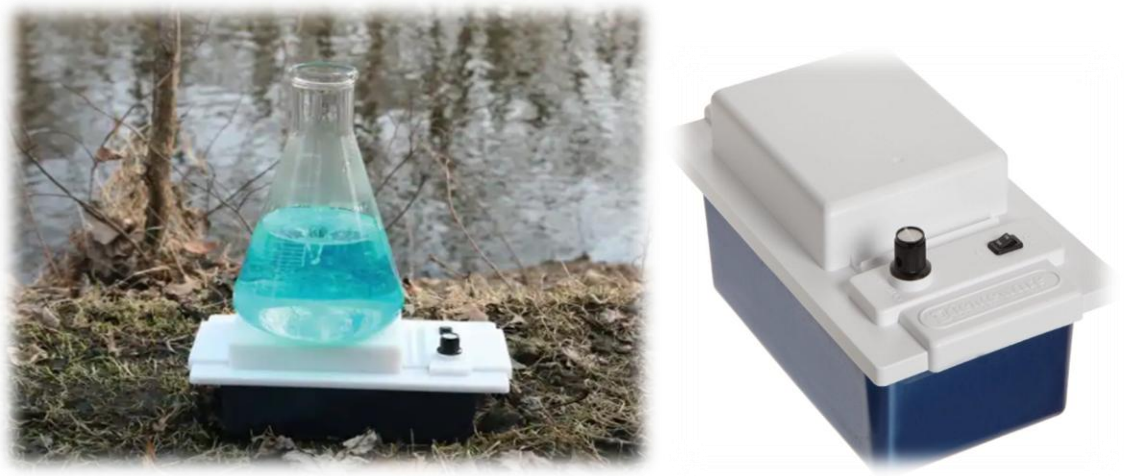

Figure I.4: Battery-powered magnetic stirrer.

I.3.5 Air-operated turbine magnetic stirrer :

The air-operated turbine magnetic stirrer is a popular device used in laboratory and industrial settings to quickly and efficiently mix large volumes of solutions. It operates using air pressure to drive a turbine, allowing for efficient mixing of viscous solutions that may be difficult to mix using other types of stirrers. The main advantage of this type of stirrer is that it eliminates the risk of sparks or electrical interference, making it ideal for hazardous substances. The stirrer can achieve relatively high speeds of 200-500 rpm and is commonly used in chemical processing, petrochemical, and pharmaceutical industries. The optimal air pressure range for the device is 0.5-1 atm, which can be precisely adjusted using a regulator [Kor80].

Figure I.5: Air-operated turbine magnetic stirrer**.**

I.4 Working Principle of magnetic stirrers :

The working principle of magnetic stirrers involves the use of a magnetic stir bar, which is a small magnet placed inside a container with the solution to be stirred. The stir bar is rotated by a magnetic field generated by an external magnetic stirrer device placed beneath the container.

The magnetic stirrer device consists of a motor that rotates a magnetic field generator, typically a small magnet or a set of magnets, inside a circular base. The circular base contains a rotating magnet and a speed control mechanism, which allows the user to adjust the speed of the stirrer.

When the magnetic stir bar is placed in the solution and the magnetic field generator is turned on, the magnetic field generated by the stirrer device rotates the magnetic stir bar inside the container, thereby stirring the solution. The speed of the stir bar can be controlled by adjusting the speed of the magnetic field generator using the speed control mechanism.

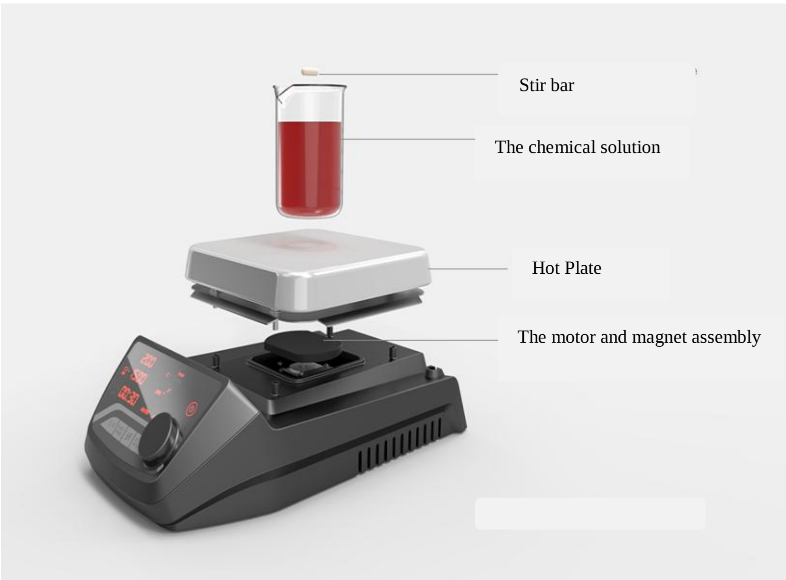

Figure I.6: The components of magnetic stirrer.

A stir bar is a magnetic bar that is used to agitate a mixture or solution. The plastic-coated bar magnet was independently invented in the late 1940s by Edward McLaughlin of the Torpedo Experimental Establishment (TEE) in Greenock, Scotland, who named it the 'flea' because of the way it jumps about if the rotating magnet is driven too rapidly. Stirring bars are typically coated with Teflon or glass, making them chemically inert and preventing contamination or reaction with the system they are submerged in. Their shape may vary to enhance stirring efficiency, and their size ranges from a few millimeters to a few centimeters. The parameters of the stir bar have a more significant effect than the container's geometry, and these parameters have an impact on the vortex flow and are essential for accurate reporting [Mah 20].

I.5 Heating Magnetic Stirrers :

Heating plates are used as a surface support and can be made of aluminum, glass-ceramic, polypropylene, or stainless steel. They typically operate at temperatures ranging from 100 to 750 °C and require power in the range of 120 to 480 volts. Most industrial hot plates can withstand loads of more than 150 pounds . Aluminum hot plates are an economical option that can withstand mechanical shock but should not exceed 400°C for safety reasons [Pau 18]. Ceramic hot plates can endure temperatures of up to 350°C but are susceptible to heat shock from metal cylinders. Polypropylene hot plates cannot reach high temperatures but are resistant to chemicals such as acetonitrile, methanol, and ethanol. Stainless steel hot plates are highly resistant to corrosion, ethers, and most alcohols, making them suitable for use ISO-grade use in clean rooms and USP-compliant facilities.

I.5.1 Induction heating (IH) :

Induction heating (IH) is a highly efficient method for heating conductive materials without the need for physical contact. Due to its numerous benefits over traditional heating methods such as flame heating, resistance heating, and traditional ovens or furnaces, IH is quickly becoming the preferred heating technology across various applications, including industrial[Loz 69] ,[Cho 15] ,[Ame 14], [Ega 12] domestic[Mor 73] , [Luc 15] , [Ace 15] , [Lop 15], and medical applications, [Sta 84] , [Ton 18] , [Hua 12] , [Tai 14] , [Ish 13] , [Ole 84] .

A typical configuration of an IH system in a longitudinal flux setup involves an AC source that supplies an alternating voltage to an IH coil. This coil generates an alternating magnetic field that immerses the induction target, or load. As a result, the induction target is heated through two physical phenomena: eddy currents and magnetic hysteresis, [Luc 14]. Eddy currents resist the magnetic field applied to the induction target and produce heating through the Joule effect, which is the primary heat source in IH processes. Additionally, magnetic hysteresis creates additional heating in ferromagnetic materials. IH systems operate at different frequencies, ranging from line frequency for industrial and high power applications to a few MHz's for medical systems.

.

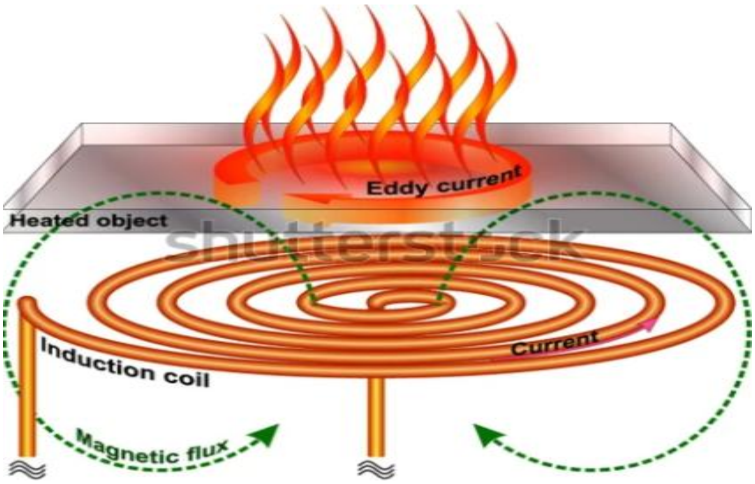

Figure I.7: heating by Induction

I.5.2 Resistance heating :

Resistance heating, also known as heating by electric alloy wire, is a widely used method of heating that involves passing an electric current through a wire made of an alloy with high electrical resistance. The wire heats up, and this heat is transferred to the surrounding area through conduction. This method is used in various heating applications, such as heating elements for ovens, water heaters, and hair dryers. The alloy used in the wire is typically a mixture of nickel, chromium, and iron, which provides high resistance to the electric current and can withstand high temperatures without melting or breaking.

Ohmic heating, also called Joule heating, electrical resistance heating, direct electrical resistance heating, electro heating, or electro conductive heating, that is defined as a process where heat is internally generated due to electrical resistance when electric current is passed through it [Alw 90] , [Kau15]. Ohmic heating involves passing an electrical current through a body to heat it, and the current can be either DC or AC. AC is more commonly used in industrial applications because with DC, the current density and power density are uniform in the cross-section of the body, unless the body has a non-straight shape or varying cross-section. With AC, the distribution of current density and power density is influenced by various factors, including the skin-effect, proximity effect, and eddy currents. These phenomena affect the distribution of the current density and the power density in the work piece and can be taken into account by appropriate design of the heating system.

Resistance heating is considered to be an efficient and safe method of heating, as it allows for precise temperature control and does not produce emissions or pollutants. However, it can be costly to operate resistance heating for extended periods, as the high electrical resistance of the wire can cause it to consume a significant amount of energy.

I.6 Applications of magnetic stirrer :

Magnetic stirrers are commonly used in chemistry and biology laboratories to mix solutions or suspensions. Some advantages of using a magnetic stirrer include:

- **Efficient mixing :** Magnetic stirrers can rapidly and efficiently mix solutions or suspensions by using a rotating magnetic field to move a stir bar within a container .and the magnetic one is also critical for reproducible mixing or mixing over long time scale. For example, protein dialysis requires multi hour or overnight sample mixing and is sensitive to bacterial contamination[Sør 03].
- ❖ **Consistent stirring :** The speed and direction of the stir bar movement can be easily controlled, ensuring consistent and uniform mixing.
- ❖ **Reduced contamination risk :** Since the magnetic stir bar is not in direct contact with the solution, the risk of contamination is reduced compared to other mixing methods such as manual stirring with a glass rod.
- ❖ **Hands-free operation :** Once the stir bar is in place and the speed and direction of the magnetic field are set, the magnetic stirrer can operate continuously without the need for manual intervention, allowing scientists to focus on other tasks.
- ❖ **Wide range of applications :** Magnetic stirrers can be used with a variety of containers, from small test tubes to large beakers or flasks, making them versatile and useful in a range of laboratory applications .

for example, In the pharmaceutical industry Magnetic stirrers are used extensively in drug development and manufacturing to mix chemicals and active ingredients. This is an important step in creating new drugs and improving existing ones, In medical research: Magnetic stirrers are used to mix samples in medical research, including blood, urine, and other bodily fluids. This enables researchers to study the effects of different compounds and chemicals on human health, In food science Magnetic stirrers are used to mix food ingredients and flavors in the food industry, allowing for more efficient and consistent mixing. They are also used in research and development to create new food products, In environmental research Magnetic stirrers are used to mix environmental samples, such as soil and water, to study the effects of pollution and other environmental factors on ecosystems and human health.

I.7 Plasma technology :

It is a commonly accepted fact that 99% of the visible matter in the universe exists in a plasma state [che 95],[Ale 08],[Neh 08]. such as in stars and interstellar matter. While lightning and flames are also examples of naturally occurring plasma, humans have developed plasma technology and use it in various fields including surface modifications, environmental remediation, biotechnology, and medicine. Though high-temperature plasmas used for controlling and harvesting energy from nuclear fusion processes are often associated with plasma technology, plasma technologies have widespread and ubiquitous applications in everyday life. For example, one-third of the steps involved in manufacturing microelectronic circuits and processors are plasma-based. and fluorescent lighting tubes and energy-saving bulbs rely heavily on plasma processes. Plasma surface modification processes enhance the properties and functionalities of materials, such as preparing plastics for printing and improving optical properties of reading glasses. Plasma can also decompose chemical pollutants and harmful microorganisms in air and water, and the generation of ozone as a disinfecting agent is one of the oldest commercially viable applications of plasma technology, [Wel 18].

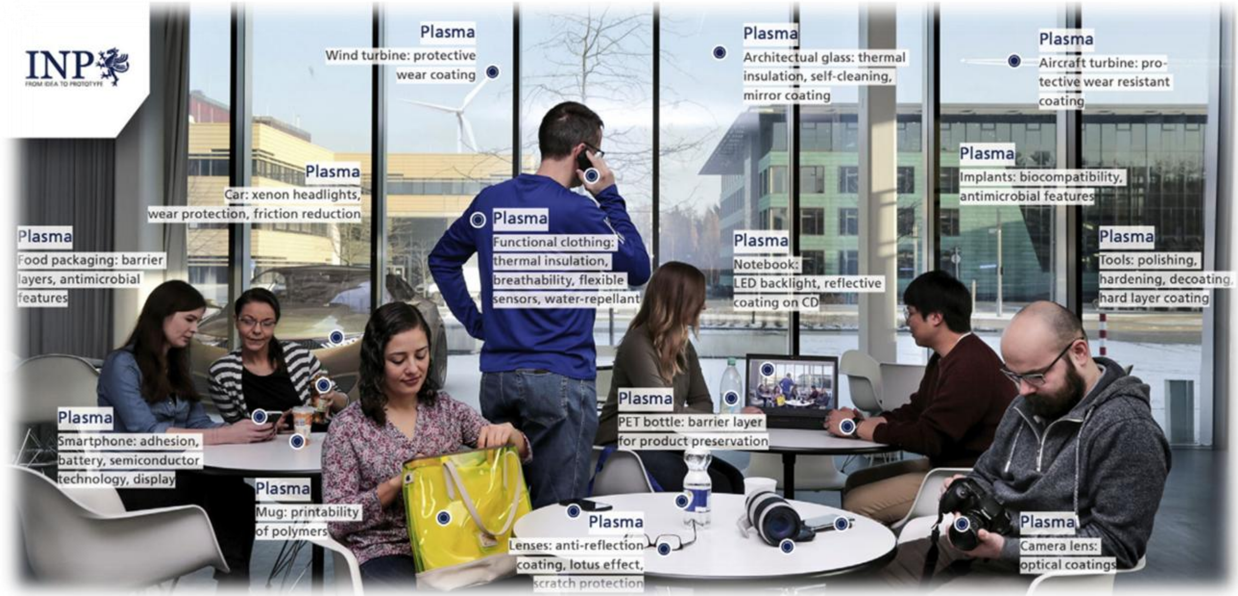

Figure I.8: The Crucial Role of Plasma Technologies in Modern Manufacturing Processes , [Wel 18].

I.7.1 Definition of plasma :

Primarily, a plasma refers to an ionized gas, formed when a gas is heated to a point where atoms collide and lose their electrons, creating electric and magnetic fields that result in unique properties. The transition from a weakly ionized gas to a plasma is a matter of nomenclature. This state of matter was named 'plasma' in 1928 by Irving Langmuir , [Šim 19], [Pau 08] , [Bel 19] , [Tho 62], a Nobel laureate who pioneered the scientific study of ionized gases. Langmuir chose this name due to its meaning in Greek, лλαoμα means 'moldable substance' or 'jelly', which accurately describes the behavior of mercury arc plasmas. These plasmas tend to diffuse throughout their glass vacuum chambers, filling them like jelly in a mold. The properties of plasmas give rise to a range of phenomena that are complex, useful, and sometimes even beautiful.

Plasma states are divided into natural and artificial states ,These states vary depending on the conditions and properties of the plasma.

I.7.2 Plasma in the nature and space :

Plasma is abundant in the universe, and can be found in various natural phenomena such as the solar corona, solar wind, nebula, lightning, and Earth's ionosphere. At an altitude of approximately 100 km, the atmosphere becomes conductive due to ionization by solar radiation, and the Earth's magnetic field interacts with charged particles from the sun, which can be seen as the aurora borealis. Natural and man-made plasmas can occur under different conditions of pressure, temperature, and electron density. The interior of stars and their atmospheres are hot enough to be in the plasma state, and plasma theories have been used to explain various phenomena in astrophysics, such as the acceleration of cosmic rays, the development of galaxies, and the sources of radiation in the universe. The Crab nebula, for example, contains a magnetic field and a visual pulsar, which are believed to be rapidly rotating neutron stars with plasmas see figure 2 , [Pau 08] , [Ale 08.]

Figure I.9: cosmic phenomena

I.7.3 Plasma in the laboratory :

Man-made plasmas, also known as artificial plasmas, are generated in gas discharges through the application of electric or magnetic fields. The study of these plasmas is a crucial area of research, as scientists strive to comprehend their behavior and develop new applications for them. As our knowledge of plasmas increases, we can expect to see even more innovative uses for man-made plasmas in the future.

These plasmas can have a broad temperature range, varying from slightly above room temperature to temperatures resembling those found in the interior of stars. While the electron density can span over 15 orders of magnitude, for practical applications, the electron temperature is typically between 1- 20 eV, with electron densities ranging from 10^6 - $10^{18} cm^{-3}$ [Ale 08].

Man-made plasmas are employed in numerous applications, including plasma processing, plasma medicine, plasma propulsion, and plasma displays. They are widely used in industrial processes, such as plasma cutting, welding, and etching, as well as in research settings, including laboratory experiments.

I.7.4 Plasma temperature :

Plasma is a state of matter in which some or all of the particles are ionized, meaning they have lost or gained electrons, resulting in a collection of positively and negatively charged particles. The diverse array of particles in plasma includes neutral atoms and molecules, charged particles such as electrons and ions, metastable particles like excited atoms and molecules, radicals, and photons [Pau 08].

Plasma temperatures can be determined by the average energies of the particles and their relevant degrees of freedom. In thermal plasmas, which are in local thermodynamic equilibrium, there is a single temperature at each point of space, and ionization and chemical processes are determined by temperature. Non-thermal plasmas, on the other hand, are far from thermodynamic equilibrium and exhibit multiple different temperatures related to different particles and degrees of freedom. In non-thermal plasmas, the electron temperature is often significantly higher than that of heavy particles, and ionization and chemical processes are directly determined by electron temperature [Ale 08].

So we can say Plasma can be divided into two types based on particle temperature: thermal or equilibrium plasma, and non-thermal or non-equilibrium plasma. Thermal plasma is characterized by an almost fully ionized gas and a high temperature of at least 15,000 K [Šim 19] .

This type of plasma is typically found in stars and in some industrial processes, such as plasma cutting and welding. Non-thermal or cold plasma, on the other hand, is a partially ionized gas with a temperature that is generally close to room temperature, with a maximum of 340 K. This type of plasma has numerous applications in fields such as medicine, agriculture, and environmental remediation.

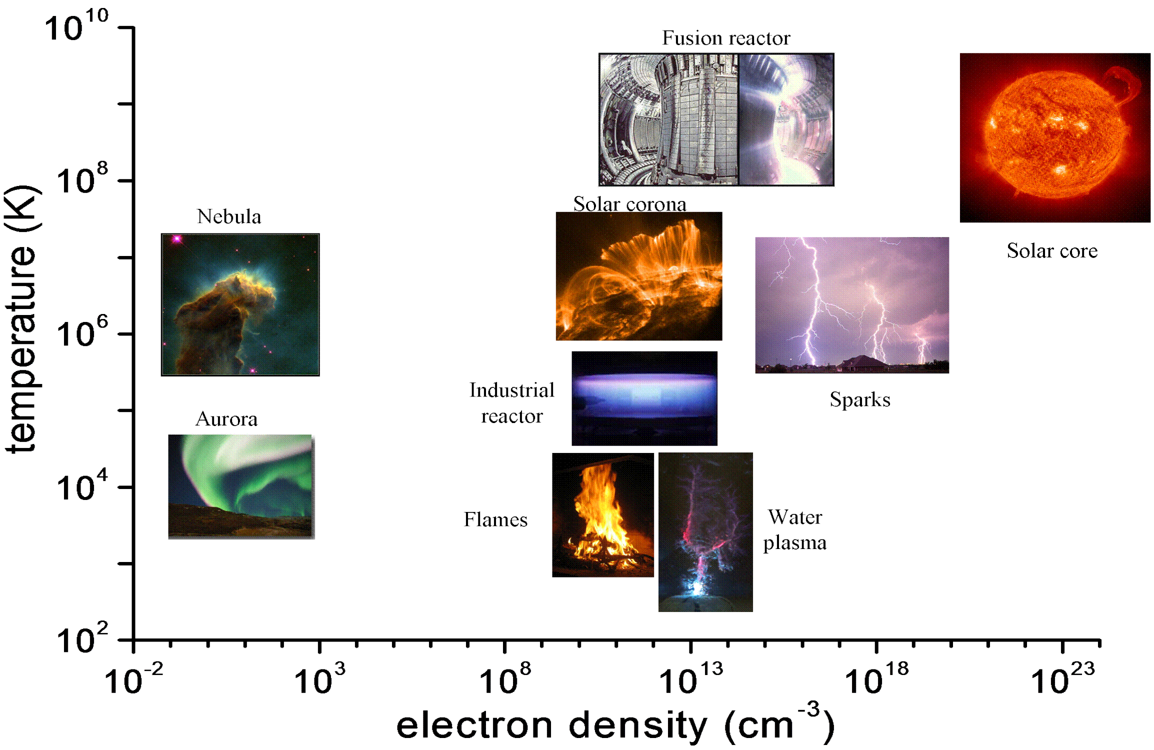

Figure I.10: Order of magnitude of temperatures and densities of some plasmas. The logarithmic scales show the extent of the range of parameters found in nature and in laboratory plasmas.

I.7.5 Atmospheric non-thermal plasmas :

In the past twenty years, there has been significant interest in Atmospheric Non-Thermal Plasmas (ANTPs) due to their breakthroughs in various scientific fields. The industrial applications of ANTPs are rapidly growing, making them a hot topic in the scientific community. ANTPs can be generated using various electrical discharges such as corona discharges, Dielectric Barrier Discharges (DBD), Atmospheric Pressure Plasma Jets (APPJ), and Micro Hollow Cathode Discharges (MHCD), each with its unique properties and applications.

❖ Corona discharge :

A corona discharge occurs when a high voltage electrode emits a current into a neutral fluid, usually air, by ionizing the fluid to create a plasma region around the electrode. The generated ions then pass the charge to nearby areas of lower potential, or recombine to form neutral gas molecules. The electric field strength near a charged object's sharp point can become so high that air near the electrode becomes conductive, increasing the apparent size of the conductor. The charged particles outside the conductive region slowly find their way to an oppositely charged object and become neutralized. The first method used to generate ANTP was through corona discharge [Neh 08].which exists in different forms depending on the polarity of the field and electrode geometrical configuration. Corona discharge is a non-uniform discharge that develops in the high field region near the sharp electrode, spreading towards the planar electrode, and can be found in inhomogeneous electrode arrangements powered by a continuous or pulsed DC voltage.

Figure (9)shows a schematic a model of point-to-plane corona. A positive corona occurs when the electrode with the strongest curvature is connected to the positive output of the power supply, while a negative corona occurs when this electrode is connected to the negative terminal of the power supply [Fri 05].

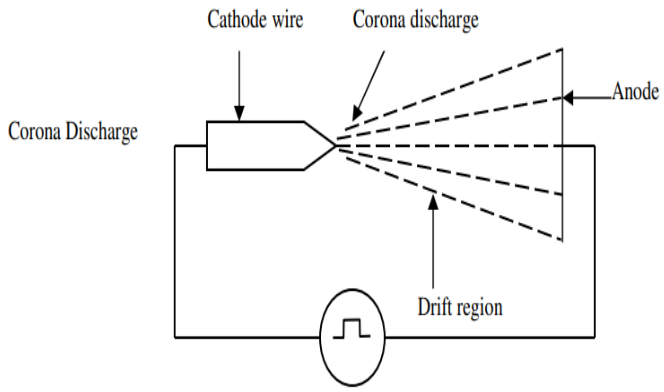

Figure I.11: Schematic of corona discharge [Neh 08].

Corona discharge is primarily used in electrostatic precipitators (ESP) for dust collection in many industrial off gases . It is also used in water purification, electrophotography, copying machines, printers, liquid spray guns, and powder coating.

static control in semiconductor manufacture, and atmospheric pressure ionization-mass spectrometry.

For the corona-induced plasma reactor applications, con trol of NO,, SO,, CO,, toxic gases, volatile organic compounds, hazardous emissions[Cha 91].

Some applications of coronas include the activation of polymer surfaces and the enhancement of SiO growth during the thermal oxidation of silicon wafers (Sch,98)

Chemical synthesis Many chemical products can be synthetized by corona discharges, but ozone is so far the only one of industrial importance. It is used for the treatment of water, preserving its natural taste and avoiding the smell of chlorine, and for other applications utilizing its large oxidation power. for instance in textile and paper industries. The streamer type coronas used for ozone generation generally use air or oxygen[Gol 85] .

I.8 Internet of things :

In 2011, made a bold prediction that by 2020, 50 billion things would be connected to the Internet [Eva 11] , with the aim of facilitating autonomous intelligent decision-making [Gar 14].Regardless of which prediction is accurate, it is clear that smart devices will far outnumber the estimated world population.

The IoT is rapidly expanding across all sectors, creating new opportunities and becoming a key competitive weapon in industries worldwide, as primary benefits shift from internal to external improvements [Gar 16]. Various sectors are benefiting from the IoT, including transportation, smart cities, smart homes, healthcare, e-governance, assisted living, e-education, retail, logistics, agriculture, automation, industrial manufacturing, and process management, among others[Gub 13][Mio 12][Sil 18].

The IoT has many different definitions, but some popular ones include:

"A dynamic global network infrastructure with self-configuring capabilities based on standard and interoperable communication protocols, where physical and virtual 'things' have identities, physical attributes, and virtual personalities and use intelligent interfaces, and are seamlessly integrated into the information network" [Van 08] [Ars 14].

"Things having identities and virtual personalities operating in smart spaces using intelligent interfaces to connect and communicate within social, environmental, and user contexts" (INF, 08).

The "Internet of Things" (IoT) typically refers to devices with unique identities that can perform remote sensing, actuating, and monitoring functions. These devices can communicate with other devices and applications, collect and process data locally or send it to centralized servers or cloud-based applications. IoT devices have various interfaces for connections to other devices, including sensors, internet connectivity, memory and storage, and audio/video interfaces. These devices can collect data from attached sensors, such as temperature or humidity, and communicate that data to other devices or cloud-based storage. IoT devices can also interact with physical entities in their vicinity through actuators, such as turning appliances on/off. There are many types of IoT devices, including wearable sensors, smart watches, LED lights, automobiles, and industrial machines. Sensor data generated by IoT devices can be processed by data analytics systems to guide further actions locally or remotely.

Figure I.12: Internet of Things devices.

I.8.1 IOT protocols :

The protocols used in IoT can be classified into four layers: Link layer, Network/Internet layer, Transport layer, and Application layer [Ars 14].

- ✓ The Link layer protocols determine how data is physically sent over the network's physical medium, such as copper wire, coaxial cable, or a radio wave. Hosts on the same link exchange data packets over the link layer using link layer protocols, which encode and signal the packets by the hardware device over the medium to which the host is attached.

- ✓ The Network/Internet layer protocols are responsible for sending IP datagrams from the source network to the destination network. This layer performs host addressing and packet routing, with datagrams containing the source and destination addresses used to route them across multiple networks.

- ✓ The Transport layer protocols provide end-to-end message transfer capability independent of the underlying network. The transport layer can be set up on connections, either using handshakes (as in TCP) or without handshakes/acknowledgements (as in UDP). The transport layer provides functions such as error control, segmentation, flow control, and congestion control.

- ✓ The Application layer protocols define how applications interface with lower layer protocols to send data over the network. The application data is typically in files, encoded by the application layer protocol and encapsulated in the transport layer protocol, which provides connection or transaction-oriented communication over the network. Port numbers are used for application addressing, enabling process-to-process connections using ports.

I.8.2 Benefits of IoT in Laboratory Science :

The Internet of Things (IoT) has revolutionized the way we interact with technology, and its impact is evident in many industries, including laboratory science. IoT devices in laboratory settings provide an efficient and cost-effective way to monitor, control, and analyze data in real-time.

IoT devices in the laboratory can be used for a wide range of applications, such as environmental monitoring, equipment maintenance, and experiment control. For instance, IoT sensors can be used to monitor temperature, humidity, and air quality, providing real-time data that enables scientists to make informed decisions about their experiments.

Additionally, IoT devices can be used to automate laboratory processes, reducing the time and effort required for data collection and analysis. For example, an IoT-enabled instrument can automatically adjust its settings based on real-time data, ensuring consistent and accurate results.

IoT technology can also enhance the safety of laboratory personnel. IoT sensors can detect hazardous conditions and send alerts to laboratory personnel, preventing accidents before they occur. Moreover, IoT devices can be used to monitor the status of equipment and send alerts when maintenance is required, minimizing the risk of equipment failure.

Overall, the integration of IoT devices in laboratory science has numerous benefits, including enhanced accuracy, reliability, and safety. As the technology continues to evolve, it is likely that IoT devices will become even more prevalent in laboratory settings, providing scientists with new and innovative ways to conduct their research.

(a)

(b) (C) (d)

Figure I.13: a) identification of unknowns, verification of raw materials, quality control

b)air quality monitoring**. c)** security camera. **d)** Lab Unit for applications with plasma water.

I.9 Conclusion :

In conclusion, this chapter provides an overview of magnetic stirrers and their different types and applications in laboratory science, as well as the concept of plasma technology and its various applications . The chapter also touches on the topic of IoT devices and their growing importance in laboratory settings

Regarding magnetic stirrers, we can expect continued advancements in their design and functionality. With the increasing demand for automation and precision in laboratory processes, magnetic stirrers are likely to incorporate more advanced features such as programmable timers, temperature control, and compatibility with digital interfaces for data monitoring and analysis. Additionally, there may be developments in miniaturized magnetic stirrers for portable and field applications.

As for plasma technology, its future holds promising prospects across various industries. In space research, plasma propulsion systems can revolutionize space travel by providing efficient and high-speed propulsion methods. In industrial processing, advancements in plasma technology may lead to more energy-efficient and environmentally friendly manufacturing processes. In the medical field, plasma-based treatments such as plasma medicine and plasma sterilization techniques are expected to gain further recognition and adoption.

Looking ahead, the Internet of Things (IoT) is poised to play a crucial role in both magnetic stirrers and plasma technology. Integration of IoT devices with magnetic stirrers can enable remote monitoring, control, and optimization of stirring parameters, enhancing efficiency and allowing for real-time data analysis. Similarly, IoT-enabled plasma systems can facilitate remote operation, diagnostics, and data collection, leading to improved process control and productivity.

In conclusion, the future of magnetic stirrers, plasma technology, and their integration with IoT holds great potential for advancements in laboratory science, industrial applications, and medical treatments. Continued research and innovation in these areas will undoubtedly contribute to further progress and improvements in these technologies.

Chapter II: Identification parameters and Control of DC motor

II.1 Introduction :

Electric mixers are widely used in various industrial and laboratory applications for the purpose of stirring and mixing liquids.

The motors used in these mixers play a crucial role in providing the necessary rotational power to drive the stirring mechanism.

In this chapter, we will explore the different types of motors used in stirrers and focus specifically on DC motors in electromagnetic mixers[SiM 09], [Ori 16].

Furthermore, we will delve into the characteristics of permanent magnet DC motors and discuss various control techniques employed for DC motors[San 17], [Lab 21].

Additionally, we will examine the electronic converters used for DC motor control and the identification of parameters specific to DC motors[Tor 18].

Finally, motor simulation and results(MATLAB) will be presented to illustrate the practical implementation and effectiveness of the discussed concepts.

II.2 Types of Motors used in Stirrer :

The types of electric motors found in electric mixers vary. Here are some examples of these motor types :

- DC motors.
- AC motors.

II.2.1 DC motors :

The DC motor is an electromechanical energy converter. It allows the transformation of DC electrical energy into mechanical energy to drive a load in motion[SiM 09].

These motors are widely used in many applications, including robotics, automation, and electric vehicles.

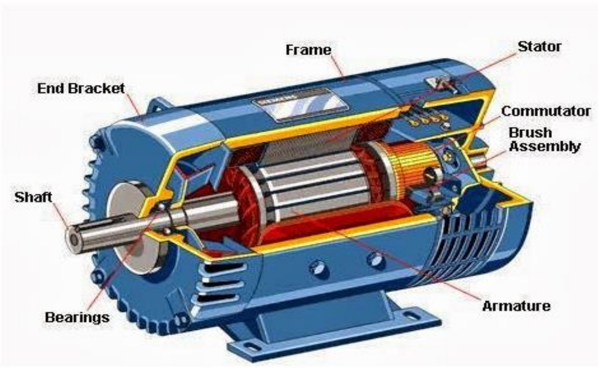

Figure II.1: Construction of DC Motor.

The DC motor consists of two main parts :

- ❖ inductor (stator).
- ❖ induced (rotor).

➢ inductor (stator) :

The stator produces the magnetic field (excitation field) from the winding supplied by direct current or by permanent magnets glued inside the stator. The flow is oriented from the north pole to the south pole.

The multipolar excitatory coils are connected so that adjacent poles have opposite magnetic polarities[Gér 12].

Figure II.2: stator of DC Motor.

➢ armature (rotor) :

It is formed by a stack of magnetic sheets and is subjected to torque and rotated in the inductor field[Gér 12].

Figure II. 3: rotor of DC Motor.

II.2.2 AC motors :

An AC motor is an electric machine that converts alternating current electrical energy into mechanical energy in the form of rotary motion. This is accomplished through the interaction of the magnetic fields of the stator and rotor, which induce a rotating magnetic field. AC motors are the most widely used type of electric motor due to their efficiency, reliability, and ease of use. They are found in a wide range of applications, from industrial machinery to household appliances [Ori 16].

Figure II.4: AC Motor.

Below are some examples of AC motors:

- **Synchronous motor :**

The synchronous motor is an alternating current machine The rotational speed of the rotor is constant and proportional to the frequency of the voltage of the electrical current to which it is connected. This speed is known as the "synchronous speed"[Ori 16].

The rotor can be of two types:

- Permanent magnet synchronous motor.
- Wound rotor synchronous motor, where the magnets are replaced by electromagnets.

Figure II. 5: AC Synchronous motor.

- **motor (Asynchronous) :**

The asynchronous motor is characterized by the fact that the rotational speed of the rotor is lower than the speed at which the rotating magnetic field caused by the electric current flowing in the stator coil rotates[Ori 16].

we find two types of motor: asynchronous motor with wound rotor and squirrel cage.

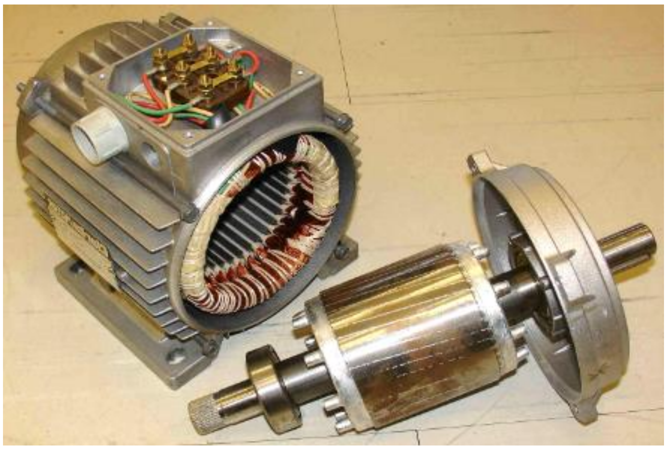

Figure II. 6: AC Induction motor.

II.3 DC Motor in Magnetic Stirrers :

II.3.1 Brush motor :

A DC motor is composed of a stationary stator consisting of two permanent magnets, and a rotor wound with coils and mounted on bearings, allowing it to rotate freely. The rotor is made up of a crossbar that is wound with wire to create a coil, but with the direction of winding changed from one side of the crossbar to the other. According to Ampere's Law, the current passing through each set of windings generates a magnetic flux distribution, resulting in the creation of a pair of electromagnets. Due to the wire being wound in opposite directions on each side, the electromagnets have opposite polarities [Gam 10].

Figure II.7: Examples of Standard brush DC motor.

II.3.2 Brushless motors :

The brushless motors used in mixers provide more power, speed, and longer run times than conventional brushed motors of the same size. The superior power and efficiency of the brushless motor makes it the ideal choice for high performance electromagnetic mixers.

Figure II.8: Brushless motor.

Brushless motors utilize coils and magnets to generate rotational force, similar to traditional DC motors. However, unlike traditional DC motors, brushless motors do not have a commutator brush that switches the direction of current flow in the coils. This absence of a brush is what characterizes them as "brushless". Instead of a commutator brush, brushless motors incorporate three stationary coils that are affixed to the motor's stator. The rotor of a brushless motor consists of a cylinder with a series of magnets attached to its outer circumference that rotates around the stator. Since the coils are stationary, wires can be directly attached to them, eliminating the need for a brush [Rah 16].

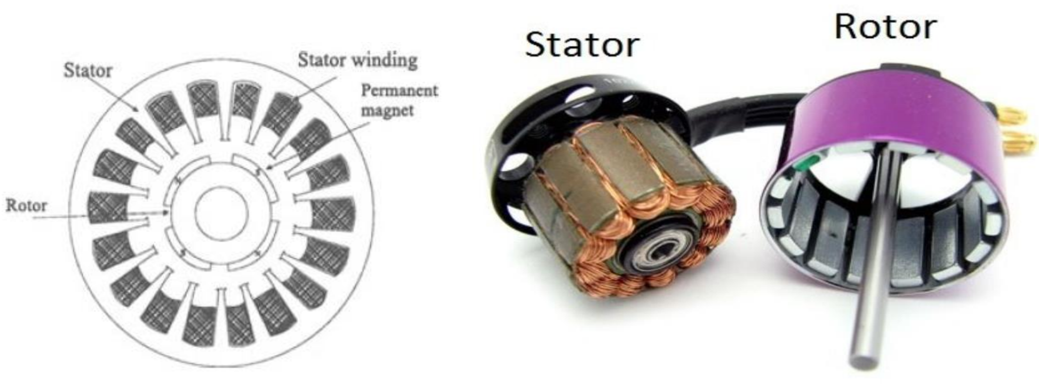

Figure II.9: Stator and rotor of brushless motor.

II.4 Model of DC Motor :

- ### Permanent magnet DC motor :

To better understand the concept of the brushed DC motor, let's look at a more realistic example. The basic structure of a brushed DC motor was introduced in the previous section on the Lorentz force, we can see a typical rotor and mechanical commutation mechanism for a brushed DC motor [Tor 18].

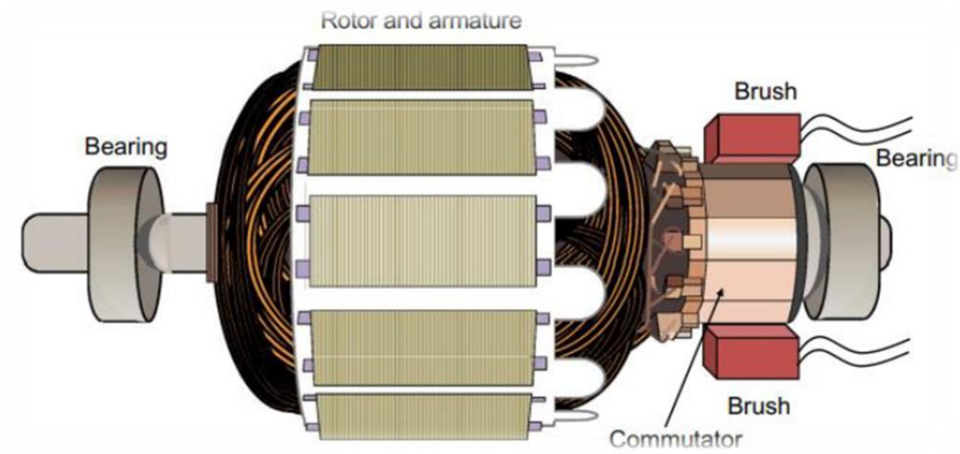

Figure II.10: The components of a brushed DC motor include the rotor, distributed windings, commutator, brushes, and stator.

The rotor of a brushed DC motor is made up of distributed windings and is constructed using thin, insulated slices of highly permeable ferromagnetic material, usually electrical steel. These insulated plates increase the resistance of the material in the perpendicular direction to the magnetic field, thereby reducing eddy-current losses. The windings are wrapped around the teeth that are cut axially into the rotor material. These windings can be either concentrated, wound around a single tooth, or distributed, wound across multiple teeth.

Electric current is supplied to these windings by brushes that come into contact with the commutator. The commutator is made up of radially insulated conductive segments that are connected to the corresponding windings. As the rotor rotates, the brushes maintain contact with the commutator, which helps to ensure that the current is always flowing in the correct direction through the windings.

The design of the commutator and the distribution of the windings on the rotor will affect the motor's performance characteristics, such as torque and speed. By controlling the current flowing through the windings, it is possible to control the speed and direction of the motor.

Overall, brushed DC motors are simple and efficient devices that are widely used in a variety of applications, including electric vehicles, industrial machinery, and robotics [Tor 18].

II.5 Different control techniques for DC Motor :

In this study, this type of engine was used

II.5.1 MCC with constant excitation :

the MCC model is the simplest and the equivalent electrical diagram of this model can be presented in figure (11) below [Lab 21], [Rac 11], [San17].

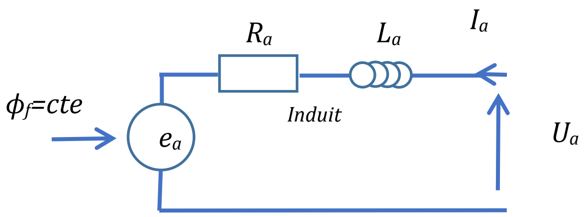

Figure II.11: Equivalent circuit diagram of MCC with constant excitation.

The equation of the counter-electromotive force is always written

$$e_a = \omega . K . \phi_f \; et \; K . \phi_f = cte = \; K' \; alors \;\; e_a = K' . \omega \tag{II.1}$$

In transient state the electrical model

$$U_a = R_a . I_a + \frac{d\phi_a}{dt} + e_a \tag{II.2}$$

The flow equation

$$\phi_a = L_a . I_a \tag{II.3}$$

By replacing the flux equation and the FCEM equation in the electrical model, we therefore find

$$U_a = R_a . I_a + L_a \frac{dI_a}{dt} + \omega . K' \tag{II.4}$$

And the mechanical model is written

$$C_e = K . \phi_f . I_a \;\; et \;\; K . \phi_f = cte = \; K' \;\; \Rightarrow C_e = K' . I_a \tag{II.5}$$

$$J \frac{d}{dt}(\omega_m) = C_e - C_r - F\omega \tag{II.6}$$

II.5.2 Transient Response Characteristic of MCC :

We studied the steady-state characteristics of MCCs, which demonstrate speed control by armature voltage or field flux and mechanical characteristics. The steady-state characteristic shows what the final speed is, while the transient response shows how to reach the final speed. The transient response characteristic is critical for high-performance motor drives, even though all three responses reach the same final speed, their response times and displacement trajectories to reach the final speed differ. Although an oscillatory or slow response may eventually reach the speed command, it has no practical usefulness[Lab 21], [Rac 11]. Therefore, we must consider both the transient and steady-state characteristics for high-performance motor drives.

Now, we will examine the transient response of achieving the final speed by the applied armature voltage for a DC motor. One simple way to examine the transient response is to use the system's transfer function [Lab 21], [Rac 11].

We can obtain the transfer function for the DC motor drive system by taking the Laplace transform of the differential equations as follows:

By equation (5)

$$U_a = R_a . I_a + L_a \frac{dI_a}{dt} + \omega . K' \Rightarrow U_a = I_a(R_a + L_a . s) + \omega . K' \quad \textbf{(II.7)}$$

And by equation (6)

$$J \frac{d}{dt}(\omega_m) = C_e - C_r - F\omega_m \Rightarrow C_e = \omega_m(s.J + F) - C_r = K'.I_a \quad \textbf{(II.8)}$$

So through the Laplace operator and Equations (7)and (8)can be represented by the closed loop block diagram as shown in Figure (12).

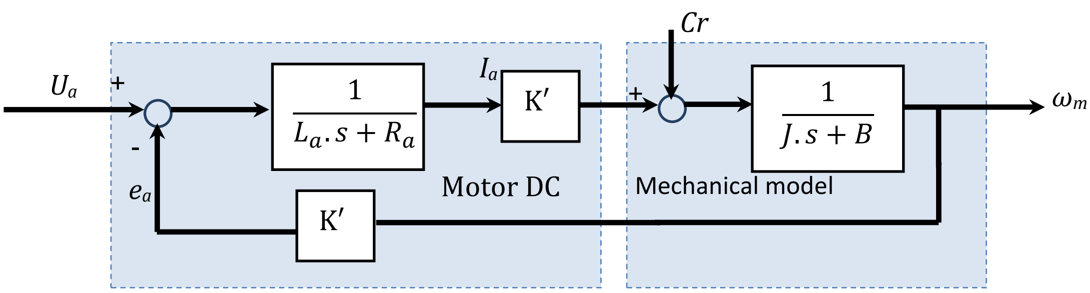

Figure II.12: Constant Flux MCC Block Diagram.

From the block diagram in Fig12, the transfer function of the input armature voltage U_a and the output by the angular velocity $\boldsymbol{\omega_m}$ is given by:

$$\frac{\omega_m}{U_a} = \frac{\frac{1}{L_a.s + R_a}.K'.\frac{1}{J.s + B}}{1 + \left(\frac{1}{L_a.s + R_a}.K'.\frac{1}{J.s + B}.K'\right)} \quad \textbf{(II.9)}$$

$$\frac{\omega_m}{U_a} = \frac{\frac{K'}{J.L_a}}{s^2 + \left(\frac{R_a}{L_a} + \frac{B}{J}\right).s + \left(\frac{R_a}{L_a}.\frac{B}{J} + \frac{K'^2}{J.L_a}.\right)} \quad \textbf{(II.10)}$$

The transfer function is a second-order system comprising two poles, which are critical factors in determining the transient response of the system. Based on the locations of the two poles in equation (10), we can predict the transient response of speed to the applied armature voltage. Therefore, the transient response heavily depends on system parameters such as motor parameters R_a and L_a and mechanical parameters J and B, as shown below[Lab 21], [Rac 11].

Assuming B=0 in Eq. (10) to easily analyze the system, one can obtain a simplified transfer function as:

$$\frac{\omega_m}{U_a} = \frac{\frac{K'}{J.L_a}}{s^2 + \left(\frac{R_a}{L_a}\right).s + \left(\frac{K'^2}{J.L_a}.\right)} = \frac{\frac{1}{K'}\left(\frac{R_a}{L_a}.\frac{K'^2}{J.R_a}\right)}{s^2 + \left(\frac{R_a}{L_a}\right).s + \left(\frac{R_a}{L_a}.\frac{K'^2}{J.R_a}\right)} \quad \textbf{(II.11)}$$

By using the electromechanical time constant Tm = J.Ra/k2 and the electrical time constant Ta = La/Ra, Equation (11) can be rewritten as:

$$\frac{\omega_m}{U_a} = \frac{\frac{1}{K'}\left(\frac{1}{T_m.T_a}\right)}{s^2 + \left(\frac{1}{T_a}\right).s + \left(\frac{1}{T_m.T_a}\right)} \quad \textbf{(II.12)}$$

The poles can be obtained from the roots of the denominator (also called the characteristic equation) of equation (12) :

$$s_{1,2} = -\frac{1}{2.T_a} \mp \frac{1}{T_a}\sqrt{\frac{1}{4} - \frac{1}{T_a}} \quad \textbf{(II.13)}$$

We can also find the response characteristic from the damping ratio for this second-order system. To do this, we compare this equation with the following prototype of the second-order system.

$$G(s) = \frac{{\omega_n}^2}{s^2 + 2.\zeta.\omega_n.s + {\omega_n}^2} \quad \textbf{(II.14)}$$

The equation (14) provides the expressions for the undamped natural frequency ω_n and the damping rate ζ of the DC motor drive system.

$$\omega_n = \frac{1}{\sqrt{T_m.T_a}} = \frac{k}{\sqrt{J.L_a}} \quad \textbf{(II.15)}$$

$$\zeta = \frac{1}{2}\sqrt{\frac{T_m}{T_a}} = \frac{1}{2}\frac{R_a}{k}\sqrt{\frac{J}{L_a}} \quad \textbf{(II.16)}$$

Normally, small motors have Tm>4.Ta(ζ>1), while servo motors or large power motors have Tm<4.Ta(ζ <1), resulting in oscillatory response. Even though the system response is inherently oscillatory, we can achieve the desired response by adopting an adequate controller.

Depreciation rate	Response Status	Graphic presentation
ζ <1	underdamping	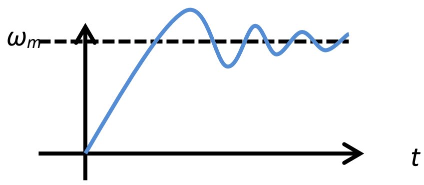
ζ =1	Critical damping	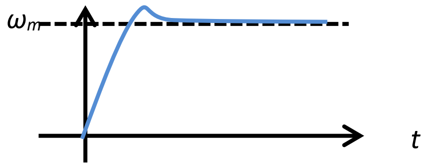
ζ>1	over-amortization	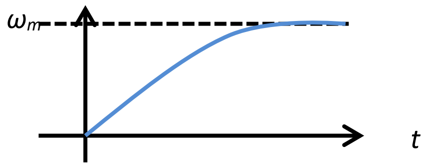

Table II.1: In the following table we summarize the different response depends and the damping rate ζ.

II.5.3 Control of the RL circuit in closed loop :

Closed-loop control is a control technique that adjusts the control input Us based on the feedback of the output Y(s). In motor drive systems, closed-loop control is commonly used to regulate the position, speed, current, or flux of the motor.
The performance of the closed-loop control system relies heavily on the controller Gc(s), which adjusts the control input U(s) to minimize the error between the output and the desired reference. Therefore, selecting the appropriate feedback controller for the motor drive system is crucial to achieve optimal performance[San 17],[Fra 06].

In our application of the RL circuit, the closed-loop control relies on measuring the output vectors, specifically the electrical current. We assume that the ideal electronic converter provides us with **U*=U**, and our system incorporates a feedback loop that includes a current sensor and regulation through a PI controller. [San 17],[Fra 06] , [Lab 21].

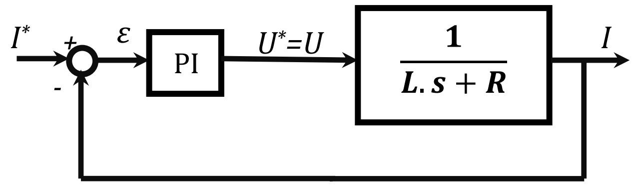

Figure II.13: Block diagram of current regulation1.

The control law is:

$$u(t) = k_p \varepsilon(t) + k_i \int \varepsilon(t) \quad \textbf{(II.17)}$$

- If k_(p) is large, the correction is fast. The risk of overshoot and oscillation in the output increases

- If k_(p) is small, the correction is slow, there is less risk of oscillations.

The integral action reacts slowly to the variation of the error and ensures progressive catching up of the set point.

As long as the positive (or negative) error remains, the action u(t) increases (or decreases) until the error is canceled[Lab 21].

To calculate the parameter of the PI regulator (Ki and Kp) it is necessary to study the stability of the system according to the following block diagram :

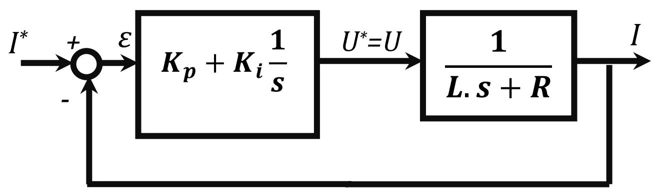

Figure II.14 : Block diagram of current regulation2.

The speed regulation of all types of rotating machinery is based on a unified model. By utilizing the Laplace transformation of the mechanical model, we obtain a Linear Time-Invariant System (L.S.I).

Therefore, the block diagram and transfer function of this circuit can be represented as follows :

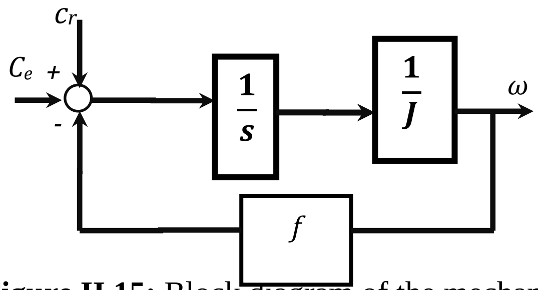

Figure II.15: Block diagram of the mechanical mode l.

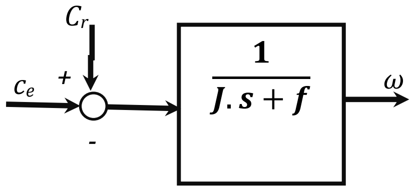

Figure II.16: Block diagram of the mechanical mode2.

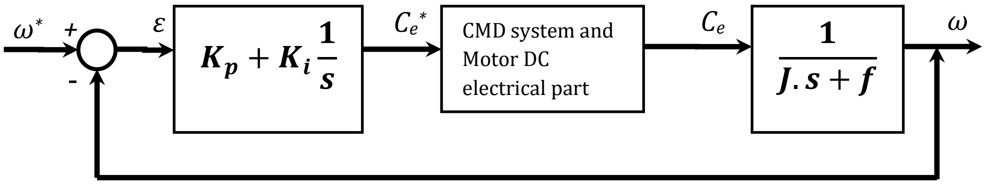

Figure II.17: Speed control block diagram.

To calculate the parameters of the PI controller (Ki and Kp), it is necessary to analyze the stability of the system using the following block diagram.

The open-loop transfer function with zero load torque is given by:

$$F(s)_{\text{ouvert}} = \frac{\omega}{\omega^*} = \frac{k_p s + k_i}{s(Js + f)} \quad \textbf{(II.18)}$$

The closed loop transfer function is written:

$$F(s)_{\text{closed}} = \frac{k_{p3} s + k_{i3}}{Js^2 + \left(k_{p3} + f\right)s + k_{i3}} \quad \textbf{(II.19)}$$

This transfer function has a 2^{nd} order dynamics, whose canonical form

$$F(s)_{\text{canonical}} = \frac{1}{\frac{1}{\omega_n^2} s^2 + \frac{2\xi}{\omega_n} + 1} \quad \textbf{(II.20)}$$

By comparison, we then get

$$\frac{J}{k_{i3}} = \frac{1}{\omega_n^2} \quad \textbf{(II.21)}$$

$$\frac{2\xi}{\omega_n} = \frac{k_{p3} + f}{k_{i3}} \quad \textbf{(II.22)}$$

II.5.4 Control System Configuration :

The configuration of controllers in motor drive systems typically involves a cascade connection of controllers for position, speed, and current control. The current controller is placed at the innermost loop and has the widest bandwidth. since speed and position can be controlled through current control, the response time of the current control should be the fastest among the three. Similarly, the response time of the inner loop control should be faster than that of the outer loop to improve the response performance and stability of the outer control loop. For instance, the bandwidth of the current loop should be at least five times wider than that of the speed loop to ensure that the current control does not affect the speed control performance[San 17].

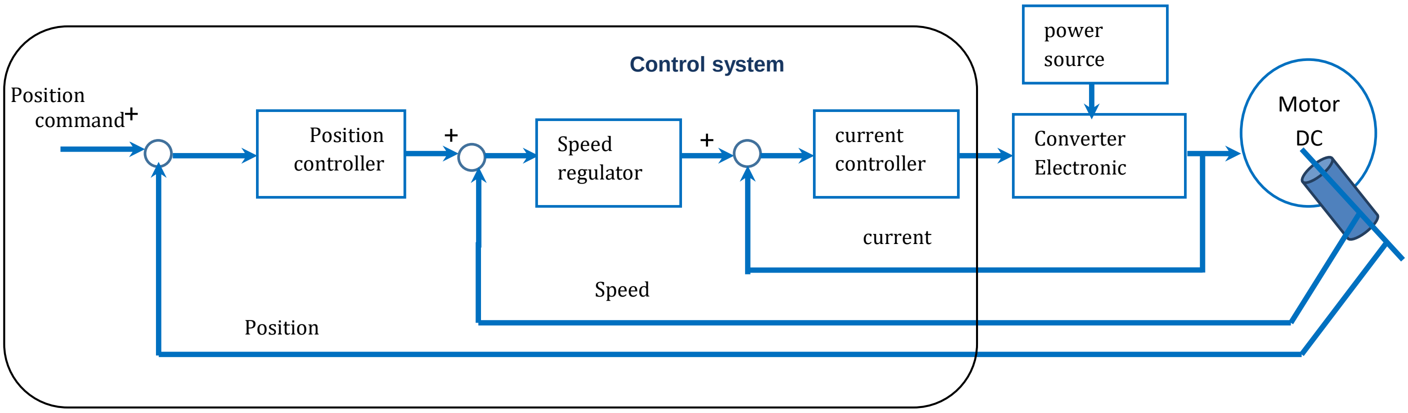

Figure II.18: Configuration of the motor control system [Lab 21].

II.5.5 Motor DC current regulation :

➢ Motor DC current control loop :

The PI controller is most commonly used in DC motor drive systems for current control. In the previous part we presented the regulation of the current but for an RL circuit[Lab 21].

It is almost similar to this control, but there are differences which we will explain in this part.

In transient state the electrical model of the MCC includes the back emf effect with the RL circuit, so the current regulation scheme will be :

To calculate the parameter of the PI regulator (Ki and Kp) it is necessary to study the stability of the system according to the following block diagram :

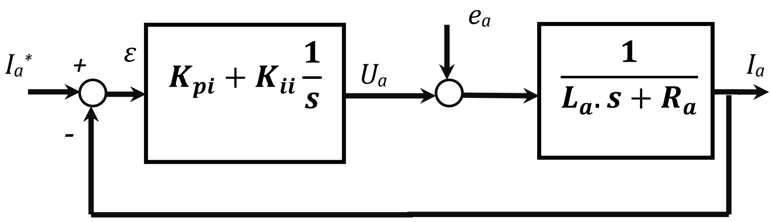

Figure II.19: Block diagram of current regulation.

Now let's assess the performance of the PI controller in regulating the current of a DC motor. The transfer function of the DC motor system, incorporating a PI current controller as depicted in Figure (17), is expressed as follows:

$$I_a = \frac{K_{pi}.s + K_{ii}}{L_a.s^2 + (R_a + K_{pi}).s + K_{ii}} {I_a}^* - \frac{s}{L_a.s^2 + (R_a + K_{pi}).s + K_{ii}} e_a \quad \textbf{(II.23)}$$

We can see from Equation (23)that the back EMF ea of the DC motor will act as a disturbance to the current control system. If the current reference of the DC motor remains a constant value (i.e. s=0), then ea will have no influence on the current control performance[Lab 21] .

However, when the current reference I* is modified, ea can have an influence on the dynamic performance of the real current following its reference[Lab 21].

For a large system inertia, the effect of ea on the current command can be ignored because the variation of ea due to speed variation is very small.

However, for servo motors designed with low inertia for fast velocity response, the effect of ea cannot be ignored. To obtain a good performance of current control by eliminating this undesirable effect of back EMF, one can adopt the feed forward control of a DC motor which is **Ea=k.φf.ω** , it can be easily estimated from the speed information. When the **disturbance** ea is compensated as shown in Figure (20), the DC motor will be simplified to an RL circuit shown in Figure (21), [Lab 21].

To calculate the parameter of the PI regulator (K_i and K_p) it is necessary to study the stability of the system according to the following block diagram:

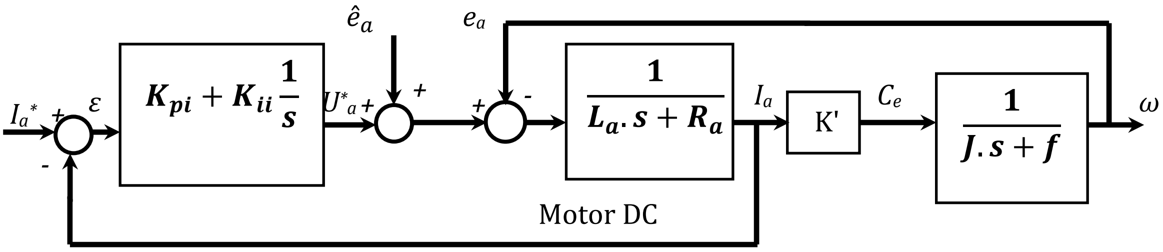

Figure II.20: Current control block diagram1.

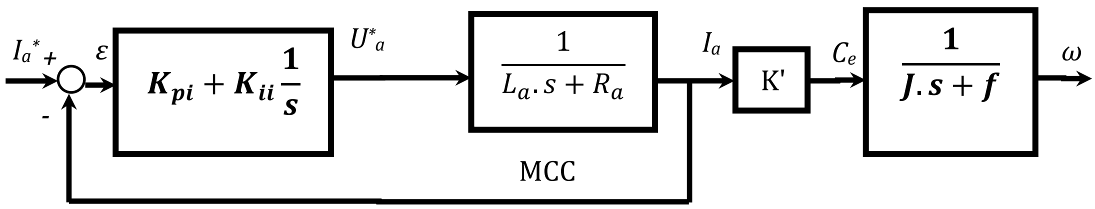

Figure II.21: Current control block diagram2**.**

- ## MCC speed regulation in cascade with the current by PI regulator:

This part is an integration of speed control and current control as previously presented.

In the speed control, as shown in Figure (17),we have the electrical control system and the electrical part of the Motor Control Center (MCC). In this context, in this section, we replace this control system with Figure(21), which represents the current control, in order to have a complete speed regulation system for the MCC. However, the output of the speed regulation is the reference torque Ce*, and the input to the current control system is the reference current Ia*. Therefore, for this problem, we will use the inverse torque model based on Equation (5)to obtain:

$$I_a^* = \frac{C_e^*}{K'} \tag{II.24}$$

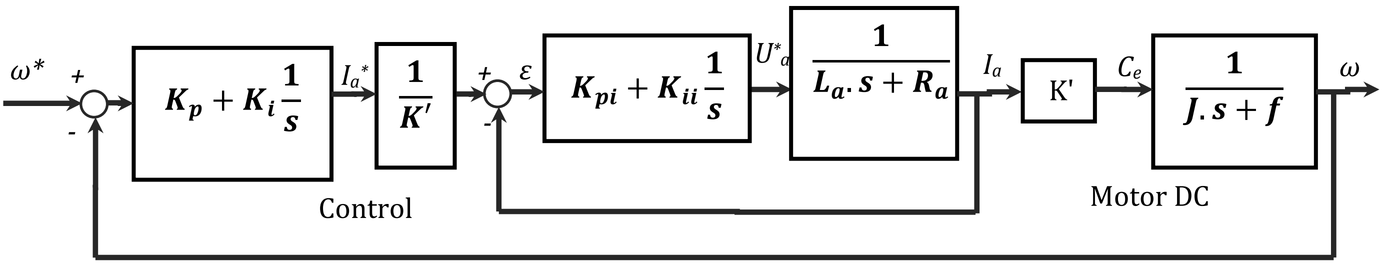

Figure II.22 : Current control block diagram**.**

- ## Cascaded MCC speed regulation with current hysteresis regulator :

This section is an integration of speed control and current control as previously presented.

In the speed control, as shown in Figure (17), we have the electrical control system and the electrical part of the Motor Control Center (Motor DC).

In this regard, in this section, we replace this control system with current regulation using a hysteresis controller to achieve a complete speed regulation system for the Motor DC, as shown in Figure (22).

This type of comparator does not require prior process analysis. The choice of hysteresis cycle length determines the accuracy of the currents as well as the switching frequency[Lab 21].

Si : $|I_{ref} - I| \langle \frac{h}{2}$ alors Kj=1 et $\bar{s}=0$

Si : $|I_{ref} - I| \rangle \frac{h}{2}$ alors Kj=0 et $\bar{s}=1$

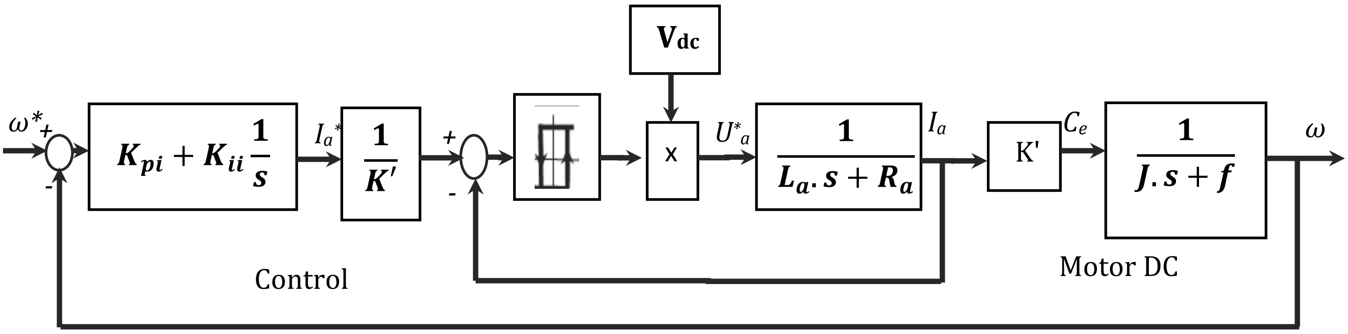

Figure II.23: Block diagram of cascaded DC motor speed control with current hysteresis controller**.**

➢ Direct speed control of DC motor :

This type of Motor DC speed control is the simplest and most cost-effective, but it is still less accurate than cascade control due to deliberate assumptions and neglects.

In most motor drive systems, the response time of an electrical system is faster than that of a mechanical system. In this case, we can ignore the transient time of the electrical circuit, so $L_a = 0$. As a result, the transfer function (10) of the Motor DC can be written as:

$$\frac{\omega}{U_a} = \frac{K'}{R_a.J.s + K'^2} = \frac{1}{K'}\frac{\omega_c}{s + \omega_c} \text{ où } (\omega_c = \frac{K'^2}{R_a.J}) \quad \textbf{(II.25)}$$

This equation implies that the relationship between the speed ω and the armature voltage U_a in a DC motor can be considered as a first-order low-pass filter with a cutoff frequency ω_c. This means that the speed ω is directly proportional to the armature voltage Ua, with its rate of change limited to ω_c, although there is a delay between the two. Generally, it can be assumed that the rotational speed of a DC motor is proportional to the applied voltage[Lab 21] .

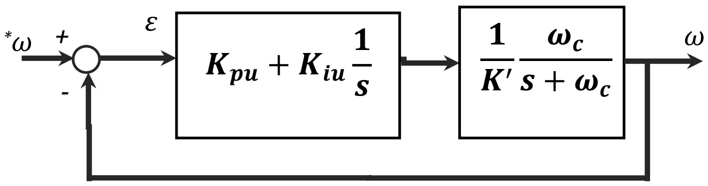

Figure II.24: MCC direct speed control block diagram.

II.6 Electronic converter for DC motor :

To control the voltage applied to a DC motor, a power electronic converter can be used, as shown in Figure(25). The switching states of the power devices in the converter are determined by the pulse width modulation (PWM) technique to achieve the required voltage control. The voltage control is provided by the current controller,as described earlier [San 17].

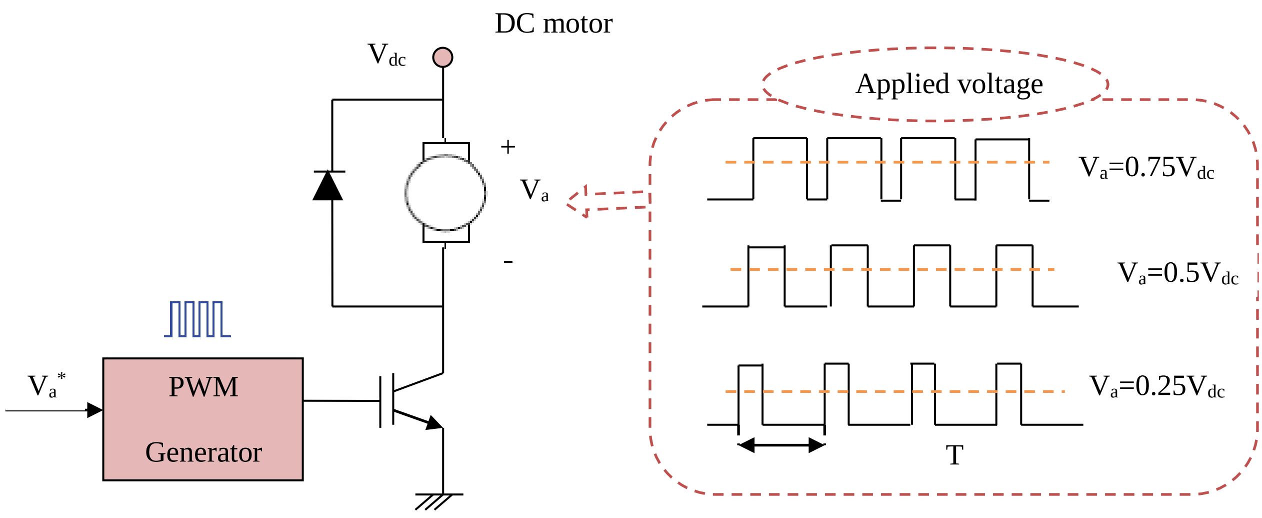

Figure II.25: A basic circuit for driving a DC motor (simple).

In order to operate a DC motor in both forward and reverse directions, as well as in both motoring and braking modes, a four-quadrant chopper or H-bridge circuit is commonly used. This circuit consists of four power switching devices[San 17].

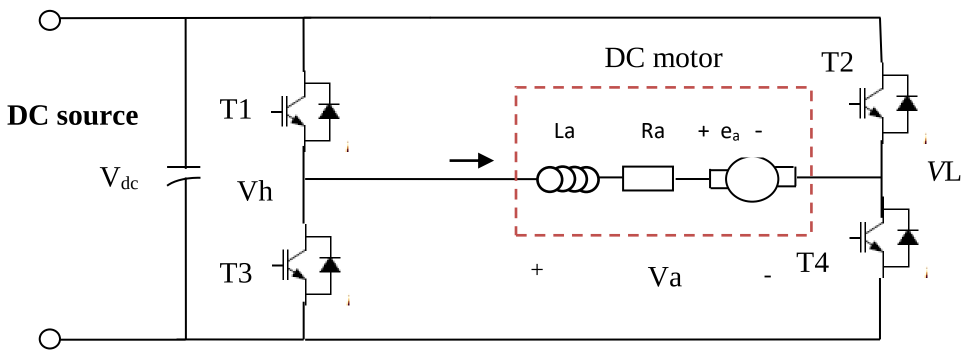

Figure II.26: H-bridge circuit.

The H-bridge circuit is widely used in DC servo drive systems due to its ability to provide high-performance current control with a bandwidth of several thousand radians per second. There are two PWM techniques used in this circuit to adjust the output voltage: the bipolar switching scheme and the unipolar switching scheme[San 17].

2.6.1 Switching Schemes :

➢ Bipolar switching scheme :

The bipolar switching scheme uses a triangular carrier wave and a voltage reference, Va, to determine the switching states of devices. The process involves comparing Va with the triangular carrier wave [San 17].

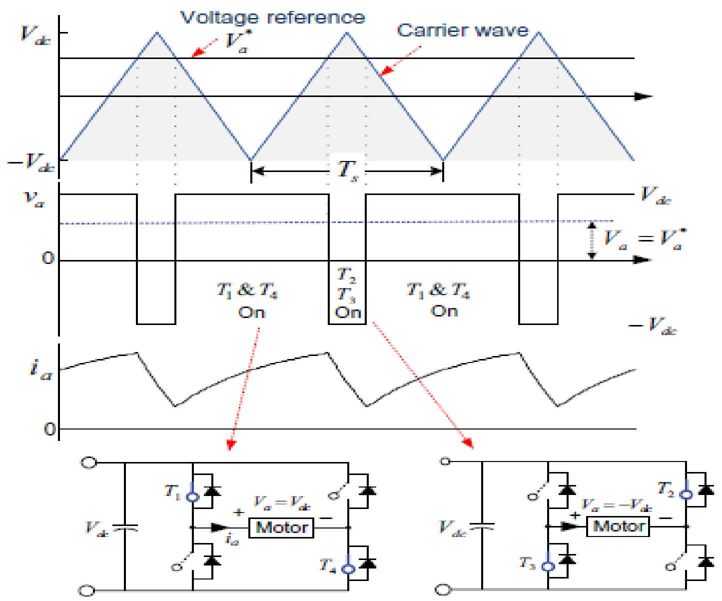

Figure II.27: Bipolar switching scheme.

If Va is greater than the triangular carrier wave, both T1 and T4 are turned on, resulting in an output voltage of 1Vdc. Alternatively, if Va is less than the triangular carrier wave, both T2 and T3 are turned on, and the output voltage becomes 2Vdc. In this way, the switching devices placed diagonally (T1 and T4, T2 and T3) are turned on or off simultaneously, resulting in a positive or negative DC output voltage.

The bipolar switching scheme derives its name from the two possible output voltage levels (positive or negative), which are generated as a result of the switching actions[San 17].

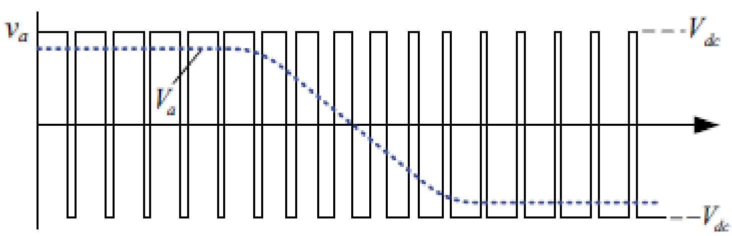

Figure II.28: Output voltage of bipolar switching.

In this scheme, the switching frequency equals to the frequency (1=Ts) of the triangular carrier wave. This scheme has an advantage of smoothly changing the average output voltage from 1Vdc to 2Vdc as shown in Fig. II.26. However, the instantaneous output voltage becomes as wide as 2Vdc, resulting in a large current ripple of the motor[San 17].

➢ Bipolar switching scheme :

In this scheme, the switching of the devices is also determined by comparing the voltage reference with the triangular carrier wave as in the bipolar switching scheme, but the switching in the H-pole and the L-pole is performed independently according to its own reference. The reference voltage VH of the H-pole is given as Va . Meanwhile, the reference voltage VL of the L-pole is given as 2Va . The output voltage (i.e., the motor voltage) Va is given by the voltage difference between the H-pole and the L-pole, i.e., VH 2 VL. Since

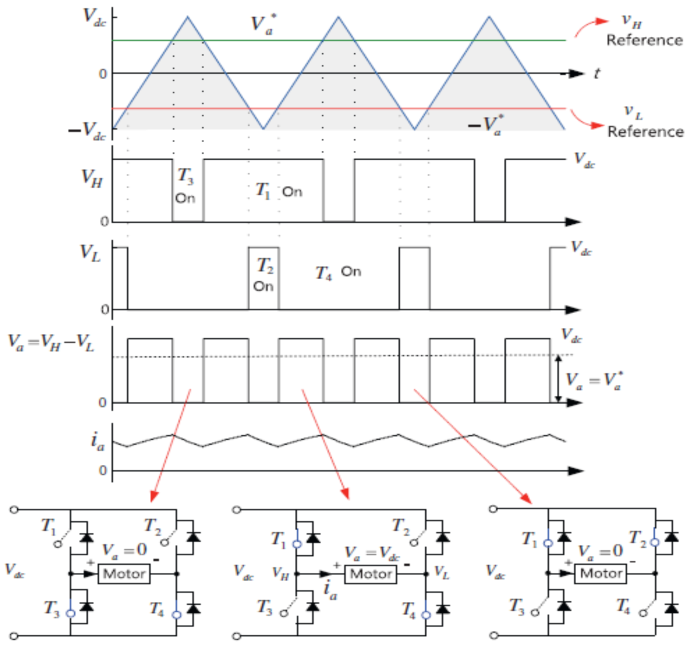

Figure II.29: Unipolar switching scheme.

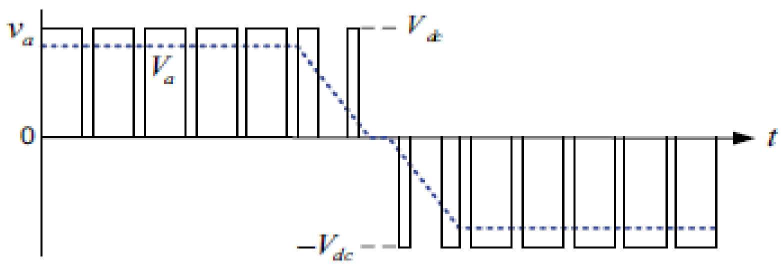

Figure II.30: Output voltage of unipolar switching.

II.7 Identification of parameters DC motor :

Identification of parameters refers to the process of determining the values based on external data for a model or system consisting of adjustable parameters. This process plays a crucial role in various fields such as engineering, physics, and computer science. In the case of a DC motor, the identification of parameters involves determining the values of key parameters that characterize the motor's behavior and performance.

DC motors are widely used in many applications, including robotics, industrial automation, and electric vehicles. The accurate identification of DC motor parameters is essential for studying and simulating their dynamic behavior. By knowing the precise values of parameters such as armature resistance, inductance, back-EMF constant, and mechanical inertia, it becomes possible to develop accurate mathematical models and simulations that accurately represent the motor's response to different input signals and operating conditions.

The importance of parameter identification for studying and simulating DC motors lies in its ability to provide insights into the motor's performance characteristics and aid in designing control algorithms. By accurately estimating the motor parameters, engineers and researchers can develop effective control strategies, optimize energy efficiency, and ensure reliable operation. Furthermore, accurate parameter identification enables the prediction of motor behavior under various load conditions, which is crucial for system integration and performance analysis.

Numerous studies have been conducted on parameter identification for DC motors to enhance their modeling and control. For example, researchers have employed techniques like least squares estimation, Kalman filtering, and system identification methods to estimate the motor parameters from experimental data. These studies have focused on different aspects such as speed control, torque control, position control, and efficiency optimization. By accurately identifying the motor parameters, these studies have contributed to the development of advanced control strategies and the improvement of DC motor performance in various applications.

These studies provide valuable insights and novel techniques for identifying the parameters of DC motors, contributing to the field of motor control and automation .The following studies are listed below:

In 1973, W. Lord and J. H. Hwang conducted a study on separately excited DC servomotors and identified eight practical models for these motors. Each model's parameters were clearly defined. They developed testing procedures to determine the model type and parameters of a servomotor solely based on its current response to a step input of armature voltage. The study demonstrated excellent agreement between actual and predicted current responses, highlighting the effectiveness of the technique [Lor73].

In 1975, W. Lord and J. H. Hwang further investigated linear modeling techniques for separately excited DC motors. They showed that dynamic operating conditions are crucial for obtaining accurate model parameters. Pasek's technique was employed to identify the model type and parameters using a single current response to a step input of armature voltage [Lor75].

In 1983, R. Schulz introduced a frequency response technique for measuring the parameters of high-performance DC motors. It was demonstrated that, under certain conditions, a second-order motor model is equivalent to a series resonant electrical circuit. By treating the motor's frequency response measurements as electrical impedance, a measurement technique with practical advantages was established. The results were compared to those obtained from conventional methods [Sch 83].

In 1988, A. D. Rajkumar and R. Somanatham proposed a practical method for determining DC motor transients using an 8085-based microcomputer. Typically, sophisticated transient recorders or storage oscilloscopes are required for such determinations. The proposed method was tested in the laboratory and verified [Raj88].

In 1991, S. Weerasooriya and M. A. El-Sharkawi introduced an artificial neural network-based high-performance speed control system for DC motors. The objective was to achieve accurate trajectory control of the speed, especially when motor and load parameters are unknown. An artificial neural network was employed to capture the unknown nonlinear dynamics of the motor and load. The performance of the identification and control algorithms was evaluated through simulations using a typical DC motor model [Wee 91].

In 1992, Y. Jung, K. Cho, Y. Lim, J. Park, and Y. Chang focused on developing a microcomputer-based parameter identification system for a brushless DC motor (BDCM). A BDCM is equivalent to a DC motor in terms of the equivalent circuit. Therefore, Pasek's equation for parameter determination of a DC motor is applicable to a BDCM. An identification algorithm specifically for BDCM parameters using Pasek's technique was developed and implemented on an IBM-PC/AT using the C language [Jun 92].

In 1996, D. M. Gillard and K. E. Bollinger investigated the use of a multilayered neural network for measuring the transfer function of a power system. The purpose was to utilize this information for power system stabilizer (PSS) tuning and assessing PSS damping. The study aimed to quickly and accurately measure the transfer function relating electric power output to the AVR PSS reference voltage input under normal operating conditions. Additionally, the excitation signal used in the identification procedure was designed not to adversely affect the terminal voltage or system frequency [Gil 96].

In 2000, A. Rubbai and R. Kotaru introduced the concept of online identification and control of a DC motor using learning adaptation. They utilized the power of feedforward artificial neural networks to capture and replicate intricate nonlinear mappings, enabling the implementation of a comprehensive nonlinear control law [Rub 00].

In 2000, X. Liu, H. Zhang, J. Liu, and J. Yang described a parameter estimation technique based on block-pulse function series to estimate the continuous-time model of a motor. The electromechanical parameters of the motor can be obtained from the estimated model parameters [Xia 00].

In 2001, S. Saab and R. Abi Kaed-Bey demonstrated that the parameters of a DC motor can be estimated through discrete measurements obtained from an integrated dynamometer. The dynamometer provides discrete measurements of the armature current, angular velocity, armature voltage (system input), and motor torque. They utilized a least-squares algorithm for parameter identification of the DC motor without the need for a D/A converter and a power amplifier. A Kalman filter was also implemented as a state observer to estimate the angular acceleration and the derivative of the armature current. To enhance the overall identification performance, the DC parameters were initially estimated by decoupling the AC parameters using a DC input signal [Saa 01].

In 2004, A. Dupuis, M. Ghribi, and A. Kaddouri proposed a simplified offline parameter identification method for motors based on optimization using a multiobjective elitist genetic algorithm. They employed the non-dominated sorting genetic algorithm (NSGA-II) to minimize the error between the measured current and velocity responses and the corresponding model estimates. The method's robustness was demonstrated by estimating parameters for a DC motor in four different scenarios. Simulation results showed successful motor parameter estimation and the ability to simultaneously identify load torque [Dup 04].

In 2005, R. Krneta, S. Antic, and D. Stojanovic investigated the application of the recursive least squares method for parameter identification of DC motor models. The proposed method's validity was demonstrated through simulations and experiments. By comparing real motor speed with the speed of investigated models in the Z and S domains, satisfactory quality of DC motor parameter identification was achieved [Rad 05].

In 2006, R. Garrido and R. Miranda introduced a novel approach for closed-loop identification of position-controlled DC servomechanisms. The servo loop is closed using a Proportional Derivative (PD) controller, while a model of the servo is simultaneously controlled using a second PD controller. By comparing the output of the real servo and its model, the error and its time derivative are utilized to identify the motor parameters, which are then used to update the model. The properties of this identification scheme are analyzed using Lyapunov stability theory [Gar 06].

In 2007, W. Aung conducted an analysis on the modeling and simulation of DC motors and their driving systems, both in terms of hardware and software. MATLAB Simulink is used for analyzing DC motor models through control techniques such as step response, impulse response, and Bode plots. The analysis encompasses the internal circuit of a simple DC motor and its characteristics, employing both control system design calculations and MATLAB software [Aun 07].

In 2009, M. Hadef and M. Rachid proposed a parameter identification method using inverse problem methodology. The key procedure in solving the inverse problem is minimizing the objective function with respect to the desired vector of design parameters. The conjugate gradient method is employed to determine the unknown parameters, and Tikhonov's regularization method is utilized to transform the original ill-posed problem into a well-posed problem [Had 09].

in 2019, Shah and Sekhar presented a study focused on identifying the parameters of a DC motor. The authors utilized a fractional order model to perform system identification in a closed-loop setup. The objective of their research was to accurately estimate the parameters of the DC motor within a closed-loop control system. The paper was presented at the 2019 International Conference on Mechatronics, Robotics, and Systems Engineering MoRSE [Sha19].

II.7.1 Identification of Back-EMF constant (K') :

The relationship between the back electromotive force (EMF), E, and the rotational velocity can be expressed through the constant factor K', as shown in the following equations (26):

$$E = K'.\omega \qquad \textbf{(II.26)}$$

gives us:

$$K' = \frac{E}{\omega} \qquad \textbf{(II.27)}$$

We conducted an experiment to extract or determine the Back-EMF constant specific to a direct current (DC) motor.

In this experiment, we applied different rotational speeds to the DC motor using a drill, which acted as a reverse motor, thereby rotating the DC motor. The speed of the DC motor was monitored using a speed sensor, and the speed readings were displayed on the computer. Additionally, we measured the voltage corresponding to each speed using a dedicated voltmeter.

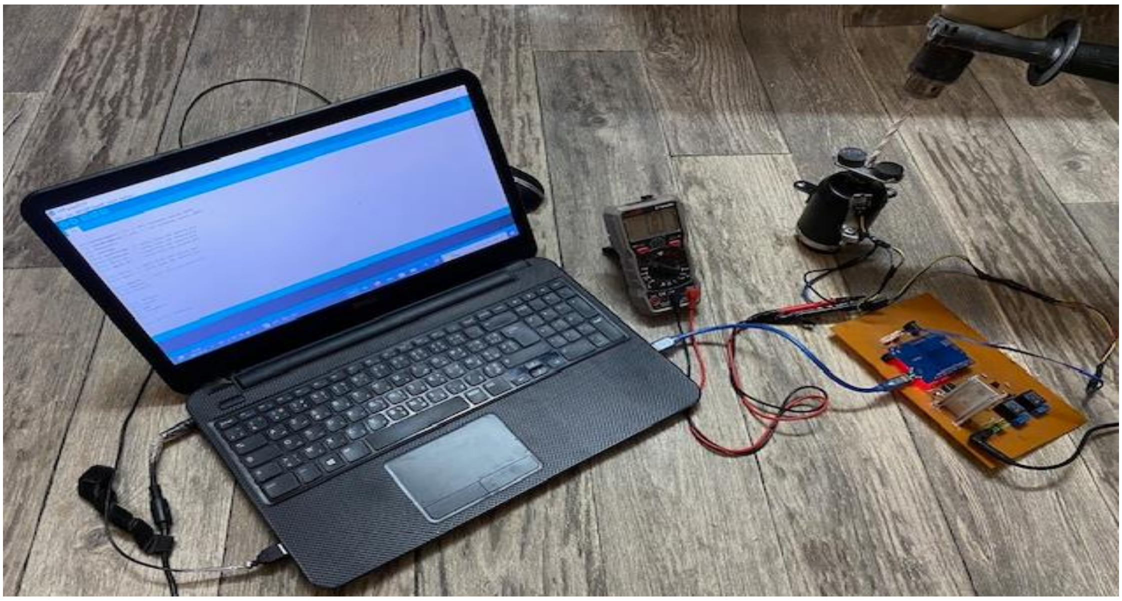

FigureII.31: Experimental Setup for Back-EMF Constant Determination in DC Motor**.**

The results from each experiment, including the recorded values, are presented in the following table:

(rpm)ω	60	120	180	240	660	900	1020	2100	2580
(v)E	0.20	0.40	0.66	0.85	1.65	2.87	3.46	4.03	5.80

Table II.2: Experimental Results for Back-EMF and Speed Measurements for Back-EMF Constant Calculation.

based on these results and to the law , the Back-EMF constant will be determined :

- K=0.03

II.7.2 Identification of Armature Inductance L and armature R resistance :

Accurate determination of the armature inductance and resistance is crucial for understanding and analyzing the behavior of a DC motor. In this case, the measured inductance value of 0.58mH represents the motor's inherent opposition to changes in current flow. This information is important for developing motor simulation models that accurately reflect the motor's dynamic response.

Similarly, the measured resistance value of 1.1Ω provides insights into the inherent resistance in the motor's armature winding. Incorporating this resistance value into motor simulations enables accurate assessment of power losses, heat generation, and overall motor efficiency.

By utilizing these identified parameters in motor simulations, we can accurately predict and analyze the motor's behavior under different operating conditions. This knowledge is crucial for designing efficient control strategies, optimizing performance, and ensuring reliable operation.

It can be said that the inductance and resistance values equal these values :

- R=1.1Ω
- L=0.58mH

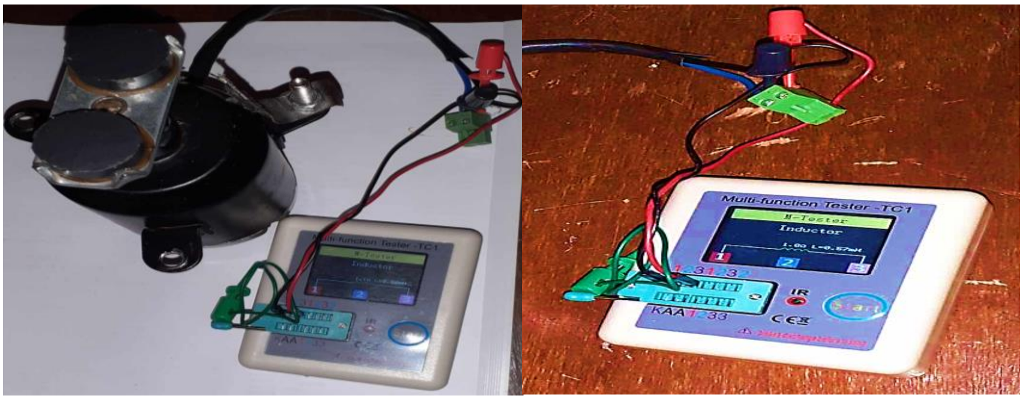

Figure II.32: the Armature Inductance of the DC Motor.

II.7.3 Identification of rotor inertia J and damping constant B :

The rotor inertia J is a crucial parameter in motor simulation as it represents the resistance of the rotor to changes in rotational motion. It plays a significant role in determining the motor's response time, stability, and overall performance. Accurate identification of J allows for more precise motor control and simulation.

Similarly, the damping constant B is essential in motor simulation as it characterizes the level of damping or resistance to motion within the motor system. It influences the rate at which the motor's rotational speed decreases after the power is removed. Proper estimation of f enables more accurate modeling of the motor's behavior and enhances the accuracy of simulations and control algorithms.

Therefore, by accurately identifying the rotor inertia and damping constant through the experimental procedure described, one can significantly improve the simulation and control of the motor, leading to better performance and optimized system design.

The motor torque T is related to the armature current I_a by a constant factor K' **,** so The load torque T can be expressed as

$$T = K'.I_a \qquad \textbf{(II.28)}$$

$$\sum T = J.\frac{d\omega}{dt} + \omega.B \qquad \textbf{(II.29)}$$

If we substitute in the previous equation (29) in the steady-state, we can obtain

$$T = \omega.B = K'.I_a \qquad \textbf{(II.30)}$$

Thus, we can conclude that damping constant (friction) is equal to

$$B = \frac{K'}{\omega}.I_a \qquad \textbf{(II.31)}$$

In this experiment, the aim was to calculate the damping constant B using the equation mentioned earlier, where K' is a constant that has been previously calculated in prior experiments. The unknown variables in this equation are the current and motor speed.

The recorded values from each experiment were documented and presented in the provided table. The experiment was conducted following the procedure depicted in the accompanying images. The duty cycle, ranging from 0% to 100%, was adjusted using a computer connected to the motor control electronic board. Simultaneously, the corresponding motor speed was recorded. The speed variations were detected through a speed sensor, while the current was measured and displayed on the ammeter screen.

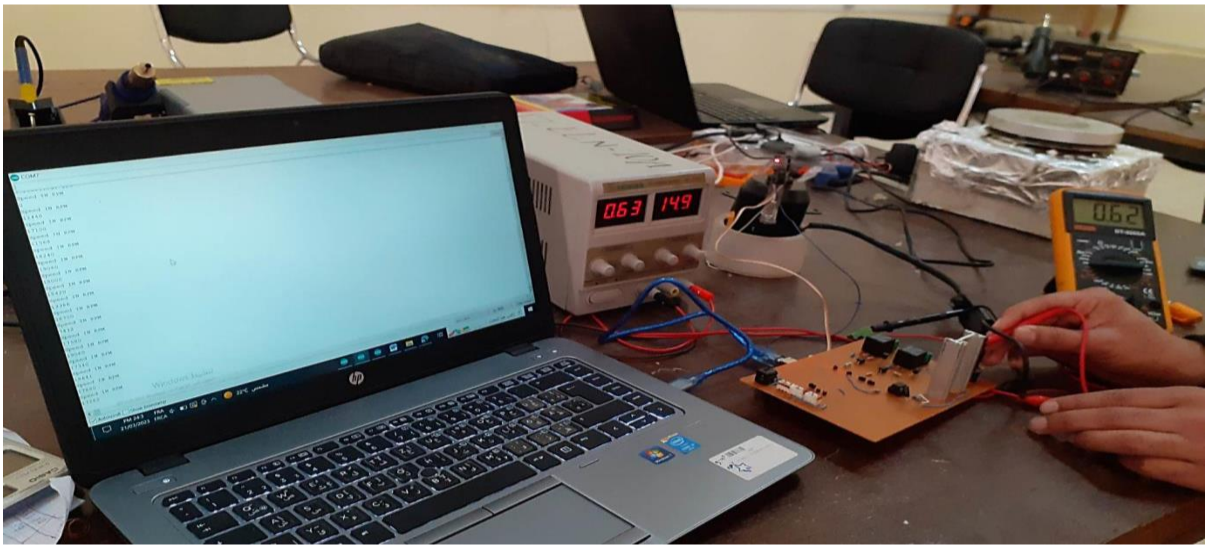

Figure II.33: Experimental Setup for Damping Constant Calculation in DC Motor.

The results from each experiment, including the recorded values, are presented in the following table:

(rpm)ω	0	850	1700	1900	2120	2500	3400
(A)I	0	0.45	0.62	0.63	0.64	0.67	0.72
B (N.m.s/rad.A)	0	10^{-4}	10^{-4}	9.3×10^{-5}	8.6×10^{-5}	7.6×10^{-5}	2.3×10^{-6}

Table II.3: Experimental Results for Damping Constant Calculation in DC Motor Experiments.

Based on the experimental results, it is possible to plot the torque as a function of speed. The recorded values of speed and the damping constant f can be used for this purpose.

In the figure(34), it is clear that the torque relationship is non-linear. However, for the sake of simplicity in our analysis, we can make the simplifying assumption of linearity. While this assumption may not fully capture the complexity of the system, it allows us to simplify calculations and gain some insights into the behavior of the system under study.

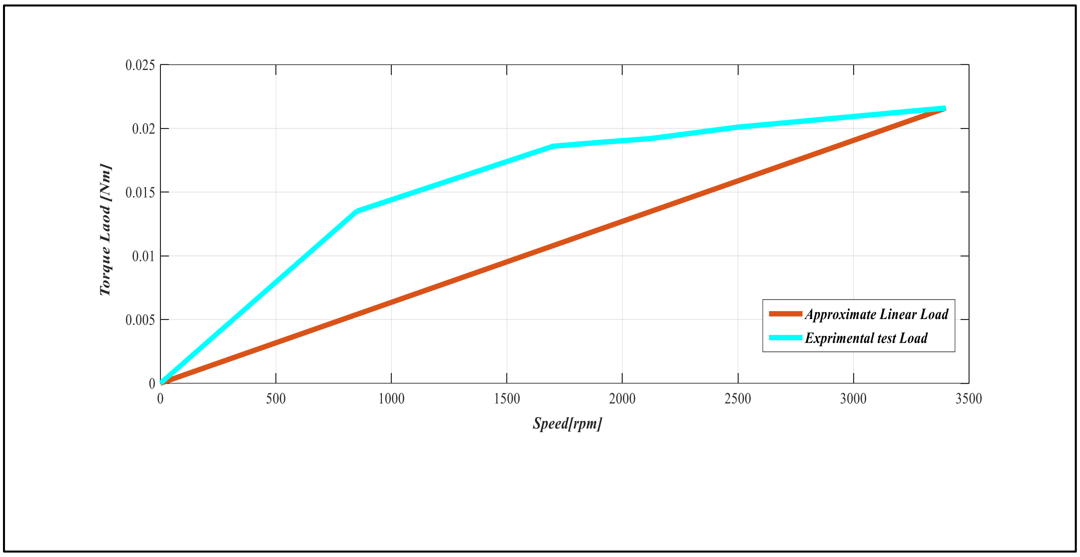

Figure II.34: Torque-Speed Relationship in the DC Motor.

Finally, after determining the value of the damping constant, we can calculate the rotor inertia using the aforementioned equation and result in Table (3).

- $f = 6.066 \times 10^{-5}$

For identification of J, in the experiment, the Arduino was programmed to rotate the DC motor at a specific speed and then stop. As the speed gradually decreased, data points were recorded from the decaying curve of the motor's rotational motion. These data points were used to calculate the rotor inertia . The results are given in Table (4) for Figure (35) …..

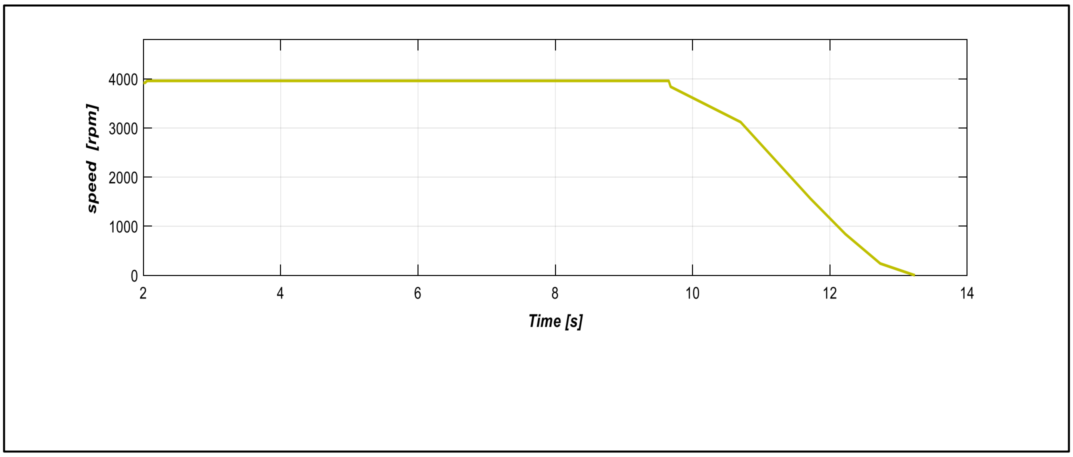

Figure II.35: speed Variation over Time in the Experiment.

(rpm)ω	3960	3840	3120	1560	840	240	0
(s)t	9.65	9.68	10.70	11.71	12.22	12.73	13.23

Table II.4: Experimental Results for Speed and Time Measurements.

Equation (29) can be rewritten as follows

$$J = -B \,.\, \omega . \left(\frac{T_1 - T_2}{\omega_1 - \omega_2}\right) \quad \textbf{(II.32)}$$

If we apply the set of data points obtained in the previous table using the following equation(32), we can find rotor inertia:

- ❖ $J = 1.2 \times 10^{-4}\ \mathrm{kg \cdot m^2}$

II.7.4 Calculating the parameters K_i and k_p :

Calculating the parameters K_i and K_P is crucial for implementing proportional-integral control in speed. This control scheme utilizes a specific diagram to determine the appropriate values for the integral gain k_i and proportional gain k_p by adjusting these parameters, the controller can achieve the desired speed control response and effectively regulate the system's behavior.

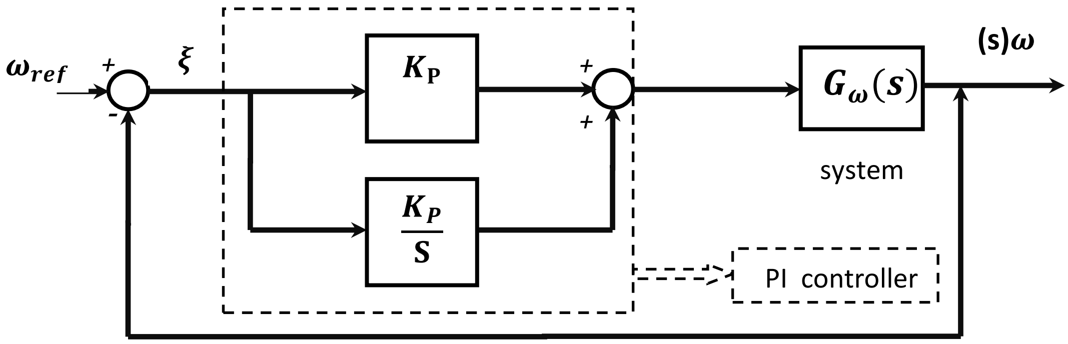

Figure II.36: Proportional-integral control in speed.

Initially, we employ a PI controller with a transfer function.

$$G_c(s) = K_p + \frac{k_i}{s} = \frac{k_p\ s + k_i}{s} \quad \textbf{(II.33)}$$

The transfer function in closed-loop is given by:

$$G_{\omega-\omega_{ref}}(s) = \frac{G_c(s).G_\omega(s)}{1 + G_c(s).G_\omega\ (s)} \quad \textbf{(II.34)}$$

With G_ω(s), is the transfer function for speed-voltage given by:

$$G_\omega(s) = \frac{K}{(L_a s + R_a)(Js + f) + k^2} \quad \textbf{(II.35)}$$

By substituting (35) and (33) into equation (34), we obtain the following closed-loop transfer function:

$$G_{\omega-\omega_{ref}}(s) = \frac{K(k_p\ s + k_i)}{s\big((L_a s + R_a)(Js + f) + K^2\ \big) + K(k_p\ s + k_i)} \qquad \textbf{(II.36)}$$

If we neglect the inductance La, we find:

$$G_{\omega-\omega_{ref}}(s) = \frac{1}{R_a\ J}\frac{k(k_p\ s + k_i)}{s^2 + \frac{(R_a f + Kk_p + k^2)}{R_a J}s + \frac{KK_i}{R_a J}} \qquad \textbf{(II.37)}$$

We can express the denominator of equation (37) as a second-order characteristic equation, such as:

$$s^2 + \frac{(R_a f + Kk_p + k^2)}{R_a J}s + \frac{KK_i}{R_a J} = s^2 + 2\xi\omega_n + {\omega_n}^2 \qquad \textbf{(II.38)}$$

Which gives:

$$K_p = \frac{2\xi\omega_n R_a\ J - (R_a f + k^2)}{k} \qquad \textbf{(II.39)}$$

$$K_i = \frac{R_a J{\omega_n}^2}{K} \qquad \textbf{(II.40)}$$

The performance indices commonly used to evaluate the performance of a second-order system:

the damping ratio ξ can be obtained as

$$\xi = \sqrt{\frac{(\ln D)^2}{\pi^2 + (\ln D)^2}} \qquad \textbf{(II.41)}$$

Settling Time by (5 %) as

$$T_s(5\%) = \frac{3}{\xi\omega_n} \qquad \textbf{(II.42)}$$

Which gives

$$\omega_n = \frac{3}{\xi T_s} \qquad \textbf{(II.43)}$$

To evaluate the performance of a second-order system, we can calculate the damping ratio and the parameters K_i and k_p for the given choices: D<0.1 and T_s < 0.8. These performance indices will be used in the simulation of the motor.

II.8 Motor Simulation and Results :

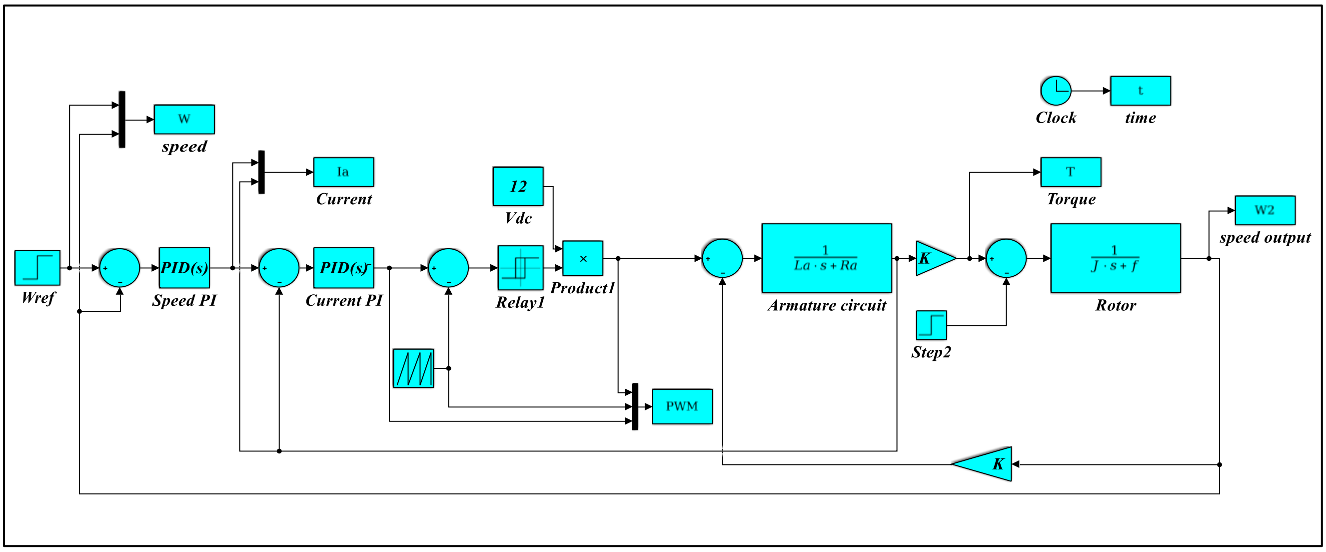

Figure II.37: Block diagram of speed cascade control for DC motor.

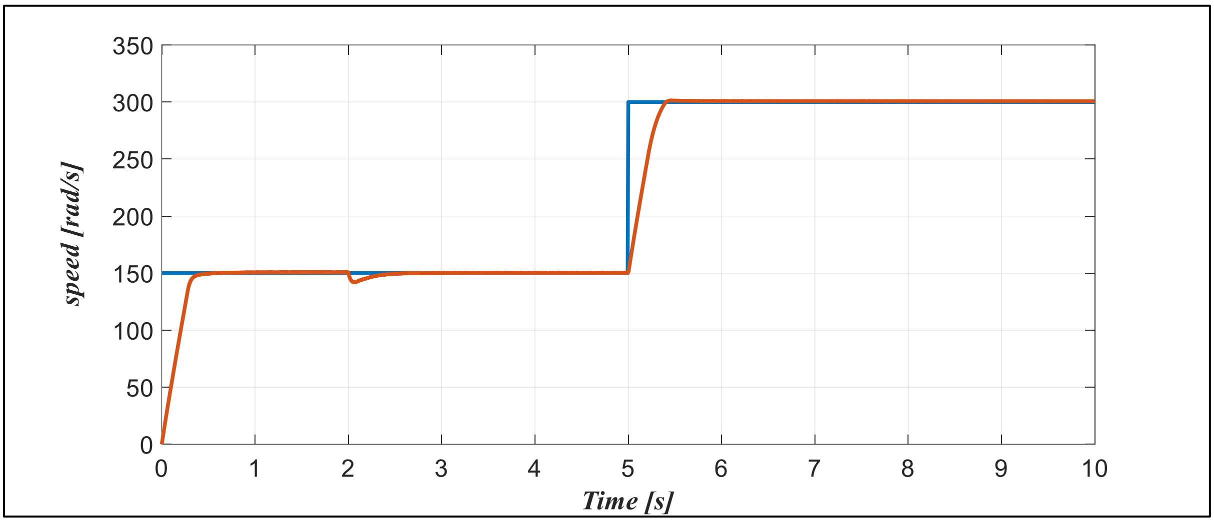

Figure II.38: Evaluation reference and measured speed for the control system.

When observing the plot (see Figure 38), it is evident that the measured speed of the motor exhibits excellent tracking performance with the reference speed. At the beginning, from 0 to 5 seconds, the reference speed is set to 150 rad/s. During this period, the measured speed steadily increases and closely follows the reference speed. Then, at 5 seconds, there is a sudden change in the reference speed to 300 rad/s. The motor quickly responds to this change and successfully tracks the new reference speed, exhibiting a rapid and accurate adjustment. This indicates a highly responsive and precise control of the motor's speed in accordance with the reference input.

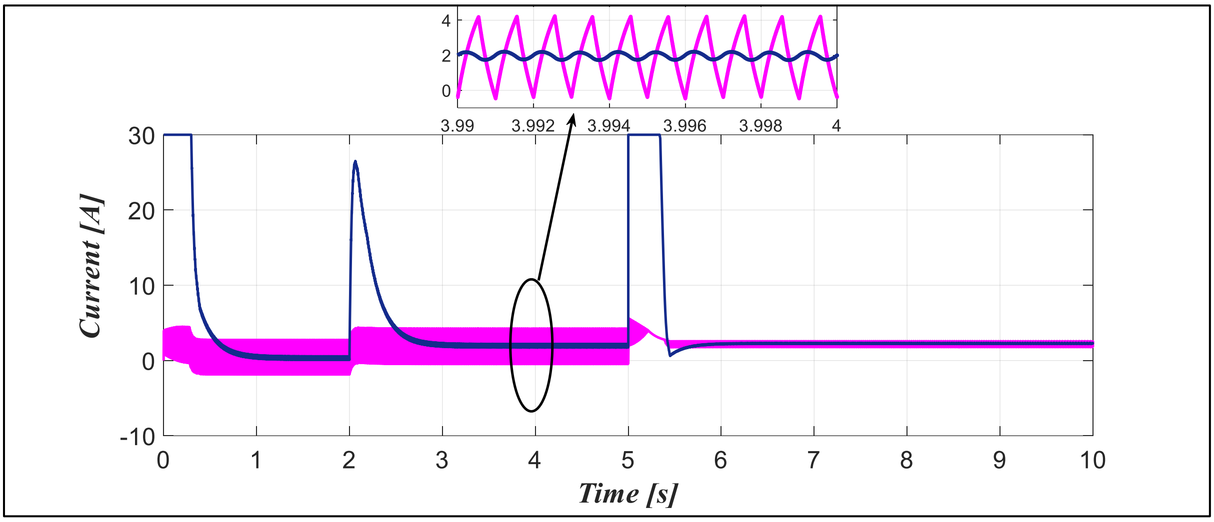

Figure II.39: measured Torque for the control system.

When observing the simulation results (see Figure39), several variations were noted in the torque curve of the DC motor. Initially, from 0 to 2 seconds, the torque remained negligible as no load was applied. At the 2-second mark, a load was introduced, resulting in a noticeable increase in torque. However, starting from 5 seconds, the torque curve exhibited ripple, oscillation, with significant variations observed between 0 and 5 seconds. Furthermore, the torque produced by the motor gradually decreased after the 5-second mark.

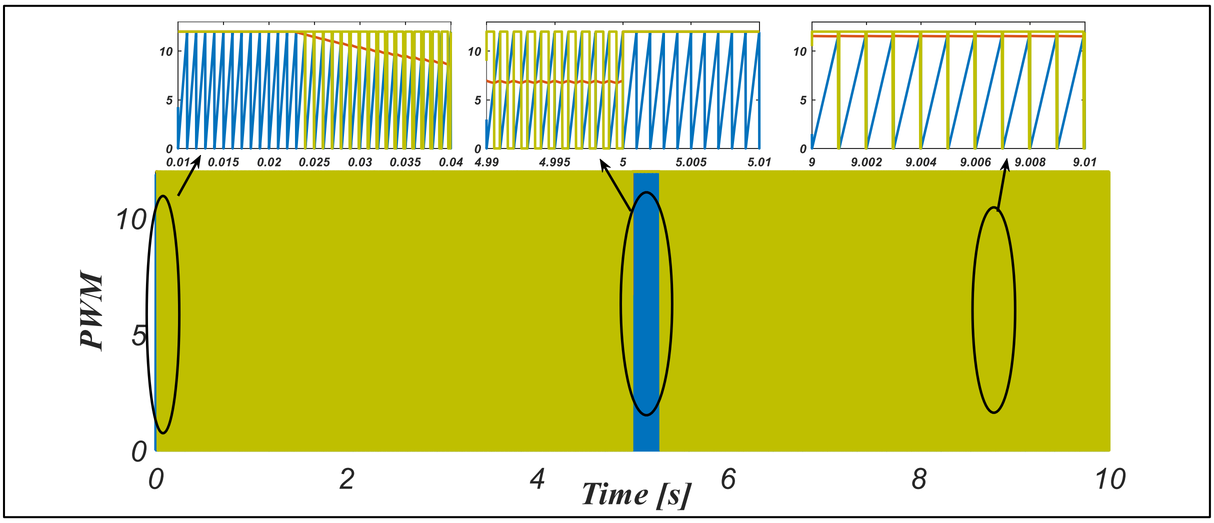

Figure II.40: Time-based representation of the PWM waveform for motor control.

Figure (40)cillustrates the time-based representation of the PWM waveform used for motor control in the cascade control system. The graph showcases the variations in the pulse width over time.

The duty cycle, represented as a percentage, determines the width of each pulse in the PWM waveform. As the speed or load of the motor increases, the duty cycle also increases. This results in wider pulses in the PWM waveform, allowing for a larger portion of the signal period to be active.

By manipulating the pulse frequency and duty cycle of the PWM waveform, precise control over the motor's speed and response to changes in load can be achieved. The wider pulses in the waveform provide increased power to the motor, enabling it to generate more torque and adapt to higher speeds or heavier loads.

Figure (40) provides a visual representation of how the pulse frequency, duty cycle, and the resulting PWM waveform interact. It demonstrates the relationship between speed, load, and the width of the pulses in the waveform, emphasizing the effectiveness of cascade control for motor control.

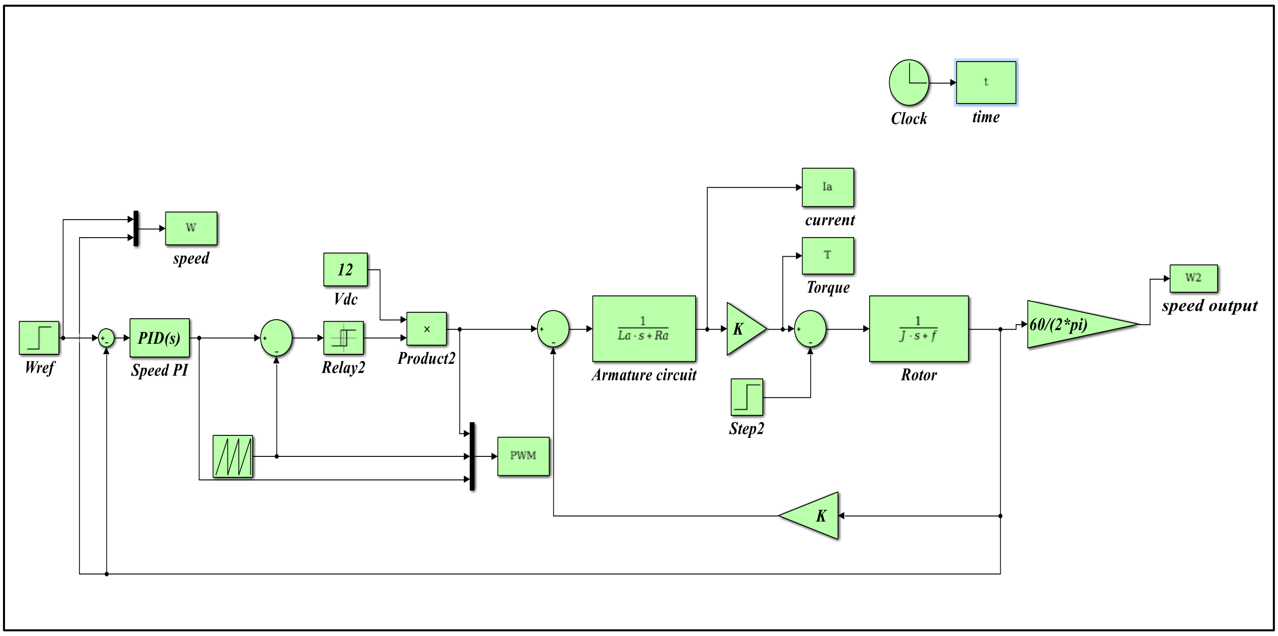

Figure II.41: Block Diagram for Direct Speed Control of DC Motor.

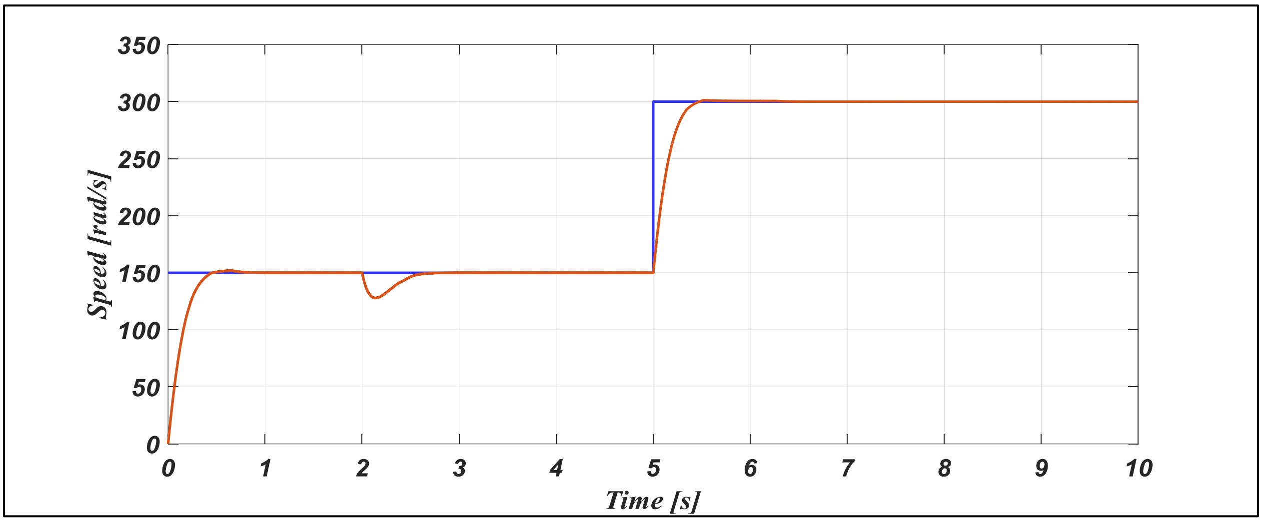

Figure II.42: Evaluation reference and measured speed for the control system.

When observing the plot (see Figure 42), it is evident that the measured speed of the motor exhibits excellent tracking performance with the reference speed. At the beginning, from 0 to 5 seconds, the reference speed is set to 150 rad/s. During this period, the measured speed steadily increases and closely follows the reference speed. Then, at 5 seconds, there is a sudden change in the reference speed to 300 rad/s. The motor quickly responds to this change and successfully tracks the new reference speed, exhibiting a rapid and accurate adjustment. This indicates a highly responsive and precise control of the motor's speed in accordance with the reference input.

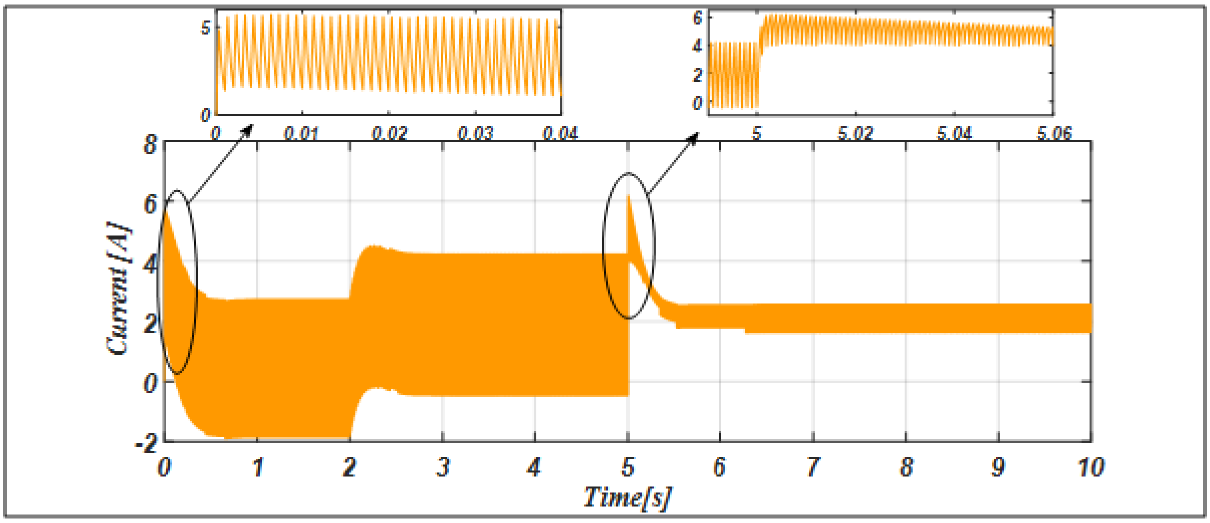

Figure II.43: Current Variation of the DC Motor over Time.

Upon examining the simulation results (see Figure 43), several noteworthy observations can be made.

Initial Current Stability: At the beginning of the simulation, the current remained stable as no load was applied to the motor. This indicates that the motor operated at a relatively low current level during this period.

Current Surge: Once the load was introduced at the 2-second mark, there was a significant surge in the current. This surge in current demonstrates the motor's response to the increased load demand.

Current Ripple and Oscillation: Starting from 5 seconds, the current curve exhibited ripple and oscillation. This suggests fluctuations in the motor's current output. The presence of ripple and oscillation indicates possible disturbances or instability in the control system.

Current Variations between 0 and 5 seconds: Significant variations were observed in the current curve within the time interval of 0 to 5 seconds. This indicates that the motor's current output was not consistent during this period, potentially due to changes in the load or disturbances in the system.

Gradual Decrease in Current: After the 5-second mark, the current produced by the motor gradually decreased. This suggests that the motor's current demand reduced over time, which could be attributed to factors like reduced load or control adjustments.

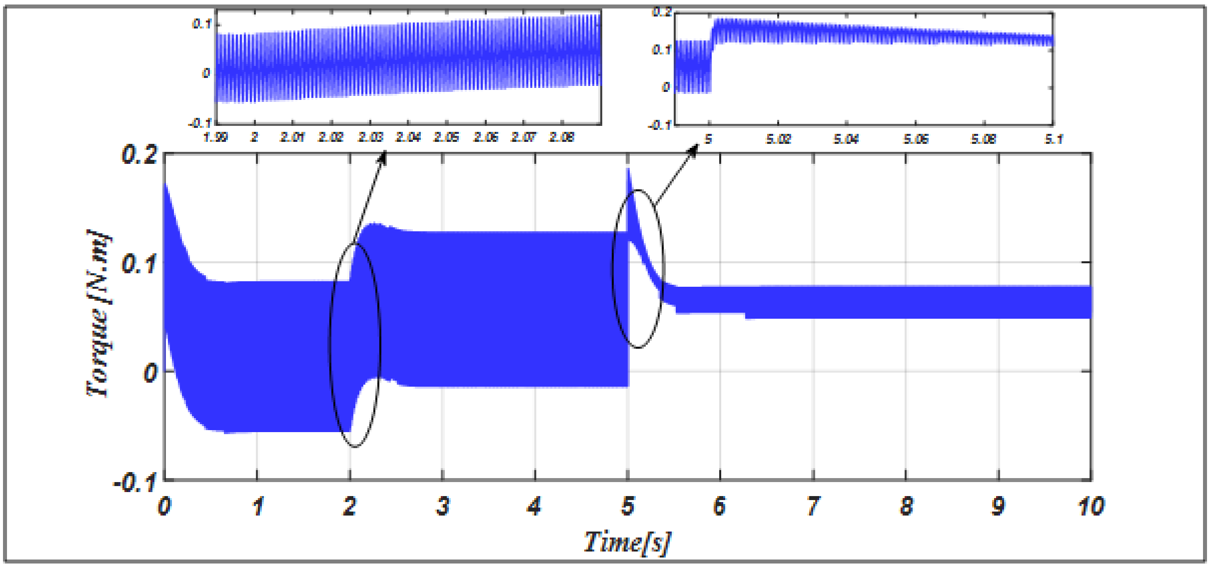

Figure II.44: Torque Variation of DC Motor Over Time.

When observing results (see Figure 44), several variations were noted in the torque curve of the DC motor. Initially, from 0 to 2 seconds, the torque remained negligible as no load was applied. At the 2-second mark, a load was introduced, resulting in a noticeable increase in torque. However, starting from 5 seconds, the torque curve exhibited ripple, oscillation, with significant variations observed between 0 and 5 seconds. Furthermore, the torque produced by the motor gradually decreased after the 5-second mark.

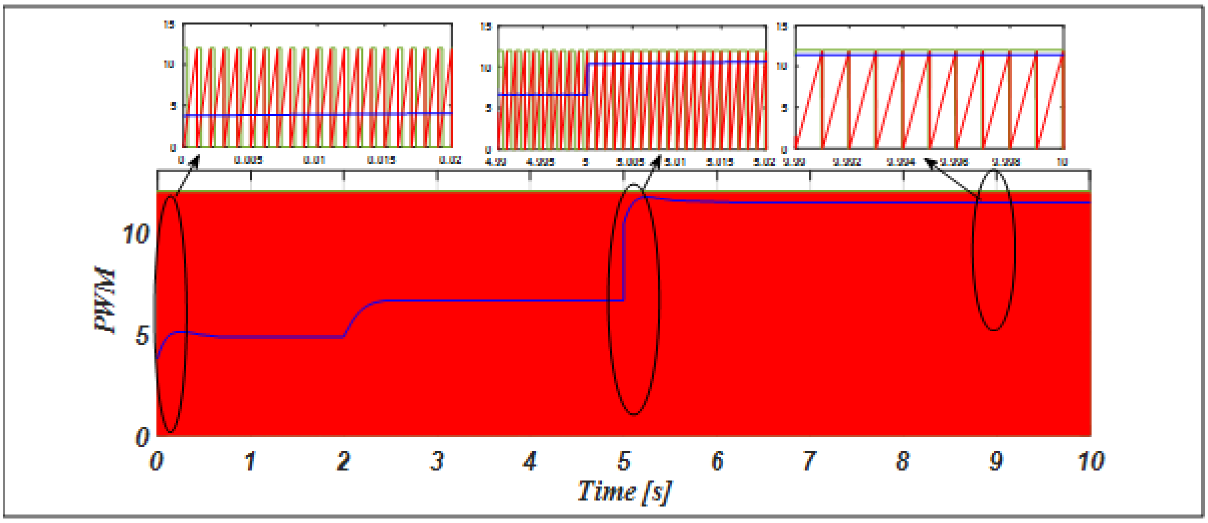

Figure II.45: Time-based representation of the PWM waveform for motor direct control.

Figure (45): Time-based representation of the PWM waveform for motor direct control) showcases the time-based representation of the PWM waveform used in direct control for motor control. The graph illustrates the variations in the pulse width over time.

The duty cycle, represented as a percentage, determines the width of each pulse in the PWM waveform. As the speed or load of the motor increases, the duty cycle also increases, resulting in wider pulses in the PWM waveform.

Direct control offers a more simplified approach compared to cascade control. By manipulating the pulse frequency and duty cycle of the PWM waveform, precise control over the motor's speed and response to load changes can be achieved. The wider pulses provide increased power to the motor, allowing it to generate more torque and adapt to different operating conditions.

Figure (45) provides a visual representation of how changes in speed and load impact the width of pulses in the PWM waveform. This emphasizes the effectiveness of direct control in achieving motor control objectives with simplicity and efficiency.

II.9 Conclusion:

In conclusion, this chapter has explored various aspects of DC motors in electromagnetic mixers. The focus was on motor characteristics and control techniques employed to regulate their performance. The electronic converters used for motor control and the identification of motor-specific parameters were also studied. Based on the simulation results, the Direct Control approach using the speed loop has shown good performance. It effectively achieved control objectives at a low cost. On the other hand, the cascaded control method demonstrated higher complexity and cost due to additional requirements such as the need for a speed sensor. Therefore, the Direct Control approach with the speed loop can be considered a promising and suitable option, delivering excellent performance and high efficiency at a low cost. This knowledge and experimentation will be applied in the upcoming chapter to implement and analyze the performance of the actual device. This theoretical and analytical study.

Chapter III: Implementation of Smart Agitator

III.1 Introduction :

In this chapter, we have explored the various stages involved in implementing the smart magnetic stirrer project, which offers intelligent features and advanced control mechanisms that revolutionize the mixing process. With its ability to regulate speed, direction, and other crucial parameters, the smart magnetic stirrer promises increased productivity, improved quality control, and reduced operating costs .

We began by visualizing the schematic diagram that represents the functioning of the smart magnetic stirrer. We discussed the main components and their roles, such as the DC motor and the control system responsible for regulating its performance. Additionally, we delved into the importance of temperature and plasma control, highlighting the methods and sensors used to maintain optimal conditions.

Furthermore, we discussed the selection of electronic components and the criteria for choosing them, including integrated controllers, sensors, motor drivers, and other essential elements. We explained the design of electronic circuits, including schematic diagrams and PCB design, illustrating the placement of components. We also explained the wiring and communication between different components in the circuit to provide a comprehensive understanding of the hardware configuration.

In this chapter, we will provide an overview of the application interface and its features, including remote control, monitoring of the mixing process, and data logging. Technical details of the application and its efficient usage will be explained.

The chapter also addressed the testing and evaluation process used to assess the performance of the smart magnetic stirrer. We discussed the results obtained from the tests and how they compare to the expected outcomes, evaluating the reliability, efficiency, and effectiveness of the system.

III.2 Flowchart of Smart Agitator :

- Flowchart of proposed smart agitator

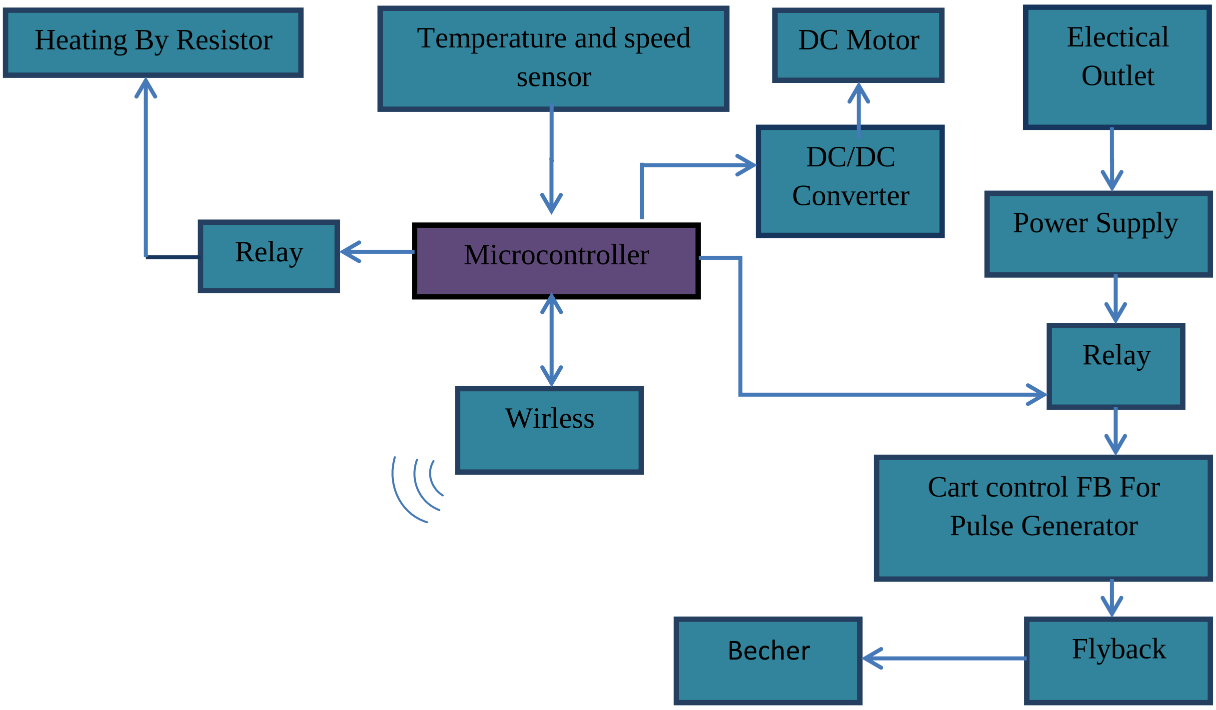

The wireless microcontroller can send commands to both the DC/DC converter to activate the motor and to the relay controlling the plasma production by operating the flyback circuit integrated in the reactor. It can also send commands to the relay controlling the heating feature in the magnetic stirrer motor. Additionally, this advanced controller receives information about changes in the liquid temperature and motor speed from the Temperature and speed sensor. By utilizing this data, the microcontroller ensures accurate monitoring and precise control of the system parameters to optimize performance and efficiency.

III.3 Choice of Electronics Components :

In this project, many electronic components were used

III.3.1 Arduino WeMo ESP8266 :

The Arduino WeMo ESP8266 is a development board that combines the functionality of an Arduino board with the power and connectivity of the ESP8266 Wi-Fi module. It is designed to enable easy prototyping and development of Internet of Things (IOT) projects [Had 09].

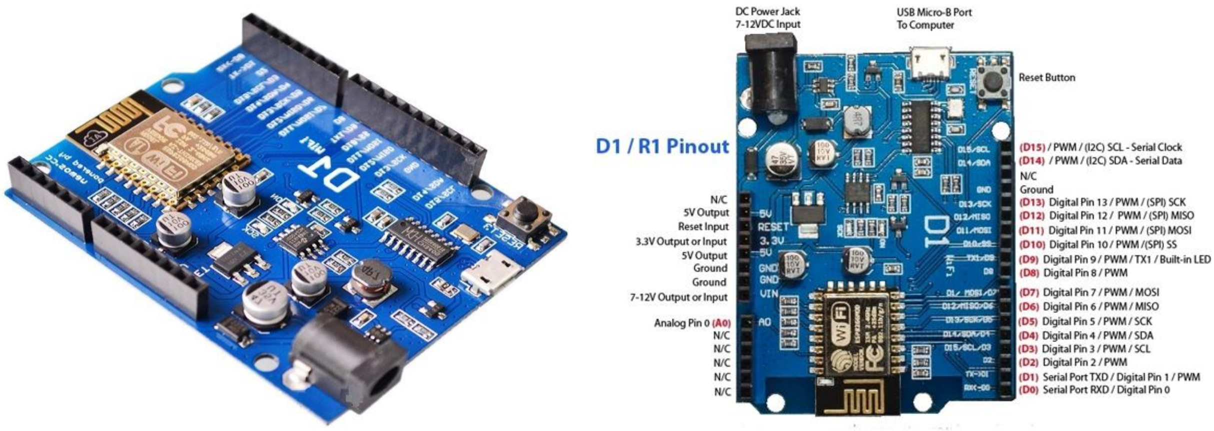

Figure III.1: Arduino WeMo ESP8266.

The WeMos D1 is an ESP8266 WiFi-based board that utilizes the Arduino Uno layout. It operates at a voltage of 3.3V and features a microcontroller called ESP-8266EX. The board offers 11 digital I/O pins and 1 analog input pin, providing flexibility for connecting and controlling external components and sensors. It has a clock speed of either 80MHz or 160MHz, depending on the configuration.

In terms of memory, the WeMos D1 boasts 4M bytes of flash, which is larger compared to the flash memory found in an Arduino Uno. The board has dimensions of 68.6mm x 53.4mm and weighs approximately 25g, making it compact and lightweight.

To connect the WeMos D1, a Micro-B type USB cable, commonly known as an "Android Cable," is used. This cable serves for both programming the board and supplying power.

Overall, the WeMos D1 combines the capabilities of the ESP8266 WiFi module with the familiar Arduino Uno layout. It offers enhanced memory capacity and provides a range of digital and analog pins for versatile project development. Its compact size and USB connectivity make it convenient for prototyping and various DIY applications [Had 09].

III.3.2 Presentation of the NE555 integrated circuit :

The 555 monolithic timing circuit is a versatile controller that serves as a highly stable and accurate timing solution. It can be used to generate precise time delays or function as an oscillator. With its flexible design, the NE555 circuit allows for precise timing control in both time delay and oscillation modes by utilizing external resistors and capacitors [Sha 19] .

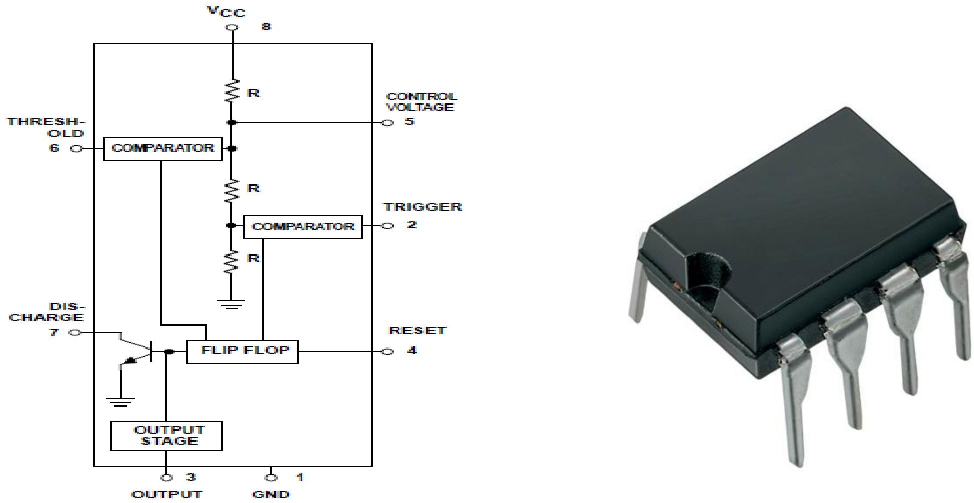

Figure III.2: Functional Diagram of NE555.

In time delay mode, the circuit achieves accurate timing by relying on a single external resistor and capacitor. On the other hand, in oscillation mode, two external resistors and one capacitor are employed to maintain precise frequency and duty cycle control.

Some key features of the NE555 timing circuit include a turn-off time of less than 2ms, a maximum operating frequency greater than 500kHz, and a wide timing range from microseconds to hours. It operates in both astable (oscillation) and monostable (time delay) modes, allowing for versatile functionality [Sha 19].

The 555 circuit is highly compatible with TTL logic, making it easy to integrate with other digital circuits. It also exhibits excellent temperature stability, with a variation of only 0.005% per °C.

Applications for the NE555 timing circuit include precision timing, pulse generation, sequential timing control, time delay generation, and pulse width modulation. It can be triggered and reset using falling waveforms, and its output structure is capable of handling high output currents up to 200mA, enabling its use in various demanding applications [Sha 19].

#	Nom	Description
1	GND	Ground
2	TRIG	Start of timing input. TRIG < $1/2$ CONT sets output high and discharge open
3	OUT	High current timer output signal
4	RESET	Active low reset input forces output and discharge low.
5	CONT	Controls comparator thresholds, Outputs $2/3\, V_{CC}$ allows bypass capacitor connection
6	THRES	Signals the end of the time delay when the voltage exceeds $2/3$ of V_{CC}
7	DISCH	Open collector output to discharge timing capacitor
8	VCC	Input supply voltage, 4.5 V to 16 V

schematic symbol of the NE555

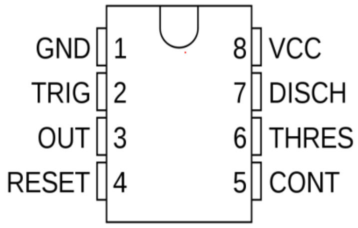

Table III.1: the pins of the NE555 .

III.3.3 Gate Drive Optocoupler HCPL-3180 :

Gate Drive Optocoupler HCPL-3180 is a family of devices that consist of a GaAsP LED optically coupled to an integrated circuit with a power stage. These optocouplers are designed for high -frequency driving of power IGBT and MOSFETs used in various applications such as Plasma Display Panels, DC/DC converters, and motor control inverters[Han 20].

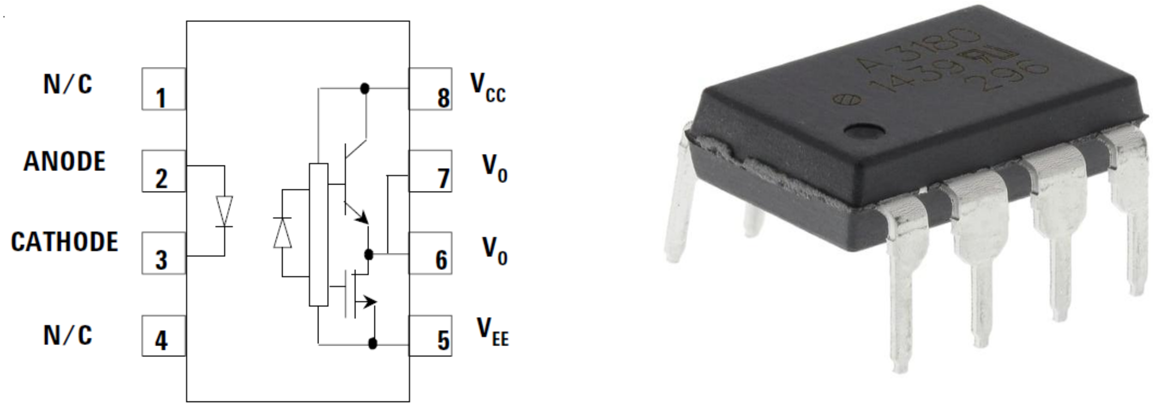

Figure III.3: Functional Diagram of Gate Drive Opt coupler HCPL-3180 .

Key Features of these optocouplers include a minimum peak output current of 2A, a maximum switching speed of 250 KHz, and a high-speed response with a maximum propagation delay of 200 ns over the temperature range. They also offer a minimum common mode rejection (CMR) of 10 KV/us at VCM=1500V, under voltage lockout protection (UVLO) with hysteresis, and a wide operating temperature range of -40 °C to +100 °C. The devices operate within a wide VCC range of 10V to 20V and have a pulse width distortion of 20 ns (typical). They comply with safety approvals such as UL, CSA, and DIN EN 60747-5-2.

Gate Drive Optocouplers find applications in Plasma Display Panels, distributed power architecture, switch mode rectifiers, high-performance DC/DC converters, switch mode power supplies, uninterruptible power supplies, and isolated IGBT/Power MOSFET gate drive systems.

Overall, these devices provide efficient and reliable opto-isolation for driving power devices, ensuring the safe and precise control of IGBT and MOSFET gates in a variety of applications[Han 20].

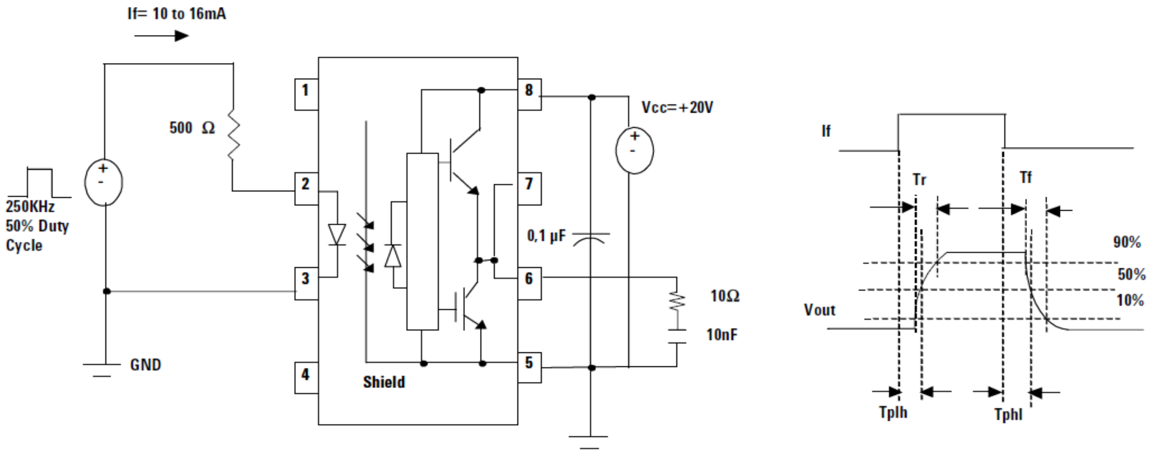

Figure III.4 : TPLH, TPHL, Tr and Tf Test Circuit and Waveform**.**

III.3.4 Phototransistor EL817 Series :

The EL817 series is a collection of optocoupler devices designed for various electronic applications. Each device in the series consists of infrared emitting diodes that are optically coupled to a phototransistor detector. These devices are conveniently packaged in a 4-pin dual in-line package (DIP), with options available for both wide-lead spacing and surface-mount technology (SMD) [Phi 94].

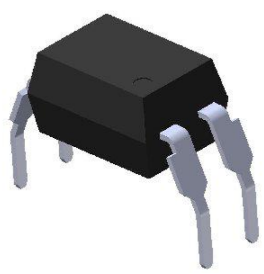

Figure III.5 : Phototransistor EL817 Series.

The EL817 series offers several notable features. It has a current transfer ratio (CTR) ranging from 50% to 600% at an input current (IF) of 5mA and a collector-emitter voltage (VCE) of

5V. This allows for efficient signal transfer between input and output circuits. Additionally, the devices provide high isolation voltage, with a rating of 5000 V rms, ensuring electrical isolation and protection.
With a creepage distance of over 7.62mm, the EL817 series provides enhanced safety measures. It is capable of operating at temperatures up to +110°C, making it suitable for a wide range of environments. The devices feature a compact small outline package, allowing for space-efficient integration into electronic systems. Moreover, they are Pb-free and RoHS compliant, meeting environmental standards [Phi 94].

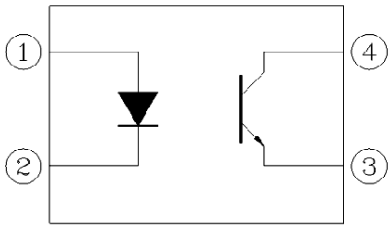

Figure III.6: Schematic of EL817

The EL817 series has obtained various certifications, including UL, VDE, SEMKO, NEMKO, DEMKO, FIMKO, and CSA. These certifications validate the quality and reliability of the devices.
Applications for the EL817 series are diverse and include programmable controllers, system appliances, measuring instruments, telecommunication equipment, and home appliances like fan heaters. The optocouplers excel at facilitating signal transmission between circuits with different potentials and impedances, ensuring secure and reliable communication.
Overall, the EL817 series offers reliable performance, electrical isolation, and versatility, making it a preferred choice for a wide range of electronic applications [Phi 94].

III.3.5 Transistors MOSFET :

The metal grid is isolated from the semiconductor substrate by an oxide layer, hence the name MOS (Metal-Oxide-Semiconductor). By controlling the gate voltage (VGS), the current flow from the drain to the source (ID) can be varied [Agi 03].

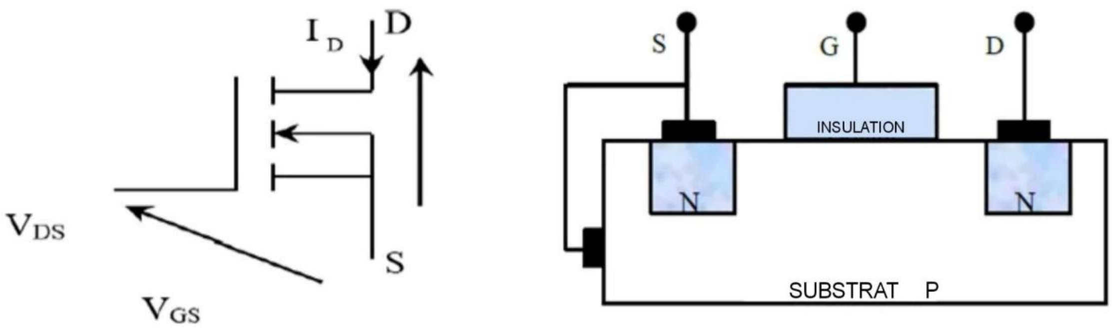

Figure III. 7: N-channel MOSFET transistor structure.

- **Le transistor IGBT** : (Insulated Gate Bipolar Transistor)

is an electronic switch that combines the advantages of MOSFETs and Bipolar transistors. It shares similarities with MOSFETs, such as a high gate impedance for fast switching and low control energy, and with Bipolar transistors, it can handle high blocking voltages and high conduction currents. It is extensively used in applications ranging from 600V to 4.5KV [Agi 03].

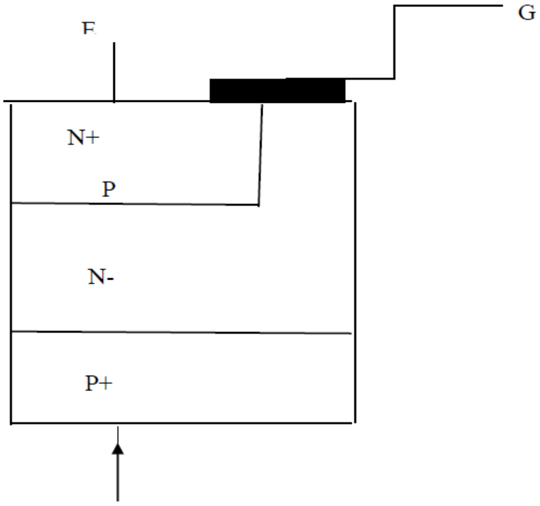

Figure III. 8: Structure of an IGBT transistor .

❖ The semiconductor used :

In this work, we will use the IGBT module UFG40N60. We focus on the dynamic estimation of dv/dt, repetitive avalanche evaluation, central isolation support hole, fast switching, ease of parallelization, and simple driving conditions.

- **IGBT UFG40N60 :**

By employing the innovative Field Stop IGBT technology, the ON Semiconductor's Field Stop IGBTs deliver outstanding performance in solar inverters, inverters, welders, microwave ovens, telecommunications, energy storage systems (ESS), and PFC applications, where low conduction and switching losses are crucial [Eve 10].

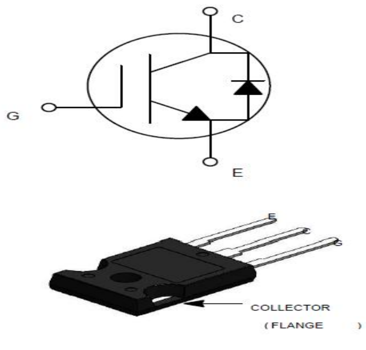

Figure III. 9: IGBT UFG40N60.

III.3.6 Radiator :

The main cause of component damage in the majority of cases is the increase in temperature. To address this, an aluminum heat sink radiator, as shown in Figure (10), will be mounted on the back of each IGBT. Aluminum is chosen for this purpose because it is a good heat conductor.

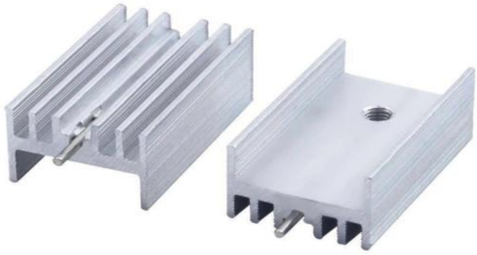

Figure III. 10: Radiator.

III.3.7 Power Relay :

A relay is an electrical device that acts as an electrically controlled switch. It consists of a coil, an armature, and one or more sets of contacts. When an electrical current flows through the coil, it creates a magnetic field that attracts or repels the armature, causing the contacts to either open or close. Relays are used to control the flow of electrical power to different circuits or components in a system. They can be used to switch high currents, control complex circuits, provide electrical isolation, or interface between different voltage levels. Relays are commonly used in various applications, including industrial control systems, automotive systems, telecommunications, home automation, and more. They are essential for enabling automation, remote control, and protection in electrical and electronic systems [Soy 93].

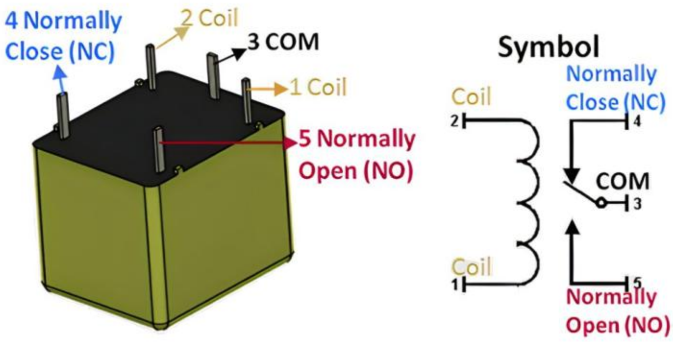

Figure III. 11: Relay .

The RELAY offers the following features: It has a miniature size with a universal terminal footprint, making it easy to install in various applications. It has a high contact capacity of 10 A, allowing for the switching of high-current loads. The TV-5 type is available as the standard version, with both the 1 Form A and 1 Form C types conforming to the TV-5 standard (N.O. side only for 1 Form C). The relay has obtained approval from VDE and TÜV, ensuring compliance with industry standards. It features a sealed construction for automatic cleaning in the standard type, enhancing reliability. It also offers options for Class B and F coil insulation types. Additionally, there is an EN60335-1 GWT compliant type available, tested and certified by VDE. Furthermore, a surge voltage 6 kV type is also available, providing protection against voltage surges.

The relay finds typical applications in various areas such as home appliances (e.g., air conditioner, heater), office machines (e.g., PPC, facsimile), and vending machines.

These features make the relay suitable for a range of applications in different industries, ensuring reliable and efficient switching operations [Soy 93].

III.4 Circuit Electronics Design :

The electronic board has been designed using Altium Designer software, which provides a powerful and comprehensive environment for (3D) electronic circuit design. This software enables accurate and realistic visualization and analysis of the board, helping to improve the device's performance and ensure its compliance with technical requirements.

We will now present the (3D) design of the device created using Altium Designer. We will focus on the distribution of components, spatial arrangement of parts, and details of the interconnections between them.

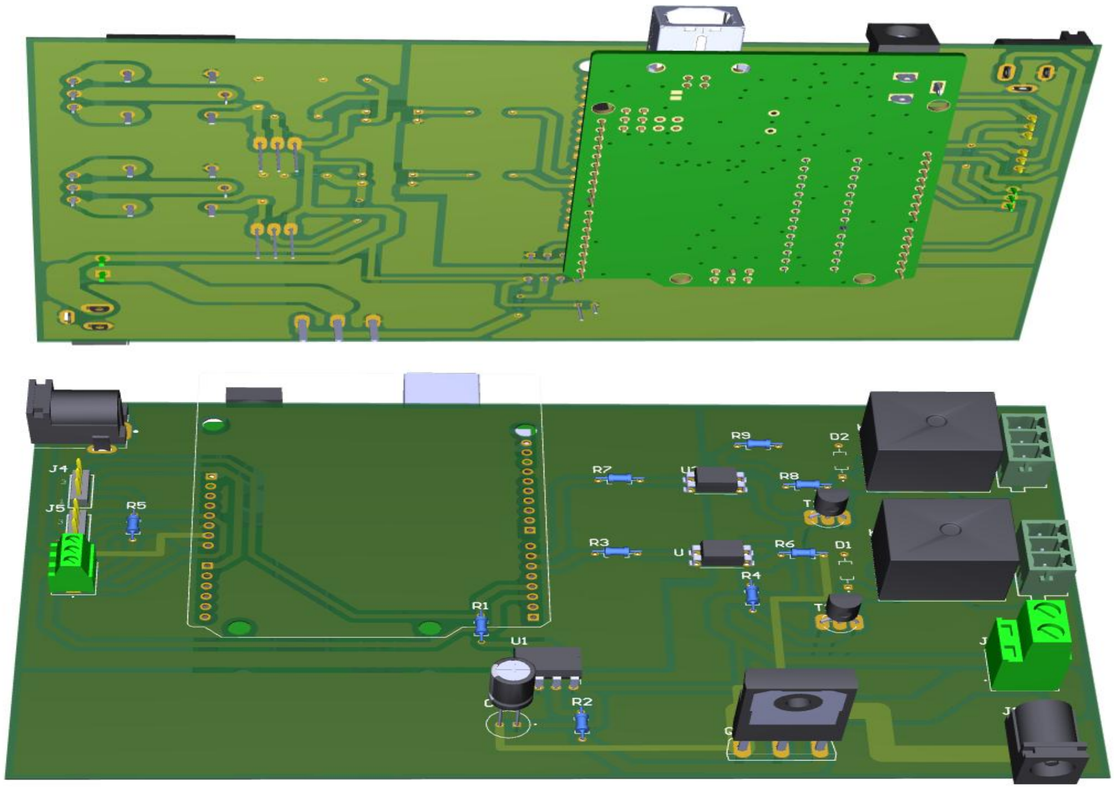

Figure III.12: Electronic board for total control (3D)

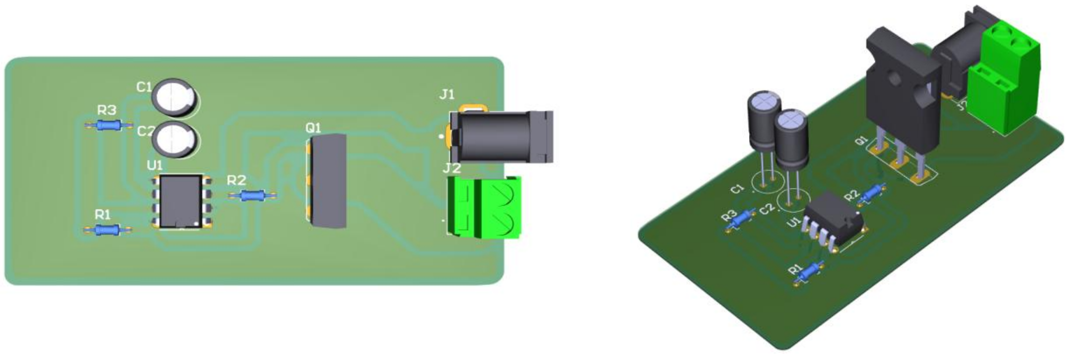

Figure III.13 design (3D) of the electronic board for plasma production

- ❖ In this section, we will showcase the detailed 2D images that depict the precise positioning of each electronic component on the circuit board. These images will highlight the strategic placement of components, taking into account factors such as signal flow, thermal considerations, and ease of assembly. Additionally, the interconnections between the components will be clearly illustrated, showcasing the intricate network of traces and vias that enable the flow of electrical signals
- ❖ It will also show the gradual stages of making this card:

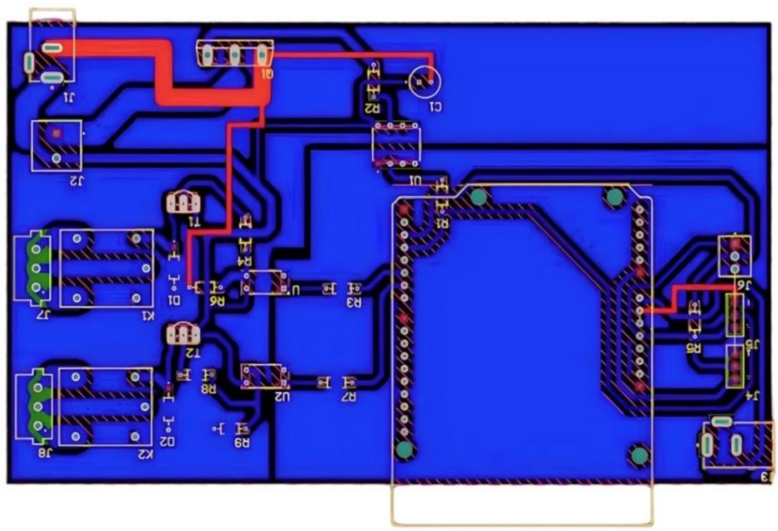

Figure III.14 Electronic board for total control (2D)

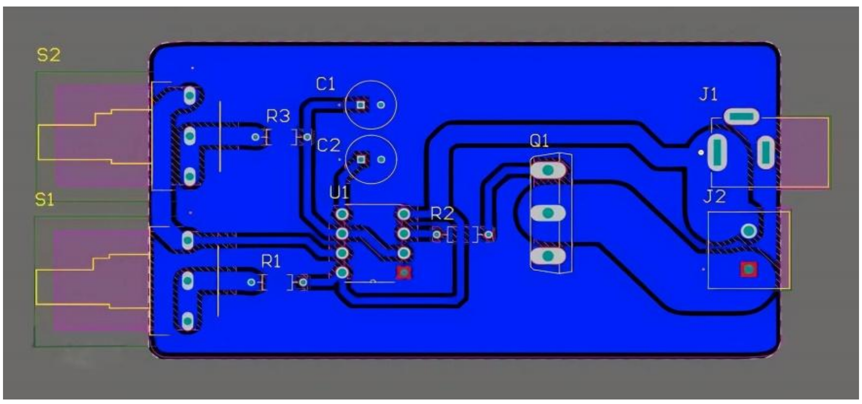

Figure III.15 Electronic board for Plasma (2D)

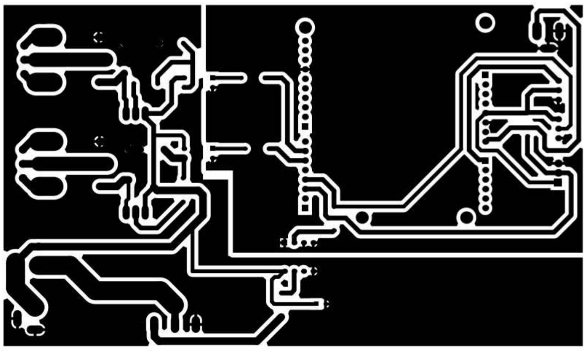

Figure III.16 Full control electronic board (2D) for CNC printing .

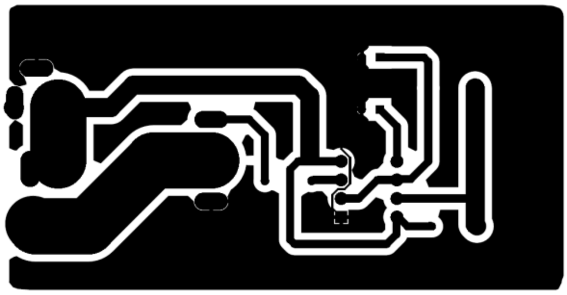

Figure III.17: Plasma Electronic board (2D) for CNC printing .

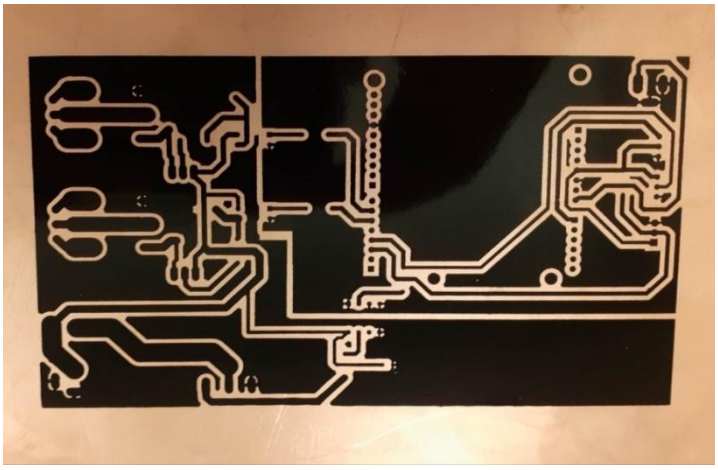

Figure III.18: format after printing.

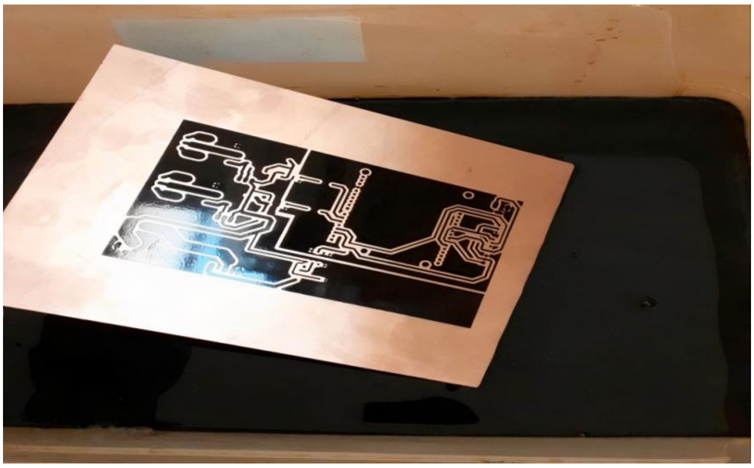

Figure III.19: Put the Electronic Board in the Acid.

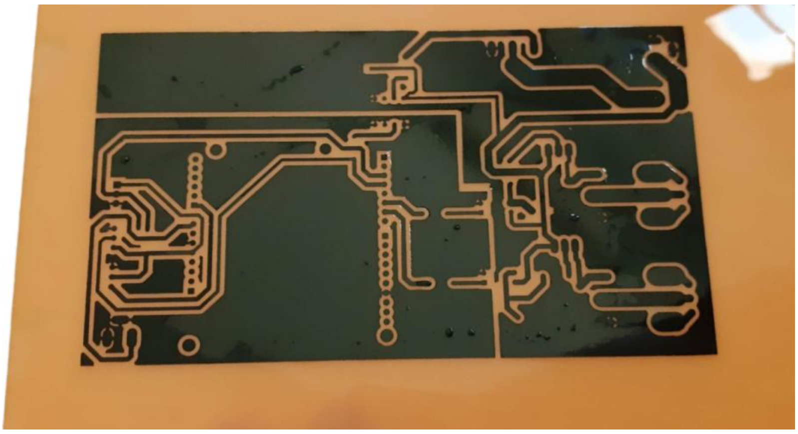

Figure III.20: Remove the Electronic Board from the Acid.

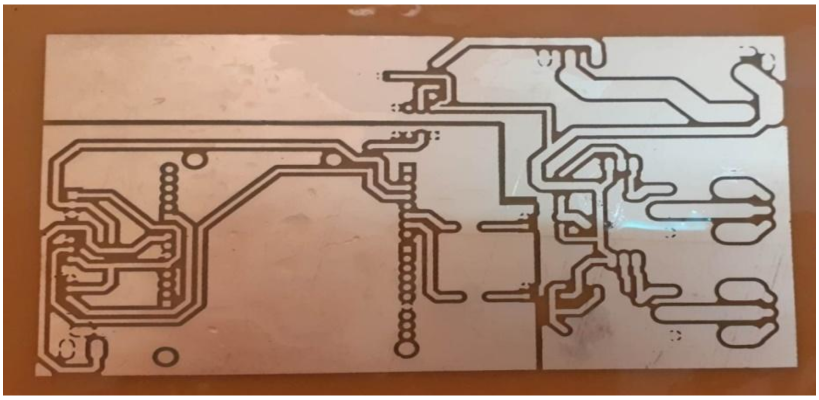

Figure III.21: Remove the printing ink from the board.

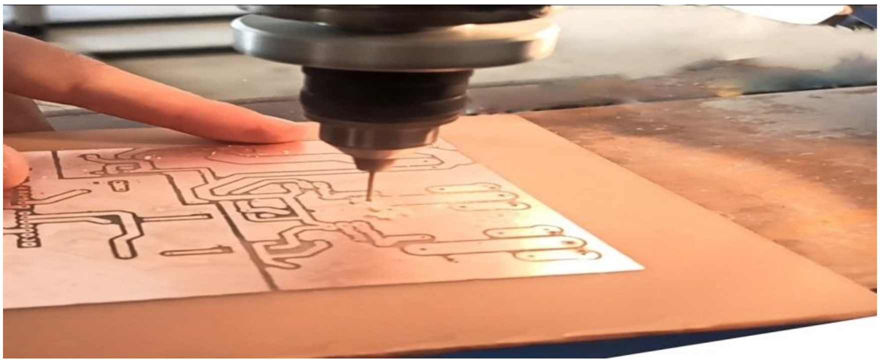

Figure III.22: Drilling places for electronic components .

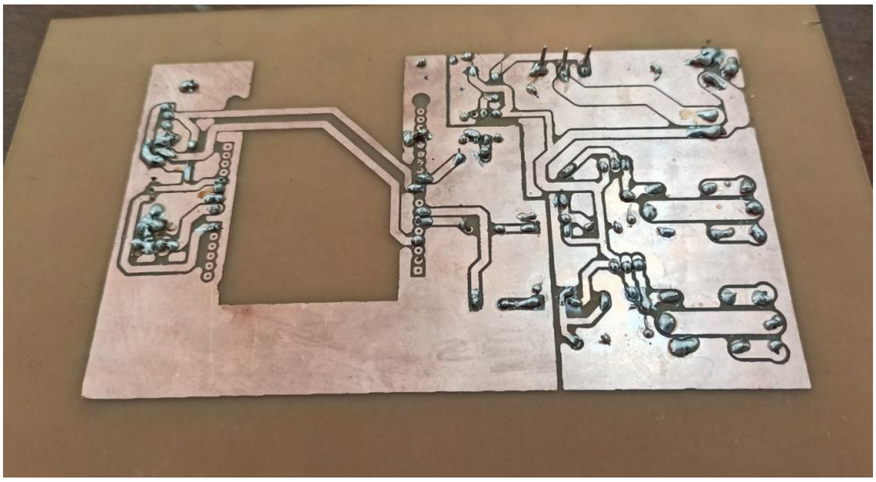

Figure III.23: Soldering electronic components.

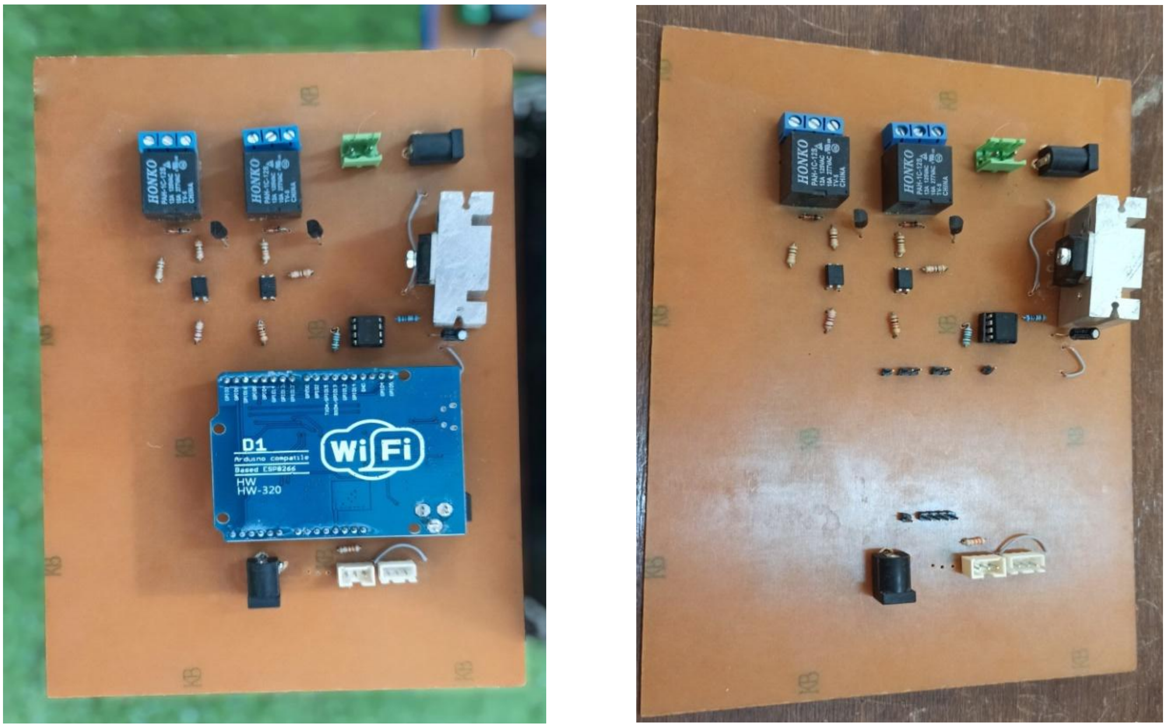

Figure III.24: The ultimate mass control Board.

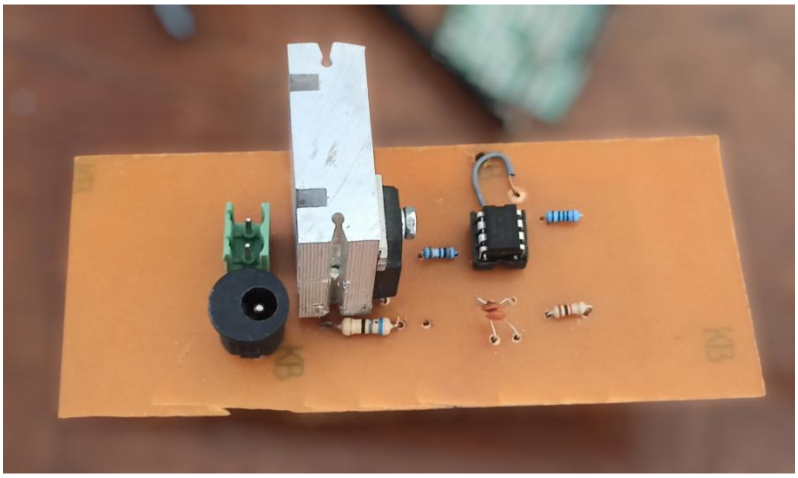

Figure III.25: The final form of an electronic plasma board.

- **Wiring and connections between the various components in a circuit :**

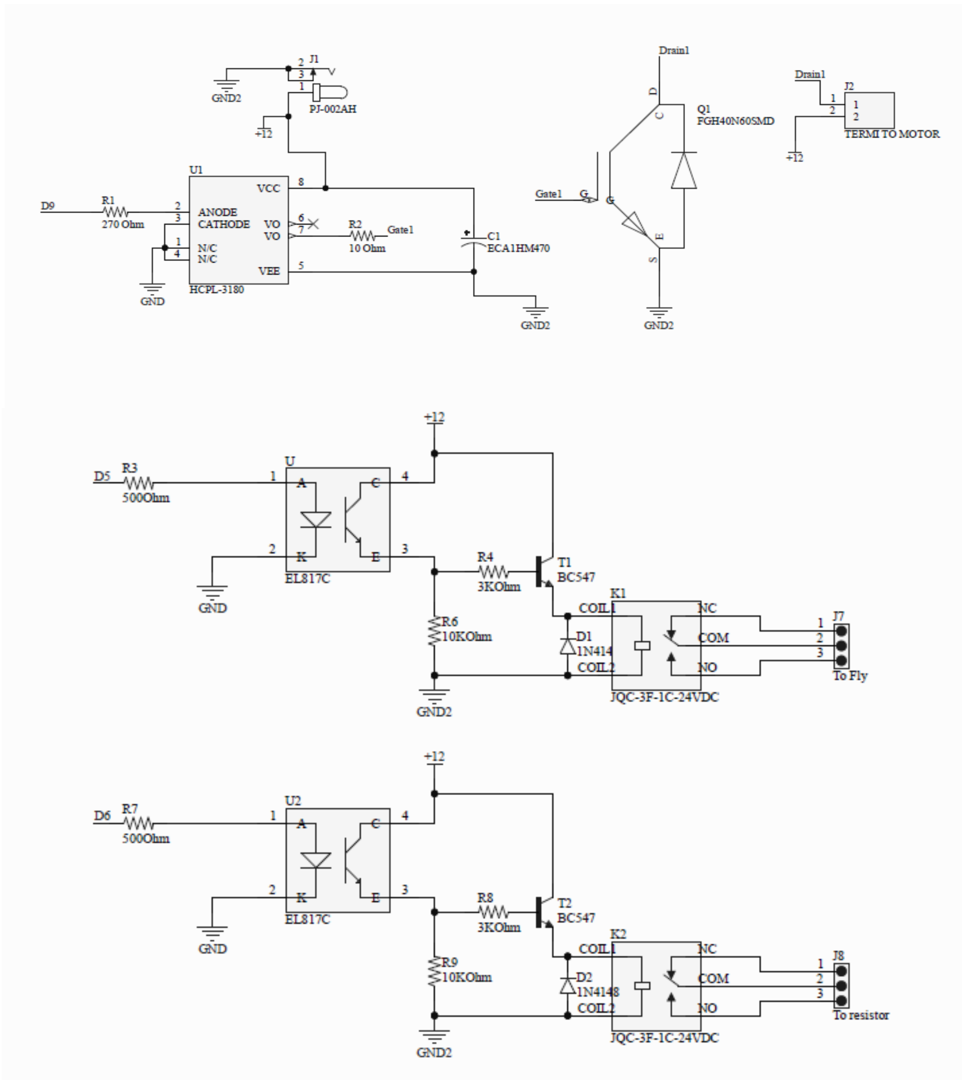

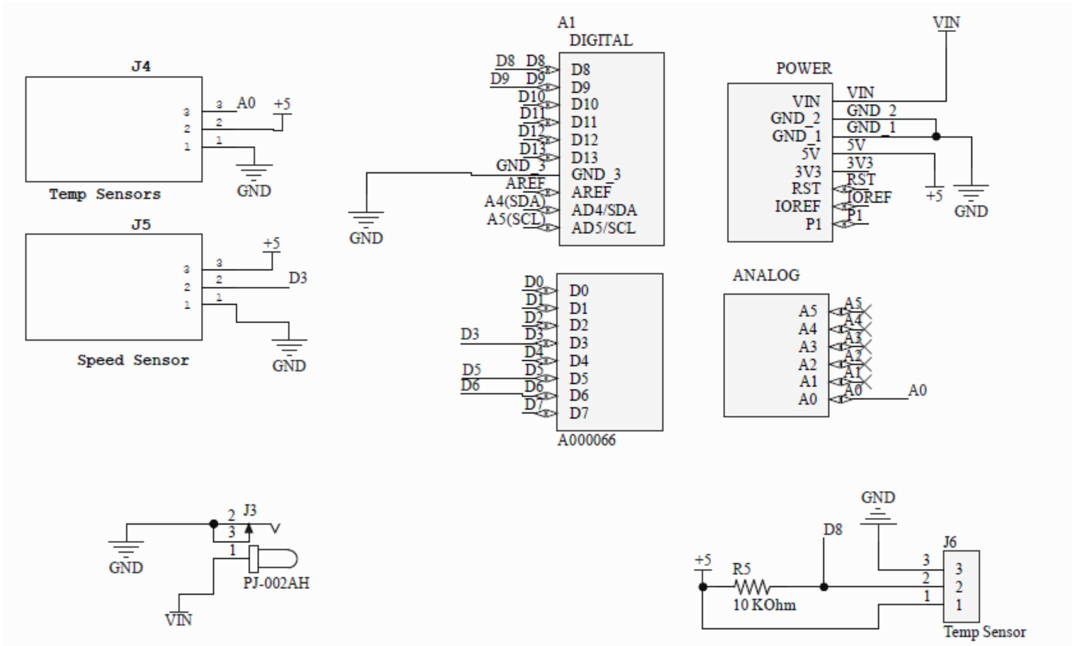

Figure III.26: schematic of the Magnetic Stirrer control board.

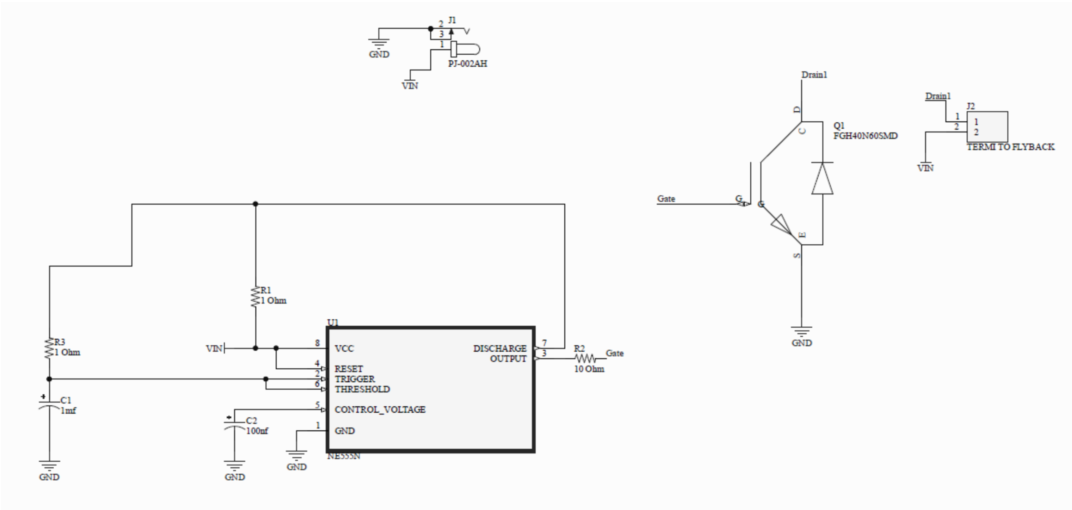

Figure III.27: Schematic of the plasma output board .

III.5 Control System of DC Motor :

III.5.1 The role of DC motor in the smart agitator :

The DC motor plays a crucial role in the operation of a smart agitator. It is responsible for providing the necessary rotational power and control to drive the agitator shaft, which in turn facilitates the mixing or agitation process. Here are some key aspects of the DC motor's role in a smart agitator:

1- **Rotational Power :** The DC motor converts electrical energy into mechanical rotational power. It generates the torque required to rotate the agitator shaft, enabling the movement of blades, paddles, or other mixing elements. The rotational power produced by the DC motor determines the agitator's ability to effectively mix or agitate substances.

2- **Speed Control :** The DC motor offers precise speed control, allowing the smart agitator to operate at different rotational speeds. By adjusting the voltage or current supplied to the motor, the speed of the agitator can be varied as per the specific mixing requirements. This speed control capability enables fine-tuning of the agitation process for optimal mixing efficiency.

3- **Direction Control :** The DC motor can be easily controlled to change the direction of rotation. This feature is beneficial when bidirectional agitation is required, such as in applications where substances need to be mixed in both clockwise and counterclockwise directions. The ability to reverse the motor's rotation allows for versatile mixing capabilities.

4- **Automation and Integration :** The DC motor in a smart agitator can be integrated with control systems and sensors to enable automation and intelligent operation. By utilizing feedback from sensors, such as those monitoring temperature, viscosity, or composition, the motor's speed and power can be adjusted automatically to maintain desired mixing parameters. This integration allows for precise and consistent mixing results.

5- **Energy Efficiency :** DC motors are known for their high efficiency and energy-saving capabilities. They convert electrical energy into mechanical power with minimal energy loss. By utilizing a DC motor, a smart agitator can optimize energy consumption, reducing operating costs and environmental impact.

6- **Compact Design :** DC motors are generally compact and lightweight, making them suitable for integration into the compact design of a smart agitator. Their small form factor allows for efficient space utilization, especially in applications where the agitator needs to fit within limited space constraints.

Overall, the DC motor serves as the driving force behind the smart agitator, providing the rotational power, speed control, and direction control necessary for effective mixing or agitation. Its integration with control systems and sensors enables automation, intelligent operation, and energy efficiency, making it a vital component in modern agitator technologies.

III.5.2 Explain the control system that regulates the speed and direction of the DC motor :

The control system that regulates the speed and direction of a DC motor using an Arduino typically involves the following components and principles :

1. DC Motor : A direct current (DC) motor is the primary actuator that converts electrical energy into mechanical motion. It consists of a rotor and a stator, and its speed and direction can be controlled by varying the voltage and polarity applied to the motor terminals.

2. H-Bridge : An H-bridge is a circuit configuration commonly used to control the direction of DC motors. It allows the motor to rotate in both clockwise and counterclockwise directions by reversing the polarity of the applied voltage. The H-bridge usually consists of four transistors or switches arranged in an H-like configuration.

3. Arduino : An Arduino microcontroller board is utilized to interface with the motor and control its speed and direction. The Arduino board receives commands from a user or an external system and generates the necessary signals to drive the motor.

4. Pulse : Width Modulation (PWM): PWM is a modulation technique used to control the average voltage applied to the motor, thereby controlling its speed. The Arduino generates a PWM signal by rapidly switching the output voltage between high and low states. By adjusting the duty cycle (percentage of time the signal is high), the average voltage and motor speed can be regulated.

5. Motor Driver : A motor driver is an electronic device that amplifies the control signals from the Arduino to provide sufficient power to drive the motor. It protects the Arduino's digital pins from excessive current and voltage.

6. Control Algorithm : The control algorithm implemented in the Arduino determines the speed and direction of the motor based on user input or system requirements. It can be as simple as reading a potentiometer value to set the desired speed or receiving commands from an external source such as a computer or sensor.

Here's a general overview of the steps involved in controlling the speed and direction of a DC motor using an Arduino:

- **a.** . Connect the motor to the motor driver and ensure the power supply is properly connected.
- **b.** Establish the connections between the Arduino board and the motor driver, ensuring the control pins are correctly connected.
- **c.** Write the Arduino code to set up the necessary input/output (I/O) pins, configure PWM output, and define the control algorithm.
- **d.** The control algorithm can involve reading input signals from sensors or user interfaces, such as potentiometers or buttons, to set the desired speed and direction.
- **e.** Use the Arduino's PWM capability to generate a varying duty cycle, which controls the average voltage applied to the motor and thus its speed.

f. Based on the control algorithm, control the motor driver's input pins to set the appropriate polarity and direction for the motor.

g. Upload the Arduino code to the board and power it up. The Arduino will execute the code and control the motor accordingly.

By manipulating the PWM duty cycle and controlling the direction of the motor through the motor driver, the Arduino can regulate the speed and direction of the DC motor. The specific implementation details may vary depending on the motor driver and Arduino model used, as well as the specific requirements of the application.

III.6 Temperature and Plasma Control :

Temperature and plasma control play crucial roles in the operation of an agitator. Here's why they are important:

III.6.1 Temperature Control :

Temperature control is vital for maintaining optimal conditions within the agitator. Here are a few reasons why temperature control is essential:

- **Process Efficiency :** Different chemical reactions or physical processes taking place within the agitator may require specific temperature ranges for optimal efficiency. Controlling and maintaining the desired temperature ensures that the reactions or processes occur at their intended rates, leading to improved productivity and desired outcomes.
- **Product Quality :** Temperature variations can significantly impact the quality of the products being processed in the agitator. Precise temperature control helps ensure consistent product quality, whether it involves mixing, blending, or chemical reactions. Maintaining a stable temperature minimizes variations that could affect product properties, such as viscosity, stability, or molecular structure.
- **Safety :** In some cases, controlling the temperature is crucial for safety reasons. Certain reactions may be exothermic, generating heat and potentially leading to hazardous conditions if not properly controlled. Monitoring and regulating the temperature mitigate the risk of overheating, thermal runaway, or other dangerous situations.

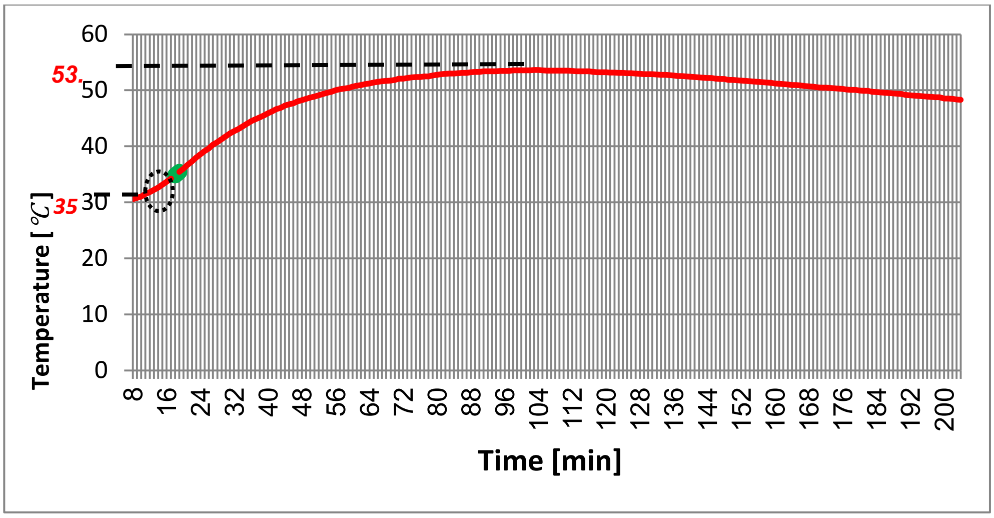

Figure III.28: The variations in liquid temperature over time.

- The difficulty in adjusting the temperature and the observed irregularity can be explained by the programming of the Arduino to control the heating element. When the command to start heating is sent to the electronic control panel, the relay connected to the heating plate is activated, and the temperature starts to rise. However, the issue lies in the delay between the moment the heating is stopped and the moment it actually stops.

In the provided scenario, the heating is programmed to stop when the temperature reaches 35 degrees Celsius. However, due to the delay in the relay response or the time it takes for the system to recognize the temperature change, the actual temperature continues to increase even after the command to stop heating is sent. This leads to an overshoot in the temperature, causing it to reach 63 degrees Celsius before it starts decreasing.

To address this issue and improve temperature control, several modifications can be made to the programming logic. These may include implementing a more responsive relay system, reducing the delay in temperature sensing and relay activation, or using feedback control algorithms to adjust the heating power based on the measured temperature. By fine-tuning the programming and ensuring a faster and more accurate response, it will be possible to achieve better temperature regulation and minimize the observed irregularities.

III.6.2 Plasma Control :

Plasma control is particularly relevant when working with plasma-based agitators, such as plasma reactors or plasma etching equipment. Here's why plasma control is important:

- **Process Optimization :** Plasma parameters, such as plasma density, ion energy, and composition, directly influence the effectiveness of plasma-based processes. Accurate control of these parameters ensures consistent and optimized process outcomes, such as surface modification, material deposition, or etching rates. Precise plasma control allows for fine-tuning the process parameters to achieve desired results.

- **Uniformity :** Achieving a uniform plasma distribution across the agitator chamber is crucial for consistent and reliable results. Plasma control mechanisms, such as gas flow rates, RF power, and electrode design, enable uniform plasma generation and distribution, reducing process variations and achieving homogenous treatment across the substrate or material being processed.
- **Equipment Protection :** Plasma control also helps protect the agitator and associated equipment. Uncontrolled or unstable plasma conditions can lead to arcing, electrode damage, or premature equipment failure. Implementing effective control strategies safeguards the longevity and performance of the agitator, minimizing downtime and maintenance costs.

In summary, temperature and plasma control are essential in agitator operations to ensure process efficiency, product quality, safety, and equipment protection. Precise control of these factors enables reliable and optimized outcomes in various applications, ranging from chemical reactions to plasma-based processes.

III.6.3 Regulate the temperature :

1. **Control System :** The control system is used to regulate the heating process. You can use the application interface to open or close the heating feature based on signals sent from the application to the device.

2. **Temperature Measurement :** Through the application interface, you can read the temperature of the liquid connected to your device. You may have a built-in temperature sensor in the device that measures the temperature and converts it into a reading displayed on the application interface.

3. **Power Control :** You can also use the application interface to control the desired heating power. You can adjust the level of power based on your personal preferences or current needs.

4. **Temperature Monitoring :** Based on the available readings from the application interface, you can monitor the temperature associated with the device. You can use this information to monitor temperature changes and ensure they align with the required needs and specifications.
5. **User Interface :** All these functions are achieved through the user interface of the developed application. The user interface provides an easy and convenient way to control and monitor the heating process and temperature readings.

By utilizing these functions in the application, you can easily control the heating process and monitor the temperature according to your needs and personal preferences.

III.6.4 Plasma Generation :

1. Flyback Converter: The device incorporates a flyback converter, which is an electronic circuit that converts the input voltage to a high-voltage, high-frequency pulse. This high-frequency pulse is then used to excite and generate plasma.
2. Power Supply: The device requires a dedicated power supply that can deliver the necessary voltage and current levels to generate and sustain the plasma. The power supply may be integrated into the device or provided externally.
3. Electronic Control: The plasma generation process can be controlled electronically through the use of specialized electronic circuits and components. These components ensure the proper generation and control of the plasma, allowing for adjustments in intensity, duration, or frequency as required.

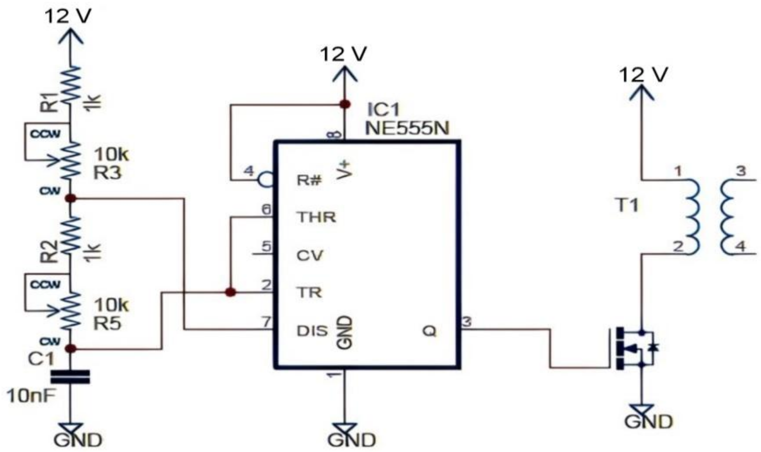

Figure III.29: Efficient Flyback Driver High Volts circuit using NE555 .

III.6.5 Liquid temperature sensor :

The DS18B20 is a digital thermometer with a 1-wire interface. It has a wide temperature range of -55˚C to 125˚C and provides temperature measurements with resolutions ranging from 9-bit to 12-bit. The sensor has a unique 64-bit serial code for addressing within the 1-wire network, allowing multiple sensors to be connected on a single data line. It operates at a voltage of 3.3~5V and consumes around 1mA of current. The DS18B20 has a quick conversion time of less than 750 ms and can be easily interfaced with microcontrollers or microcomputers, making it suitable for various temperature monitoring applications[Max 08].

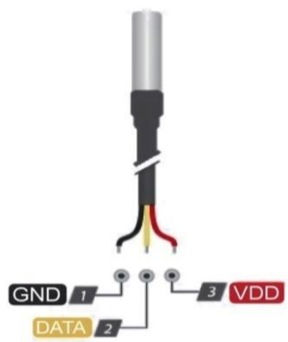

Figure III. 29: Liquid temperature sensor.

III.6.6 Speed sensor :

The KY-035 Hall Magnetic Sensor is a module based on the Hall effect principle that detects changes in magnetic fields. It consists of a Hall sensor and supporting circuitry in a compact package. The module has three pins: VCC for power, GND for ground, and Signal for the digital output [Joy 17].

When a magnet approaches the Hall sensor, it generates a voltage proportional to the magnetic field strength. The module's circuitry detects this voltage change and provides a digital signal indicating the presence or absence of a magnetic field.

The KY-035 module is versatile and used for various applications, including speed measurement, proximity detection, position sensing, and magnetic field monitoring. It can be easily integrated with microcontrollers or Arduino boards to interface with other components and perform specific tasks based on magnetic field detection [Joy 17].

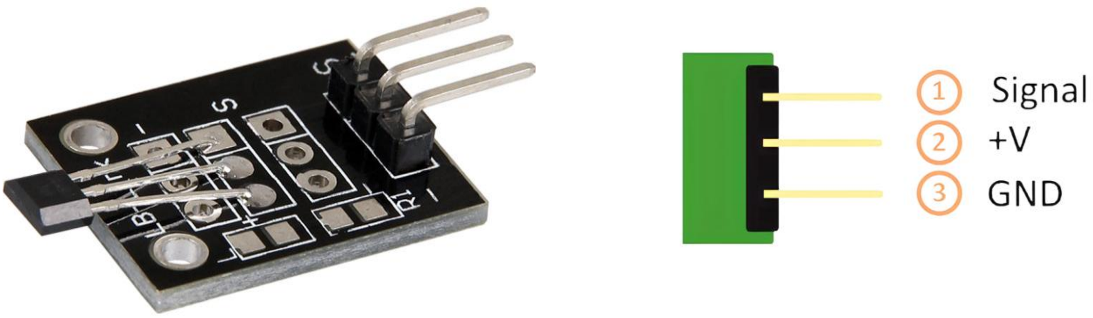

Figure III. 30: magnetic sensor module.

✓ We tested this speed sensor and it gave excellent results :

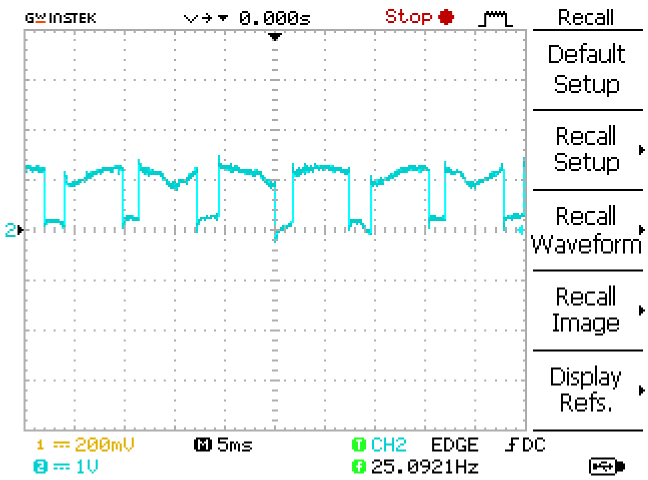

Figure III. 31: Oscilloscope result of the speed sensor.

- Based on the oscilloscope readings of the speed sensor, excellent results have been obtained. The changes in motor speed over time were accurately recorded. These results reflect the high capability of the speed sensor in accurately and effectively monitoring motor speed. This information contributes to a better understanding of motor performance and evaluation. It can be utilized to improve motor efficiency and adjust its speed for optimal performance in various applications. Additionally, it can be used for diagnostic and maintenance purposes to detect any potential issues and take necessary actions. The oscilloscope results contribute to the development of knowledge and understanding of motor performance, enabling future enhancements.

III.7 Smart android application associated with circuit electronics of agitator :

The system relies on Internet of Things (IOT) technology to control the device. The device, based on the Arduino Wi-Fi WeMo , is connected to the internet and a Wi-Fi network. It is programmed to communicate with the device through the provided IP addresses. By sending specific commands to these addresses, the application can control various functions of the device. For example, sending the command "192.168.4.1/ONPLASMA" activates the plasma generation, while "192.168.4.1/OFFPLASMA" stops it. Similarly, "192.168.4.1/ONTEMP" turns on the heating, and "192.168.4.1/OFFTEMP" turns it off. To adjust the speed, the command "192.168.4.1/PSPEED" increases the speed, and "192.168.4.1/MSPEED" decreases it. The command "192.168.4.1/SPEED" sets the desired speed. Furthermore, the application can receive information from sensors integrated into the device. The temperature reading can be obtained by accessing "192.168.4.1/TEMP," while the speed measurement is available through "192.168.4.1/SPEED." This allows the application to monitor and manage the device's operations remotely, providing enhanced control and convenience through IoT technology.

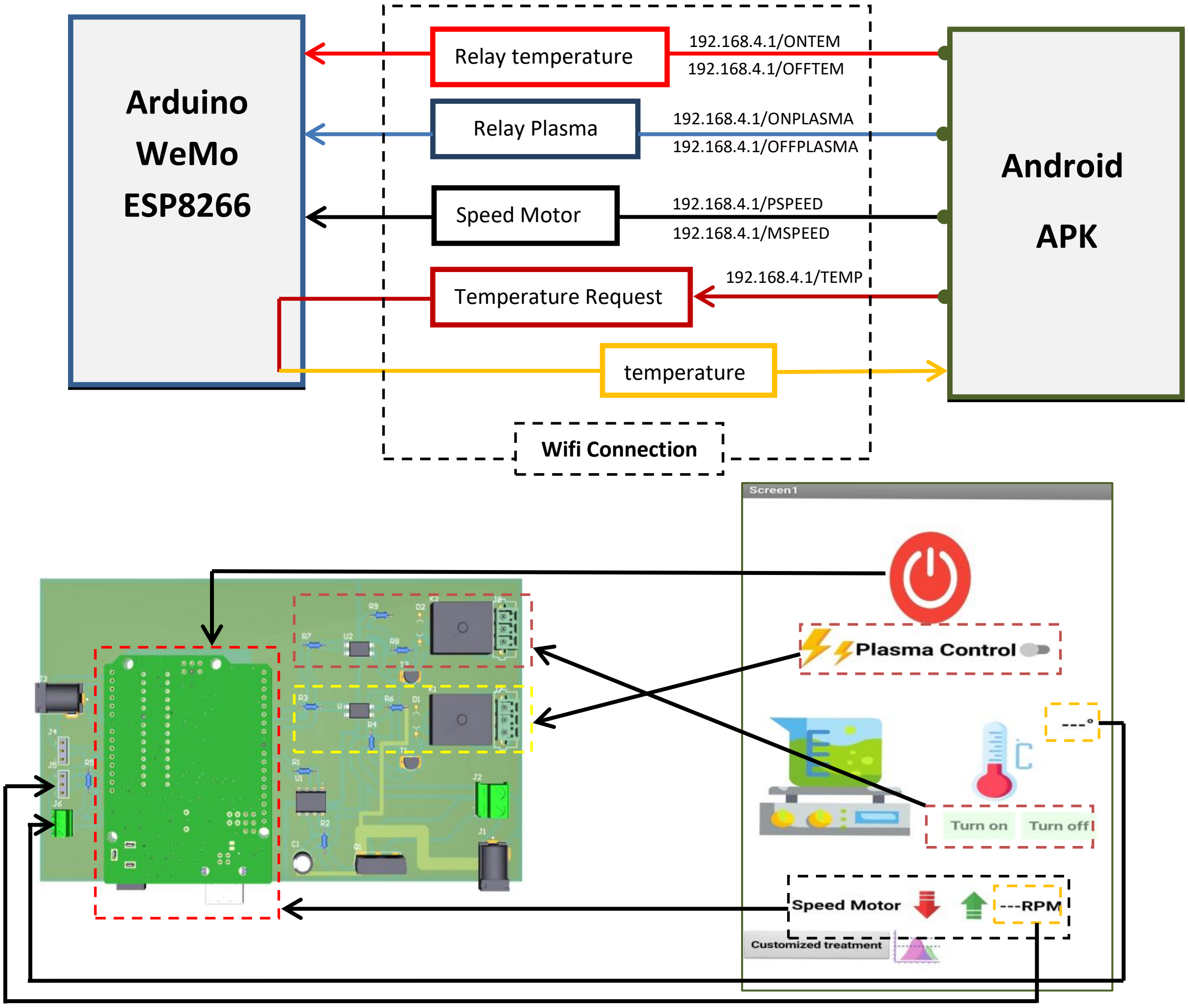

Figure III.32: Communication between the application and the control board.

A sophisticated Android application has been developed to control the magnetic stirrer device. The application features a range of functions that allow users to have complete control over the stirrer. This includes remote control, where users can turn the stirrer on/off and adjust its speed through the application on their smartphones. The application also enables monitoring of the stirrer's operation and displays status indicators such as temperature, stirrer speed, and operating status. Data logging functionality is also provided, where the application records information related to each stirring session, such as time, temperature, stirrer speed, and any additional relevant data. This feature allows users to review and analyze previous work data, obtaining accurate results and valuable information. As for the user interface, the application is designed with a simple and user-friendly layout. It includes an intuitive user interface that clearly displays elements and functions in an organized manner, making it easy for users to interact with the application seamlessly. Power On/Off button: Allows the user to turn the device on or off. Plasma On/Off button: Enables the user to activate or deactivate the plasma function in the mixer. Heating On/Off button: Allows the user to start or stop the heating function in the mixer. Solution Temperature gauge: Displays the current temperature of the mixed solution. Speed Control buttons: Provide the user with the ability to increase or decrease the mixing speed using dedicated buttons. Mixing Speed indicator: Shows the current speed of the mixing process. Data Logging area: Provides a place or log to record and store information related to each mixing session, such as time, temperature, mixing speed, and any additional relevant data. The application demonstrates excellent performance, executing commands quickly and accurately. It provides immediate response to user actions and continuously updates the displayed data. The application's performance has been extensively tested to ensure its stability and effective functionality.

III.8 Experimental Results and Discussion :

- The first image Figure(33) illustrates the successful motor speed control test, displaying excellent results as we mixed the liquids with high precision.

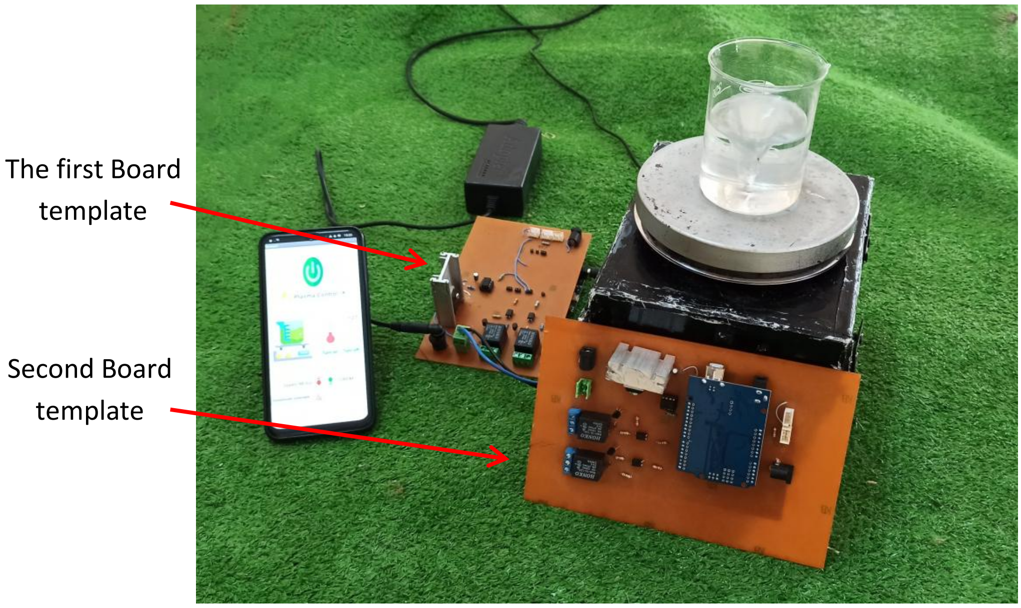

Figure III.33: Testing the effectiveness of mixing operation in the device.

- The second image Figure (34) represents the oscilloscope result, where every adjustment made to the motor speed through the application caused a change in the waveform displayed on the graph.

Figure III.34: DC motor speed control test.

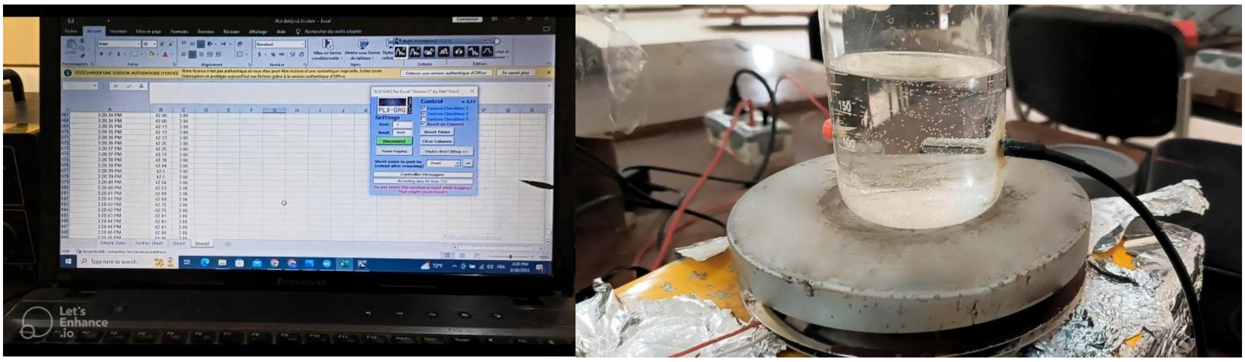

Figure III.35: Heating test.

- The third imageFigure (35) represents the heating test process in the device, where it yielded excellent results, and we efficiently heated the liquids with high efficiency.

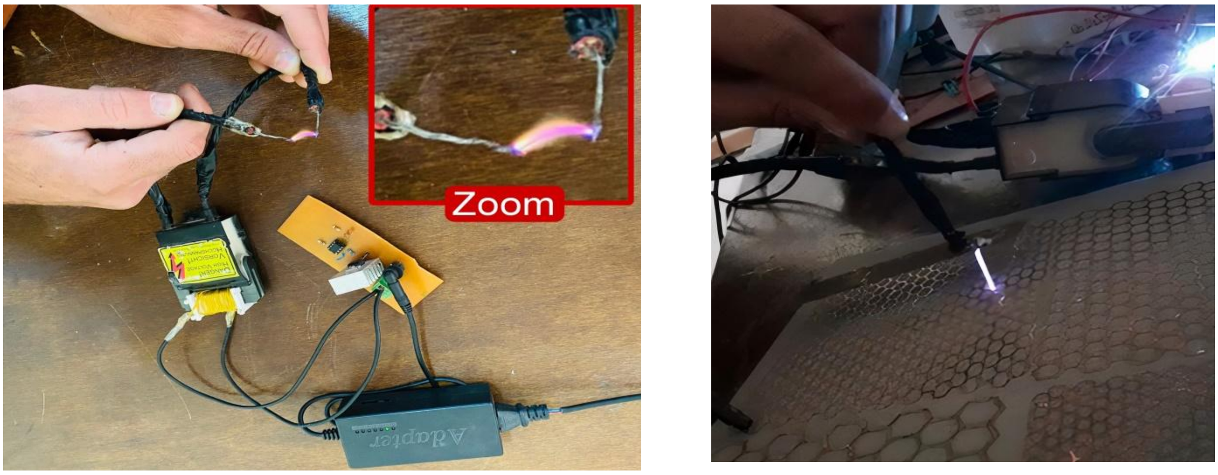

Figure III.36: Testing the effectiveness of the plasma electronic board.

- The following images Figure(36) represent the plasma generation test process, where we successfully produced plasma with high efficiency. We have also become capable of adjusting its intensity according to our needs.

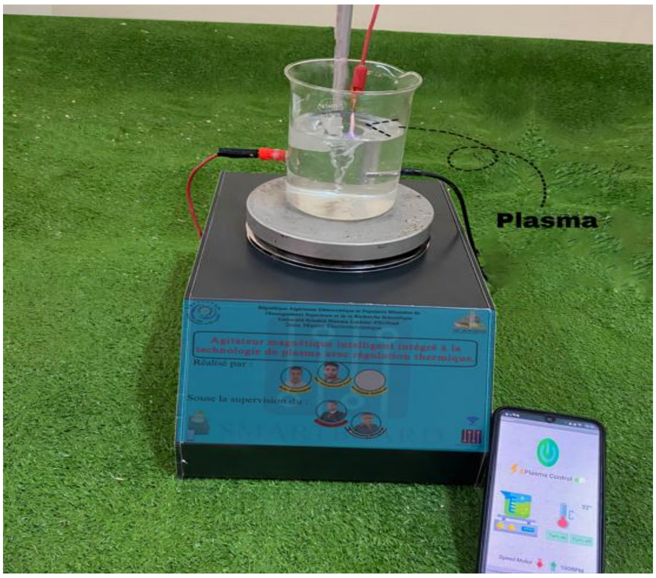

Figure III.37: The final model of the device.

III.9 Conclusion :

In conclusion, this chapter has provided an overview of the implementation of the smart magnetic stirrer, focusing on the control application that governs its operation. The smart magnetic stirrer represents a significant advancement in the field of mixing technology, offering intelligent features and advanced control mechanisms that revolutionize the mixing process.

Through the application, users have the ability to remotely control and monitor the smart magnetic stirrer, adjust speed and direction, and log important data during the mixing process.

The user interface of the application is designed to facilitate ease of use and efficient control over the smart magnetic stirrer.

The successful manufacturing and functionality of the smart magnetic stirrer signify a significant milestone in this project. The implementation process has involved the integration of various components, including the hardware and software aspects, to ensure seamless and reliable operation.

With the ability to control critical parameters and monitor the mixing process in real-time, the smart magnetic stirrer promises enhanced productivity, improved quality control, and reduced operational costs for various industries.

Moving forward, further experimentation and testing will be conducted to evaluate the performance of the smart magnetic stirrer in different scenarios and applications. This will enable us to gather valuable insights and fine-tune the system for optimal results.

General conclusion

General conclusion

In summary, this thesis aims to design and develop an intelligent electromechanical mixer that incorporates magnetic induction and plasma generation to enhance the mixing process. The previous chapters have provided comprehensive insights into magnetic stirrers, their applications in laboratory settings, and the fundamentals of plasma technology.

The studies and experiments conducted have yielded encouraging results, highlighting the effectiveness of direct control with a speed loop in achieving desired performance at a low cost. The implementation of the smart mixer has involved the integration of electronic components, design of electronic circuits, and development of a remote control application interface.

By utilizing advanced control mechanisms and intelligent features, the smart mixer promises increased productivity, improved quality control, and cost-effectiveness. It represents a significant milestone in the field of mixing technology, offering enhanced capabilities and revolutionizing the mixing process across various industries.

Looking ahead, further research and innovation in magnetic induction, plasma technology, and IoT integration hold great potential for advancements in laboratory science, industrial applications, and medical treatments. Future developments may include the incorporation of programmable features, compatibility with digital interfaces, and miniaturization for portable and field applications.

Overall, this research serves as a fundamental step in the design and development of intelligent electromechanical mixers. The successful implementation of the smart mixer and the knowledge gained from this study pave the way for future advancements and improvements in mixing technology, leading to enhanced efficiency, control, and productivity.

References

[Hal 07] Halász, G., Gyüre, B., Jánosi, I. M., Szabó, K. G., & Tél, T. (2007). Vortex flow generated by a magnetic stirrer. American Journal of Physics, 75(12), 1092–1098.

[Ros 13] A. Rosinger, “Magnetic Stirrer,”United States Patent Office, Retrieved 16 February 2013.

[Kor 80]Korpela, T. K. (1980). Air-driven magnetic stirrer for spectrophotometric cuvettes. Journal of Biochemical and Biophysical Methods, 3(4), 249–251.

[Fri 08] Fridman, Alexander. Plasma Chemistry. Cambridge University Press, 2008,p1.

[Wel 18] Weltmann, K., Kolb, J. F., Holub, M., Uhrlandt, D., Šimek, M., Ostrikov, K. (Ken), … Becker, K. (2018). The future for plasma science and technology. Plasma Processes and Polymers, 1800118.

[Šim 19] Šimončicová, J., Kryštofová, S., Medvecká, V., Ďurišová, K., & Kaliňáková, B. (2019). Technical applications of plasma treatments: current state and perspectives. Applied Microbiology and Biotechnology.

[Cha 91] Chang, J.-S., Lawless, P. A., & Yamamoto, T. (1991). Corona discharge processes. IEEE Transactions on Plasma Science, 19(6), 1152–1166.

[Gol 85]Goldman, M., Goldman, A., & Sigmond, R. S. (1985). The corona discharge, its properties and specific uses. Pure and Applied Chemistry, 57(9), 1353–1362.

[Gub 13] Gubbi, J, Buyya, R, Marusic, S, Palaniswami, M. (2013). Internet of things (IoT): A vision, architectural elements, and future directions. Future Generation Computer Systems, 29(7), 1645–1660.

[Mio 12] Miorandi, D, Sicari, S, De Pellegrini, F, Chlamtac, I. (2012). Internet of things: Vision, applications and research challenges. Ad Hoc Networks, 10(7), 1497–1516.

[Sil 18] Silverio-Fernández, M., Renukappa, S., & Suresh, S. (2018). What is a smart device? - a conceptualisation within the paradigm of the internet of things. Visualization in Engineering, 6(1).

[AUL 17] AULIA, Hanne; MUKHAIYAR, Riki. A New Design of Handless Stirred Device. 2017.

[MAH 20] MAHMOODI, Narges, et al. Are reported methods for synthesizing nanoparticles and microparticles by magnetic stirrer reproducible?. Journal of Computational Applied Mechanics, 2020, 51.2: 498-500.

[Pau 18]De Paula, L. F., & Ruggiero, R. (2018). Teaching Students How To Troubleshoot, Repair, and Maintain Magnetic Stirring Hot Plates Using Low-Cost Parts or Repurposed Materials. Journal of Chemical Education.

[Loz 69] M. G. Lozinskii, Industrial Applications of Induction Heating, 1st English ed. New York, NY, USA: Pergamon, 1969.

[Cho 15]Choi, J.; Kim, S.; Kim, K.; Park, M.; Yu, I.; Kim, S.; Sim, K. Design and Performance Evaluation of a Multi-Purpose HTS DC Induction Heating Machine for Industrial Applications. IEEE Trans. Appl. Supercond. 2015, 25, 1–5.

[Ame 14] Amestoy, P.; Buttari, A.; Joslin, G.; L'Excellent, J.Y.; Sid-Lakhdar, W.; Weisbecker, C.; Forzan, M.; Pozza, C.; Perrin, R.; Pellissier, V. Shared-Memory Parallelism and Low-Rank Approximation Techniques Applied to Direct Solvers in FEM Simulation. IEEE Trans. Magn. 2014, 50, 517–520. [Google Scholar] [CrossRef][Green Version]

[Ega 12]Egalon, J.; Caux, S.; Maussion, P.; Souley, M.; Pateau, O. Multiphase System for Metal Disc Induction Heating: Modeling and RMS Current Control. IEEE Trans. Ind. Appl. 2012, 48, 1692–1699. [Google Scholar] [CrossRef][Green Version]

[Mor 73] W. C. Moreland, "The induction range: Its performance and its development problems," IEEE Trans. Ind. Appl., vol. 9, no. 1, pp. 81–85, Jan. 1973.

[Luc 15] Lucía, O.; Sarnago, H.; Burdío, J.M. Soft-Stop Optimal Trajectory Control for Improved Performance of the Series-Resonant Multiinverter for Domestic Induction Heating Applications. IEEE Trans. Ind. Electron. 2015, 62, 6251–6259.

[Ace 15] Acero, J.; Lope, I.; Burdío, J.M.; Carretero, C.; Alonso, R. Performance Evaluation of Graphite Thin Slabs for Induction Heating Domestic Applications. IEEE Trans. Ind. Appl. 2015, 51, 2398–2404.

[Lop 15] Lope, I.; Acero, J.; Burdío, J.M.; Carretero, C.; Alonso, R. Design and Implementation of PCB Inductors With Litz-Wire Structure for Conventional-Size Large-Signal Domestic Induction Heating Applications. IEEE Trans. Ind. Appl. 2015, 51, 2434–2442.

[Sta 15] P. R. Stauffer, T. C. Cetas, and R. C. Jones, "Magnetic induction heating of ferromagnetic implants for inducing localized hyperthermia in deepseated tumors," IEEE Trans. Biomed. Eng., vol. BME-31, no. 2, pp. 235–251, Feb. 1984.

[Ton 18] Tonthat, L.; Yamamoto, Y.; Aki, F.; Saito, H.; Mitobe, K. Thermosensitive Ferromagnetic Implant for Hyperthermia Using a Mixture of Magnetic Micro-/Nanoparticles. IEEE Trans. Magn. 2018, 54, 1–6. [Google Scholar] [CrossRef].

[Hua 12]Huang, S.C.; Chang, Y.Y.; Chao, Y.J.; Shan, Y.S.; Lin, X.Z.; Lee, G.B. Dual-Row Needle Arrays Under an Electromagnetic Thermotherapy System for Bloodless Liver Resection Surgery. IEEE Trans. Biomed. Eng. 2012, 59, 824–831. [Google Scholar] [CrossRef].

[Tai 14]Tai, C.; Chen, C.; Kuo, C.; Lin, F.; Chang, C.; Chen, Y.; Wang, W. Deep-Magnetic-Field Generator Using Flexible Laminated Copper for Thermotherapy Applications. IEEE Trans. Magn. 2014, 50, 1–4. [Google Scholar] [CrossRef].

[shi 13]Ishizawa, H.; Tanabe, T.; Yoshida, D.; Hosseini, S.H.R.; Katsuki, S.; Akiyama, H. Focusing system of burst electromagnetic waves for medical applications. IEEE Trans. Dielectr. Electr. Insul. 2013, 20, 1321–1326. [Google Scholar] [CrossRef].

[Ole 84]Oleson, J.R. A Review of Magnetic Induction Methods for Hyperthermia Treatment of Cancer. IEEE Trans. Biomed. Eng. 1984, BME-31, 91–97.

[Luc 14]Lucia, O., Maussion, P., Dede, E. J., & Burdio, J. M. (2014). Induction Heating Technology and Its Applications: Past Developments, Current Technology, and Future Challenges. IEEE Transactions on Industrial Electronics, 61(5), 2509–2520.

[Alw 90]De Alwis, A. A. P., & Fryer, P. J. (1990). The use of network theory in the finite-element analysis of coupled thermo-electric fields. Communications in Applied Numerical Methods, 6(1), 61–66.

[Kau 15] Kaur, N., & Singh, A. K. (2015). Ohmic Heating: Concept and Applications—A Review. Critical Reviews in Food Science and Nutrition, 56(14), 2338–2351.

[Sør 03] Sørensen, H. P., Sperling-Petersen, H. U., & Mortensen, K. K. (2003). Dialysis strategies for protein refolding: preparative streptavidin production. Protein Expression and Purification, 31(1), 149–154.

[Che 95] Chen, F. F. (1995). Introduction to Plasma Physics.p1 .

[Neh 08] NEHRA, Vijay; KUMAR, Ashok; DWIVEDI, H. K. Atmospheric non-thermal plasma sources. International Journal of Engineering, 2008, 2.1: 53-68.

[Wel 18] Weltmann, K., Kolb, J. F., Holub, M., Uhrlandt, D., Šimek, M., Ostrikov, K. (Ken), … Becker, K. (2018). The future for plasma science and technology. Plasma Processes and Polymers, 1800118.

[Šim 19] Šimončicová, J., Kryštofová, S., Medvecká, V., Ďurišová, K., & Kaliňáková, B. (2019). Technical applications of plasma treatments: current state and perspectives. Applied Microbiology and Biotechnology.

[Pau 08] Paul M. Bellan , Fundamentals of Plasma Physics Cambridge University Press, 2008,p1.

[Bel 19] Belmont, G., Rezeau, L., Riconda, C., & Zaslavsky, A. (2019). What Is Plasma? Introduction to Plasma Physics, 1–32.

[Toh 62] THOMPSON, W. B. (1962). AN INTRODUCTION TO PLASMA PHYSICS. An Introduction to Plasma Physics, 1–8.

[Fri 05] Fridman, A., Chirokov, A., & Gutsol, A. (2005). Non-thermal atmospheric pressure discharges. Journal of Physics D: Applied Physics, 38(2), R1–R24.

[Cha 91] Chang, J.-S., Lawless, P. A., & Yamamoto, T. (1991). Corona discharge processes. IEEE Transactions on Plasma Science, 19(6).

[Sch 98] Schutze, A., Jeong, J. Y., Babayan, S. E., Jaeyoung Park, Selwyn, G. S., & Hicks, R. F. (1998). The atmospheric-pressure plasma jet: a review and comparison to other plasma sources. IEEE Transactions on Plasma Science, 26(6), 1685–1694.

[Gol 85] Goldman, M., Goldman, A., & Sigmond, R. S. (1985). The corona discharge, its properties and specific uses. Pure and Applied Chemistry, 57(9), 1353–1362.

[Eva 11] Evans, D. (2011). The internet of things: How the next evolution of the internet is changing everything. CISCO White Paper, 1(2011), 1–11.

[Gar 14] Gartner. (2014). Gartner says 4.9 billion connected “things” will be in use in 2015. Retrieved from http://www.gartner.com/newsroom/id/2905717.

[Gar 16] Gartner. (2016). Measuring the strategic value of the internet of things for industries. Retrieved from https://www.gartner.com/doc/3299317.

[Van 08] Van Kranenburg, R (2008). The internet of things: A critique of ambient technology and the all-seeing network of RFID. Amsterdam: Institute of Network Cultures.

[Han 14] Internet of Things: A Hands-On Approach," by Arshdeep Bahga and Vijay Madisetti 2014, page22.

[Han 08] INFSO, D (2008). Networked enterprise & RFID INFSO G. 2 micro & nanosystems, in co-operation with the working group RFID of the ETP EPOSS, internet of things in 2020, Roadmap for the future [R]. Berlin: Information Society and Media, Tech. Rep.

[SiM 09] Si, M. (2009). Le moteur à courant continu-publié le 02/03/2009. Publications Pimido.

[Gér 12] : Gérard Guihéneuf, « les moteurs électriques expliqués aux électroniciens (démarrage, variation de vitesse, freinage) », Deuxième édition augmentée, 2012, Publitronic_Elektor International Media, Pays -bas.

[Ori 16] :Oriol Planas « Moteurs à courant alternatif, description et types» 17/11/2016

[Gam 10] Gamazo-Real, J.C., E. Vázquez-Sánchez, and J. Gómez-Gil, Position and speed control of brushless DC motors using sensorless techniques and application trends. sensors. Vol. 10. 2010. 6901-6947.

[Rah 16] Rahman , M, et al. Implementation of quadcopter as a teaching tool to enhance engineering courses. in 2016 IEEE 8th International Conference on Engineering Education (ICEED). 2016. IEEE.

[San 17] Sang-HoonKim " Chapter 2 of Book "Electric Motor Control -Control of direct current motors", 12 May 2017

[Lab 21] Labiod Chouaib, Course Chapter 2 " Commande des machines a courant continu ", 2021/2022.

[Rac 11] Rachid Abdessamed, "Modélisation et simulation des machines électriques",Electrotechnique ,Ellipses,2011.

[Tor 18] Toru Masuzawa, Masahiro Osa, Martin Mapley" Chapter 11 of Book "Motor design and impeller suspension", 2018

[Fra 06] G. Franklin, J.D. Powell, A. Emami-Naeini, Feedback Control of Dynamic Systems, fifth ed., Prentice Hall, Upper Saddle River, NJ, 2006.

[Sug 90] H. Sugimoto, M. Koyama, S. Tamai, Practical Theory and Design of an AC Servo System, ISBN-10: 4915449580 (in Japanese) (Chapter 7), Tokyo, 1990.

[Kim 07] J.S. Yu, S.H. Kim, B.K. Lee, C.Y. Won, J. Hur, Fuzzy-logic-based vector control scheme for permanent-magnet synchronous motors in elevator drive applications, IEEE Trans. Ind. Electron. 54 (4) (2007) 2190_2200.

[Lor 73] W. Lord and J. Hwang, “ DC servomotors modeling and parameter determination ”. IEEE Trans. Industrial Applications, vol. IA-3, pp. 234-243, May/June1973.

[Lor 75] W. Lord and J. Hwang, “ DC motor model parameters ”. IEEE Trans. on Industrial Electronics and Control Instrumentation, vol. IECI-23, No.3, August1975

[Sch 83] R. Schulz, “A frequency for determining the parameters of high performance DC motors”. IEEE Trans. on Industrial Electronics, vol. IE-30, No.1, Februray1983.

[Raj 88] A. Rajkumar and R. Somanahtham, “ Determination of DC motor transients using a microcomputer ”. IEEE Trans, on Instrumentaion and Measurement, vol. 37, No.4, Dec. 1988

[Wee 91] S. Weerasooriya and M. El-Sharkawi, “ Identification and control of a DC motor using back-propagation neural networks ”. IEEE Trans. on Energy Conversion, vol. 6, No.4, December 1991.

[Jun 92] Y. G. Jung, K. Cho, Y. Lim, J. Park and Y. H. Change, “ Time domain identification of brushless DC motor parameters ”. IEEE Trans. on Industrial Electronics, vol. 2, 593-597, Februray 1992.

[Gil 96] D. M. Gillard and K. E. Bollinger, “ Neural network identification of power system transfer functions ”. IEEE Transactions on Energy Conversion, Vol. 11, No. 1, March 1996.

[Gil 00] Rubaai, A., & Kotaru, R. (2000). Online identification and control of a DC motor using learning adaptation of neural networks. IEEE Transactions on Industry Applications, 36(3), 935–942. Xiang-Qun Liu, Hong-Yue Zhang, Jun Liu, & Jing Yang. (2000). Fault detection and diagnosis of permanent-magnet DC motor based on parameter estimation and neural network. IEEE Transactions on Industrial Electronics, 47(5), 1021–1030.

[Xia 00] Xiang-Qun Liu, Hong-Yue Zhang, Jun Liu, & Jing Yang. (2000). Fault detection and diagnosis of permanent-magnet DC motor based on parameter estimation and neural network. IEEE Transactions on Industrial Electronics, 47(5), 1021–1030.

[Saa 01] S. Saab and R. Abi Kaed-Bey, “ Parameter identification of a DC motor: an experimetnal approach ”. IEEE Trans. on Electronics, Circuits and Systems, vol. 2, 981-984, 2001.

[Dup 04] A. Dupuis, M. Ghribi and A. Kaddouri, “ Multiobjective genetic estimation of DC motor parameters and load torque ”. IEEE International Conference on Industrial Technology, vol. 3, 1511-1514, Dec. 2004.

[Rad 05] Radojka Krneta, Sanja Antic and Danilo Stojanovic, “ Recursive least squares method in parameters identification of DC motors models ”. ELEC. ENERG, vol. 18, no. 3, 467-478, December 2005.

[Gar 06] R. Garrido and R. Miranda, “ Closed loop identification of a DC servomechanism ”. Power Electronics Congress, 10th IEEE, vol., no., pp.1-5, 16-18 Oct. 2006.

[Aun 07] W. P. Aung, “ Analysis on modeling and simulink of DC motor and its driving system used for wheeled mobile robot ”. International Journal of Computer, Information, and Systems Science, and Engineering, Volume 2 Number 1, Nov. 2007.

[Had 09] M. Hadef and R. Mekideche, “ Parameter identification of a separately excited DC motor via inverse problem methodology ”. Turk J Elec Eng and Comp Sci, vol. 17, No.2, 2009.

[Sha 19] Shah, P., & Sekhar, R. (2019). Closed Loop System Identification of a DC Motor using Fractional Order Model. 2019 International Conference on Mechatronics, Robotics and Systems Engineering (MoRSE).

[Han 20] : Handson Technology. "Datasheet for WeMos D1 ESP8266 WiFi Board." Accessed from https://www.handsontec.com/dataspecs/module/WeMos%20D1%20WiFi.pdf. .

[Phi 94] : Philips Semiconductors Linear Products. (1994) . " Timer NE/SA/SE555/SE555C " data sheet .

[Agi 03] : Agilent Technologies , (2003) . HCPL-3180 2 Amp Output Current, High Speed IGBT/MOSFE Gate Drive Optocoupler Data Sheet.

[Eve 10] : Everlight Electronics , (2010) " 4 PIN DIP PHOTOTRANSISTOR EL817 Series " , Data sheet .

[Soy 93] : Mr: SOYED-Abdessam Cours d'électronique de puissance 93 .

[Sem 20] : ON Semiconductor , (2020) "IGBT - Field Stop 600V, 40A FGH40N60UFD " , Data sheet .

[Pan12] : PANASONIC IDEAS FOR LIFE , (2012) , "1a/1c 10A cubic type power relays" , Data sheet .

[Max 08] : Maxim Integrated Products , (2008) . " DS18B20 " , Data sheet .

[Joy 17] : Joy-IT (2017) "DS18B20 Programmable Resolution 1-Wire Digital Thermometer". Data sheet .